Regulation of recycling endosomal membrane traffic by a γ-BAR/ kinesin KIF5 complex

PhD Thesis

in partial fulfilment of the requirements

for the degree "Doctor of Philosophy (PhD)"

in the Molecular Biology Program

at the Georg August University Göttingen,

Faculty of Biology

submitted by

Michael Schmidt

born in

Eisenach, Germany

Göttingen 2007

Affidavit

I declare that my PhD thesis entitled "Regulation of recycling endosomal membrane traffic by a γ-BAR/ kinesin KIF5 complex" has been written independently and with no other sources and aids than quoted.

Michael Schmidt September 30th, 2007

Meiner Familie

Table of Contents

Acknowledgements

First, I want to thank my supervisor **Prof. Dr. Volker Hauck**e for giving me the opportunity to perform my PhD studies in his lab. I am thankful for his excellent supervision, fruitful discussions and numerous ideas.

My thanks go to the members of my PhD committee, **Prof. Dr. Reinhard Jahn** and **Dr. Dieter Klopfenstein,** for help and support during my PhD studies. I am grateful for their encouragement and advice during our committee meetings.

I am thankful to all current and former members of the Haucke lab for their support and for creating an enjoyable working atmosphere: **Kasim Diril, Isabelle Grass, Lisa Jerndal, Junyong Jia, Nadja Jung, Nina Kahlfeldt, Yaara Kapp-Barnea, Kathrin Kastning, Michael Krauß, Viktoria Kukhtina, Tanja Maritzen, Julia Mössinger, Arndt Pechstein, Jasmin Podufall, Yijian Rao, Claus Rodemer, Stefanie Thiel, Kristin Walther, Ingeborg Walther and Marnix Wieffer**. Special thanks to my diploma and practical students **Naomi Barak, Jennifer Hanna, Claudia Krause and York Posor**.

I especially thank **Dr. Carlos Dotti** and **Dr. Frank Bradke** as well as their colleagues for allowing me to carry out parts of my PhD studies in their labs and teaching me new techniques. I truly enjoyed my visits in Torino and Munich!

I am thankful for financial support of my PhD project by a Georg Christoph Lichtenberg stipend from the state of Lower Saxony. I also thank the European Molecular Biology Organisation (EMBO) for financial support of my visit to Carlos Dotti's lab in Torino, Italy by an EMBO Short-Term Fellowship.

Abstract

Intracellular trafficking of membrane proteins and lipids between different compartments is a fundamental process underlying a variety of cell physiological functions of eukaryotic cells. Protein sorting along the secretory and endocytic pathways depends on the presence of different types of endosomal organelles. Recycling endosomes (REs) comprise a collection of vesiculo-tubular membranes that are often found in association with microtubules. In most cell types, they are concentrated in the perinuclear area in close proximity to the trans-Golgi network. REs mediate constitutive recycling of plasma membrane proteins, for example the transferrin receptor (TfR), but have also been implicated in the regulation of other cellular processes ranging from cytokinesis over morphogenesis to cellular polarity and long term synaptic plasticity.

The aim of this thesis was to analyze the role of γ-BAR, a recently identified protein that interacts with the γ-ear domain of the clathrin adaptor complex AP-1 and is implicated in post-Golgi/ endosomal trafficking events. We found that γ-BAR association with membranes is mediated by post-translational palmitoylation of three cysteine residues at its amino-terminal end. Furthermore, we discovered that γ-BAR localizes to recycling endosomal membrane profiles and associates with the microtubule-based motor protein kinesin KIF5 via direct binding to its light chains, thereby regulating RE dynamics. Overexpression of γ-BAR caused a relocalization of Rab11- and TfR- containing REs to the cell periphery and to axonal clusters in hippocampal neurons. This phenomenon was dependent on the presence of intact microtubules and functional kinesin KIF5 motor proteins. Furthermore, γ-BAR overexpression delayed recycling of transferrin (Tf) to the cell surface and impaired axonal outgrowth in developing hippocampal neurons. Conversely, siRNA mediated knockdown of γ-BAR facilitated Tf recycling as well as axonal outgrowth.

These results identify γ-BAR as a molecular link between the endosomal recycling compartment and the microtubule-based transport machinery. We propose that a γ-BAR - kinesin KIF5 complex regulates the intracellular positioning and transport of recycling endosomes. Thus, it might be implicated in diverse cell physiological processes known to involve REs.

1 Introduction

1.1 Eukaryotic compartmentalization and membrane trafficking

Eukaryotic cells contain a variety of distinct intracellular compartments and organelles that are separated from each other by surrounding single or double membranes (Alberts et al., 2002; Lodish et al., 2000). The nucleus is separated from the surrounding cytoplasm by an envelope consisting of two membranes. It contains the chromosomal DNA and is the place of DNA and RNA synthesis. The cytoplasm contains the cytosol, the place of protein synthesis and most of the cell's intermediary metabolism, as well as a variety of cytoplasmic organelles. The endoplasmic reticulum (ER), a continuous collection of flattened sheets, sacs and tubes of membrane, extends throughout the cytoplasm and is connected with the outer membrane of the nuclear envelope. It is involved in synthesis, modification and transport of secreted and membrane proteins. The Golgi apparatus, first described by Camillo Golgi in 1898 (Brambell, 1923), is a system of stacked, flattened sacs surrounded by single membranes. It is implicated in modifying, sorting and packaging of membrane proteins for secretion or the delivery to other compartments. Mitochondria are double-membrane bounded organelles that serve as the "power plant" of eukaryotic cells by producing energy in the form of ATP from sugar molecules and oxygen. A variety of smaller membrane bounded organelles and vesicles are present in the eukaryotic cell: Lysosomes contain hydrolytic enzymes involved in the degradation of macromolecules. Peroxisomes are specialized compartments that contain oxidative enzymes involved in the generation and destruction of hydrogen peroxide. Different kinds of endosomes (early, late, recycling etc.) mediate intracellular transport processes towards and from the plasma membrane. The plasma membrane itself, a continuous sheet mostly composed of phospholipid molecules and embedded membrane proteins serves as the outer boundary of the cell.

Each organelle has its unique functional identity, which is reflected by the presence of particular sets of proteins in the lumen as well as the organelle's membrane (Munro, 2004). Thus, the introduction of different compartments provides a challenge for eukaryotic cells: They have to create as well as preserve the identity and function of each organelle. Exchange of proteins, lipids and other macromolecules between compartments is effected by intracellular membrane trafficking. Such trafficking events involve the sorting of proteins and lipids destined for different organelles at several intracellular sorting stations, the generation of small carrier vesicles or tubules that

mediate transport processes between the organelles and the fusion of carriers with target membranes. At least two main trafficking routes can be distinguished: An outward so-called **secretory pathway** and an inward or **endocytic pathway**. Within the secretory pathway, proteins synthesized in the ER move to the Golgi complex as a major sorting station from where they are targeted to the plasma membrane. Proteins reaching the Golgi complex might also enter the endosomal sorting system and can either be directed to late endosomes and lysosomes or traffic to the plasma membrane via recycling endosomes (REs). The endocytic pathway starts with the internalization of membrane proteins and lipids from the plasma membrane into primary endocytic vesicles which fuse with each other or preexisting organelles to form early endosomes (EEs). From EEs proteins are either sorted towards late endosomes (LEs)/ lysosomes, return to the plasma membrane or are transferred to REs.

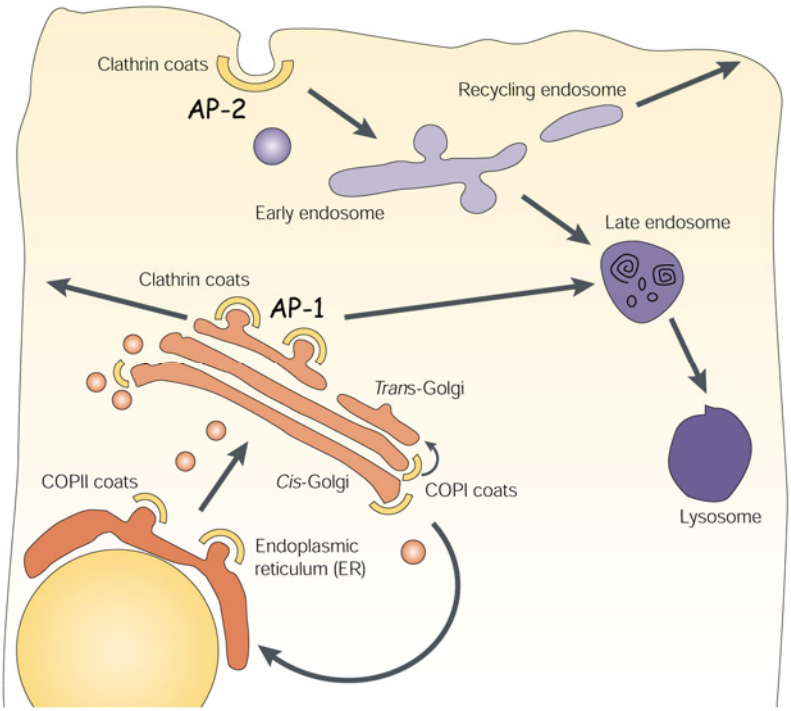

Figure 1-1: The classical view of intracellular trafficking pathways

The secretory pathway starts at the endoplasmic reticulum (ER), from where COPII carriers are transported to the Golgi complex. Proteins leave this complex at the trans-Golgi side (trans-Golgi network, TGN), where they are packaged into clathrin-coated vesicles and transported to the plasma membrane or the late endosomal/ lysosomal sytem. The endocytic pathway begins at the plasma membrane. Membrane proteins internalized in a clathrin-dependent manner are transported to early endosomes, from where they enter the late endosomal/ lysosomal pathway or are recycled to the plasma membrane via recycling endosomes. Clathrin-coated vesicle formation at the TGN/ REs depends on the adaptor complex AP-1, whereas AP-2 functions at the plasma membrane. Modified from Kirchhausen, 2000.

1.2 Vesicle formation, coat proteins and adaptors

1.2.1 Vesicles and associated coats

The trafficking pathways explained above largely depend on trafficking of membrane-bounded transport carriers and vesicles moving between intracellular compartments. There are three different ways to generate a coated vesicle and these depend on the type of compartment they are derived from (Kirchhausen, 2000b). Secretory protein trafficking from the endoplasmic reticulum (ER) to the cis-Golgi (antrograde transport) is mediated by COPII-vesicles. Retrograde transport from the cis-Golgi to the ER and transport within the Golgi involves the formation of COPI-vesicles that are distinguished by morphologically similar, yet molecularly different sets of coat proteins (Duden, 2003). The third type of vesicle formation occurs at the trans-Golgi network (secretion of proteins) and endosomes as well as at the plasma membrane (endocytosis) and is clathrin-dependent (McNiven and Thompson, 2006). COPI, COPII and clathrin are so-called coat proteins that aid vesicle formation by stabilizing curved patches of membrane at the bud site (McMahon and Mills, 2004). Vesicles are finally pinched off from the membrane and the coat proteins disassemble and dissociate from the vesicle surface, a process called uncoating.

Clathrin-dependent vesicle formation is involved in a variety of transport pathways including internalization of receptors, growth factors, ion channels and synaptic vesicle membranes from the plasmalemma as well as secretory vesicle formation at the TGN (Takei and Haucke, 2001; Traub, 2005). Clathrin was discovered already 25 years ago (Pearse, 1976) and is the most abundant protein found in the coat of clathrin-coated vesicles (CCVs). It forms a lattice at the cytosolic face of the membrane which is built up from three-legged triskelial units. Triskelia are composed of three clathrin heavy and light chains (Kirchhausen, 2000a; Smith and Pearse, 1999). CCV formation requires clathrin, adaptor proteins as well as a variety of additional factors, so called accessory proteins, that assist in invagination, fission and uncoating of vesicles and link these processes to the actin cytoskeleton (McMahon and Mills, 2004; Slepnev and De Camilli, 2000; Traub, 2005).

1.2.2 Adaptor complexes and alternative adaptors

Heterotetrameric adaptor complexes help recruiting transmembrane cargo proteins, clathrin and accessory proteins to the site of clathrin-coated pit formation. The first adaptor proteins were identified almost 30 years ago and originally referred to as "assembly polypeptides" (APs) as they were able to promote the assembly of purified clathrin into lattices *in vitro* (Ahle and Ungewickell, 1986; Keen et al., 1979). Clathrin adaptor complexes come in four different flavours, namely AP-1, 2, 3 and 4, depending on the site of vesicle formation. Whereas AP-2 is the predominant clathrin adaptor at the plasma membrane (Collins et al., 2002; Kirchhausen, 2002) facilitating clathrin mediated endocytosis, AP-1 functions at the TGN (Robinson, 1990) and perhaps at REs in packaging cargo destined for the endosomal-lysosomal (Honing et al., 1997) or secretory pathways as well as in vesicle formation on endosomes (Futter et al., 1998; Peden et al., 2004). AP-3 (Dell'Angelica et al., 1997; Simpson et al., 1996) and AP-4 (Dell'Angelica et al., 1999; Hirst et al., 1999) have been identified later and are implicated in protein sorting at the TGN and/ or endosomes (Peden et al., 2004; Robinson and Bonifacino, 2001), which might at least in part be clathrin independent. All four adaptor complexes are heterotetramers and contain related sets of subunits (see below). In addition to these adaptor complexes, a number of alternative adaptors are known that can function together with or independently from them (Robinson, 2004). GGAs (Golgi-localized, γ-ear containing, Arf binding proteins) comprise a family of monomeric adaptors (Boman et al., 2000; Dell'Angelica et al., 2000; Hirst et al., 2000; Poussu et al., 2000) that are found at the TGN and endosomal membranes and are implicated for example in mannose-6-phosphate receptor trafficking (Bonifacino, 2004; Doray et al., 2002; Ghosh and Kornfeld, 2004). Whether or not they function together with or independently of AP-1, on parallel or distinct trafficking pathways, is still under intense investigation (Doray and Kornfeld, 2001; Lui et al., 2003; Mardones et al., 2007). Another set of alternative clathrin adaptors act together with AP-2 at the plasma membrane (Traub, 2003).

1.2.3 The adaptor complex AP-1

AP-1, like the other three adaptor complexes, is a heterotetramer composed of the four subunits γ, β1, σ1 and μ1, also called adaptins (Robinson and Bonifacino, 2001). The large γ und β1 subunits of AP-1 are symmetric to each other and form structurally distinct domains of the adaptor complex: the 'trunk' or 'core' domain, two long, unstructured 'hinge' segments and two 'ear' or 'appendage' domains. The medium and small subunits μ1 and σ1 are tightly associated with the very compact structure of the core domain. The hinge regions of β1- and γ-adaptins contain so-called 'clathrin box' or related sequences that bind to the terminal domain of clathrin heavy chains (Doray and Kornfeld, 2001; Gallusser and Kirchhausen, 1993). The ears of the adaptor complex serve as platforms for interactions with a variety of accessory proteins involved in the regulation of vesicle formation, disassembly and cargo sorting (Lui et al., 2003; Page et al., 1999). The core domain mediates the recruitment of AP-1 to membranes by binding to ARF-GTP and phosphoinositides (Crottet et al., 2002; Wang et al., 2003). The μ1 subunit recognizes tyrosine-based sorting motifs (YXXΦ, where Φ is a hydrophobic residue) present in the cytoplasmic domains of cargo proteins and recruits them to the site of vesicle formation (Ohno et al., 1995), while a γ/σ1 hemicomplex has been shown to interact with dileucine-based sorting signals (Doray et al., 2007; Janvier et al., 2003). However, other studies identified the β1 subunit (Rapoport et al., 1998) or the μ1 subunit (Craig et al., 2000; Hofmann et al., 1999; Rodionov and Bakke, 1998) to be responsible for recognition of dileucine-based sorting motifs.

The large β1 and β2 subunits of the adaptor complexes AP-1 and AP-2, respectively, show very high homology to each other. However, in the case of γ-adaptin and its homologous subunit α-adaptin of AP-2, the conservation is restricted to the first 600 amino acids that form the trunk domain. The carboxy-terminal 100-300 amino acids long appendage or ear domains display divergent sequences, although they show a similar overall folding (Hirst and Robinson, 1998). As described above, the ear domains of the AP large subunits function as platforms for the recruitment of accessory proteins from the cytosol onto the membrane where they facilitate coated vesicle formation. A growing number of AP-1-associated accessory proteins binding to the γ-adaptin ear domain have emerged, including γ-synergin (Hirst et al., 2000; Page et al., 1999; Takatsu et al., 2000), rabaptin-5 (Hirst et al., 2000; Shiba et al., 2002; Zhu et al., 2001), NECAP 1 and 2 (Mattera et al., 2004; Ritter et al., 2003), aftiphilin (Mattera et al., 2004), enthoprotin/Clint/EpsinR (Hirst et al., 2003; Kalthoff et al., 2002; Mills et al.,

2003; Wasiak et al., 2002) and p56 (Lui et al., 2003). However, the functions of most of these accessory proteins remain poorly understood.

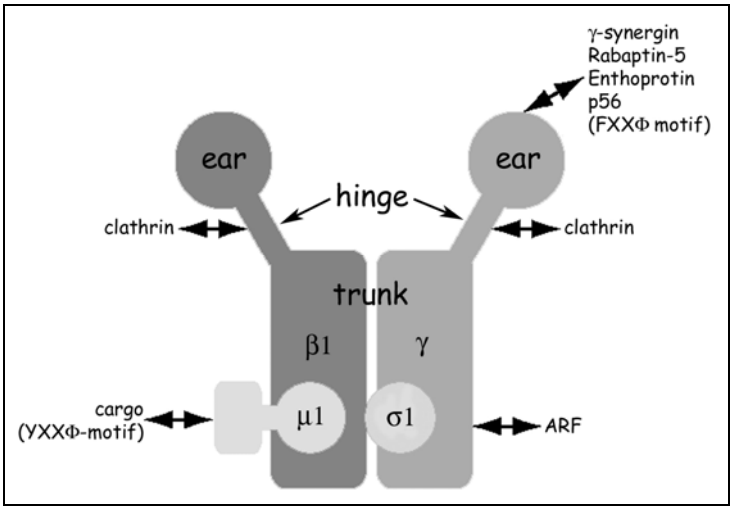

Figure 1-2: Schematic representation of the adaptor complex AP-1

The large subunits, β1 and γ-adaptin, build up the trunk, hinge and ear domains of the complex. The small subunits, μ1 and σ1-adaptin, are tightly associated with the trunk domain. The sites of interaction with clathrin, cargo proteins and accessory proteins are indicated.

1.3 Endosomes

1.3.1 Endosomal sorting

Endosomes are not a homogenous population of organelles, but rather comprise a collection of compartments with distinct properties and functions. In non-polarized cells one can distinguish three main types of endosomes: Early endosomes (EEs), recycling endosomes (REs) and late endosomes (LEs). They play key roles in sorting along the endocytic and secretory pathways.

Early endosomes serve as a major sorting station for the endocytic journeys of internalized proteins from the plasma membrane, such as cargo receptors and ligands. There are several known routes which cargo can take from EEs: First, they can be returned to the plasma membrane, which can either occur directly from EEs (fast recycling pathway) or indirectly via REs (slow pathway). Typical examples for recycled plasma membrane proteins are transferrin (Tf) and low-density lipoprotein (LDL) receptors (Maxfield and McGraw, 2004). Once transferred to REs (also called ERC for endocytic recycling compartment), cargo proteins can be sorted towards the plasma

membrane as seen for TfR, but can also traffic retrogradely towards the trans-Golgi network (TGN). Sorting to the TGN can occur from both EEs and LEs. Such retrograde pathways from endosomes (Saint-Pol et al., 2004) are taken by proteins cycling between the TGN and the plasma membrane (e.g. TGN38/ TGN46) (Roquemore and Banting, 1998) or certain toxins entering the cell, such as the bacterial Shiga toxin (Lauvrak et al., 2004). Mannose-6-phosphate receptors (MPRs) which guide newly synthesized lysosomal hydrolases from the TGN to LEs are the classical example for cargo sorted from late endosomes back to the TGN (Schweizer et al., 1997; Tikkanen et al., 2000). Alternatively, cargo from EEs can enter the late endosomal/ lysosomal pathway for degradation, as exemplified by many ligand-activated signaling receptors, such as the EGF (epidermal growth factor) receptor (Katzmann et al., 2002; Raiborg et al., 2003).

1.3.2 Rab proteins and endosome identity

Endosome identity and function is, in part, determined by members of the Rab family of small GTPases (Zerial and McBride, 2001) which function as molecular timers cycling between active GTP- bound and inactive GDP-bound states. Cycling between these two stages is regulated by GTPase-activating proteins (GAPs), guanine nucleotide exchange factors (GEFs), GDP-dissociation inhibitors (GDIs) and GDP-displacement factors (GDFs) as well as their binding partners. Rab effector proteins specifically interact with the active GTP-bound form and include membrane-tethering and docking factors, components of the vesicle budding and fusion machineries as well as cytoskeleton-associated motor proteins (Jordens et al., 2005). Different Rab proteins are associated with distinct endosomal subpopulations or delineate specific endosomal membrane domains. So far, more than 60 different mammalian Rab proteins are known. The most important and thoroughly investigated ones will be described here. Rab5 functions in the early endocytic pathway by regulating fusion of clathrin-derived primary endocytic vesicles with pre-existing EEs as well as homotypic EE fusion (Bucci et al., 1992; Gorvel et al., 1991). Rab5 effectors include the tethering factor early endosomal antigen 1 (EEA1) (Christoforidis et al., 1999) and the non-conventional kinesin KIF16B (Hoepfner et al., 2005). Rab4 is associated with early as well as recycling endosomes (Van Der Sluijs et al., 1991) and is presumed to control early sorting events in the endocytic pathway (van der Sluijs et al., 1992). Rab11 regulates membrane traffic at the recycling endosomal compartment and its boundary with the TGN (Ullrich et al., 1996; Urbe et al., 1993). This includes recycling of TfR (Ren et al., 1998) or α-amino-3-

hydroxy-5-methylisoxazole-4-propionic acid (AMPA)-type glutamate receptors to the cell surface in neurons (Park et al., 2004), as well as delivery of Shiga toxin and TGN38 to the TGN (Wilcke et al., 2000). Rab8 selectively regulates AP-1B-dependent basolateral transport via the TGN and recycling endosomes in polarized epithelial cells (Ang et al., 2003). Rab7 and Rab9 are regulators of trafficking in the late endosomal system with Rab7 controlling EE-to-lysosome sorting (Feng et al., 1995) and Rab9 being implicated in LE-to-TGN transport of MPRs (Lombardi et al., 1993). Other Rab proteins are specifically expressed in polarized epithelial (for example, Rab17 and Rab25) (Casanova et al., 1999; Zacchi et al., 1998) or specialized secretory cells (Rab27a, Rab32, Rab38) (Seabra and Wasmeier, 2004). The dynamic exchange of Rab proteins between separate membrane areas (Miaczynska and Zerial, 2002) or different types of endosomes may form the basis for the maturation and specialization of endosomes by Rab conversion (Rink et al., 2005).

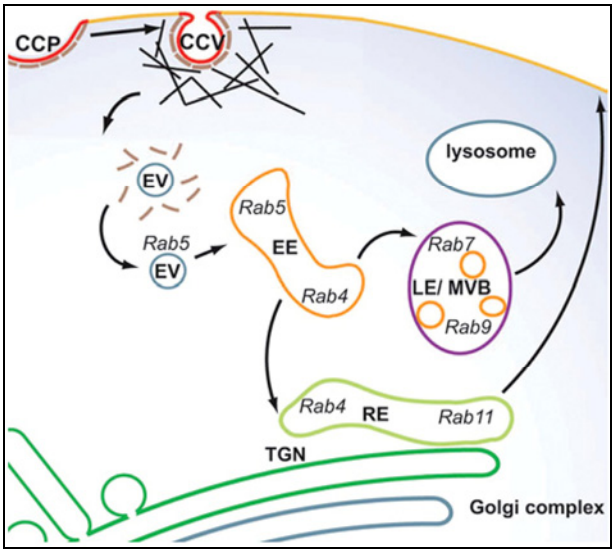

Figure 1-3: Rab protein distribution along the endosomal sorting pathways

Distinct kinds of endosomal subpopulations associate with different Rab proteins. Endocytic vesicles (EV) and early endosomes (EE) contain Rab5. Rab4 is associated with EEs and recycling endosomes (RE), whereas Rab11 is only found in the latter. Trafficking in the late endosomal (LE)/ multivesicular body (MVB) system is regulated by Rab7 and Rab9. Different Rab proteins can also delineate specific membrane subdomains within the same endosomal compartment (e.g. Rab4 and Rab11 mark different domains within RE). Taken from Schmidt and Haucke, 2007.

1.3.3 Recycling endosomes

1.3.3.1 Endosomal recycling pathways

The transferrin receptor (TfR) serves as the major example for a recycling membrane protein. It is constitutively endocytosed from the PM and reaches EEs from where it is efficiently recycled either directly or via REs (Sheff et al., 1999). Direct sorting from EEs to the plasma membrane reflects a fast method of recycling (Hao and Maxfield, 2000), whereas sorting through REs is much slower (Mayor et al., 1993). REs comprise a collection of vesiculo-tubular membrane structures that are often associated with microtubules (Hopkins, 1983; Yamashiro et al., 1984). This morphology, which is also seen for the "recycling" part of EEs, ensures a high membrane-to-volume ratio. This favors the enrichment of endosomal membrane proteins and thus facilitates their sorting into transport carriers that leave the endosomal tubules (Maxfield and McGraw, 2004). The subcellular localization of REs varies between different cell types. Most frequently, REs are found in a peri-nuclear location opposing late elements of the Golgi complex, the TGN and the centrosome with the microtubule-organizing center (Hopkins et al., 1994). However, in some cells REs are distributed more widely throughout the cytoplasm (Lin et al., 2002). REs can sort molecules to several distinct destinations, but most molecules are returned to the plasma membrane. The trafficking of molecules from REs depends on the formation of transport intermediates, vesicles or tubules, and is regulated by the small GTPase Rab11 and the Eps15-homology-domain protein EHD1/Rme1. Interestingly, these proteins seem to be required for transport towards both the TGN and the plasma membrane (Lin et al., 2001; Wilcke et al., 2000).
Another type of sorting from REs is exemplified by the endocytic trafficking of TGN38. This protein exhibits a predominant TGN distribution, but a pool of about 10% resides on the cell surface at steady state. The surface pool is internalized and returned to the TGN, passing through REs *en route* (Ghosh et al., 1998). Shiga toxin is another example for proteins that are transported from REs back to the TGN (Mallard et al., 1998).

1.3.3.2 Recycling endosomes in secretory membrane traffic

As already mentioned above, the TGN was thought to be the major sorting station for secretory membrane traffic (Pfeffer and Rothman, 1987). However, this point of view has changed dramatically over the past 15 to 20 years (Rodriguez-Boulan and Musch,

2005). Now it seems clear that not all sorting occurs at the TGN, but includes also other compartments and pathways. Sorting may occur in REs and budded tubulosaccular structures or even at the exit from the ER.

Accumulating evidence from epithelial cells suggests that REs play important roles in polarized sorting and secretory transport of at least a subset of proteins *en route* to the cell surface (Ang et al., 2004; Perret et al., 2005). For that, apical and basolateral cargos are actively segregated into separate subdomains of individual REs (Thompson et al., 2007). For example, the basolateral transport of the cell adhesion molecule E-cadherin is regulated by Rab11-mediated delivery of REs *en route* from the TGN to the plasma membrane (Lock and Stow, 2005). Thus, REs might be involved in the establishment of cellular polarity which will be discussed later on.

Other studies indicate that REs are important for the delivery of membrane to sites of plasma membrane growth. During cellularization in *Drosophila*, sub-apical REs receive vesicles from the secretory end endocytic pathways and provide material for the growth of the lateral membrane (Pelissier et al., 2003). The *Drosophila* pericentrosomal protein, Nuclear-fallout (Nuf), and Rab11 at REs are implicated in the initial stages of furrow formation during cytokinesis which requires a dramatic remodeling of the cortical cytoskeleton as well as membrane addition (Riggs et al., 2003). In mammalian cells, Rab11-containing REs accumulate near the cleavage furrow and are required for successful completion of cytokinesis. The delivery, targeting and fusion of REs with the furrow is controlled by the interaction of Rab11 and FIP3 (family of Rab11-interacting proteins 3)/ Arfophilin-1, which shares homology with *Drosophila* Nuf (Wilson et al., 2005). Thus, cells might use REs for the delivery of membranes to regions of their surface that are subject to dynamic reorganization. This process is probably mediated through regulated interactions with the exocyst, a multi-protein complex containing eight subunits that is thought to recruit material to areas of membrane fusion and growth (Lipschutz and Mostov, 2002).

Consequently, REs control a variety of cellular processes dependent on intracellular trafficking and membrane delivery to the plasmalemma including epithelial cell-cell adhesion and polarity (see below), cytokinesis as well as cell fate specification (van Ijzendoorn, 2006).

1.4 Cellular polarity

Cellular polarity is an important feature of many eukaryotic cell types including neurons and most epithelial cells. It is established by creating distinct plasma membrane domains that differ for example in their membrane lipid and protein composition. Thus, distinct sets of membrane proteins exist within a particular cellular domain, including receptors, ion channels, transporters and adhesion molecules. The mechanisms underlying establishment and maintenance of cellular polarity include: (i) differential sorting of membrane proteins to distinct plasma membrane domains along the secretory and endosomal pathways (Keller et al., 2001; Kreitzer et al., 2003), (ii) retention of proteins in membrane domains by building up barriers that prevent their free diffusion (Dotti and Poo, 2003; Kobayashi et al., 1992; Nakada et al., 2003; Winckler et al., 1999), and (iii) stabilization of protein complexes at the membrane by scaffolding proteins (Harris and Lim, 2001).

1.4.1 Polarized protein sorting in epithelial cells

The best characterized model for cellular polarity in mammalian cells is that of the polarized epithelial cell. These cells establish two distinct domains, the apical and basolateral plasma membrane surface, separated by tight junctions, each with their own specific set of membrane proteins to accomplish the unique functions of each domain (Mostov et al., 2003).

As already mentioned, the establishment of cellular polarity largely depends on the differential sorting of membrane proteins to distinct membrane domains along the secretory and endosomal membrane trafficking pathways. Thus, apical versus basolateral sorting of cargo involves an interplay between secretory and specialized endocytic organelles (Rodriguez-Boulan et al., 2005). The latter include apical REs, apical and basolateral EEs (also called sorting endosomes, SEs), as well as common REs.

The conventional model for protein sorting in polarized cells proposes that all protein sorting in the biosynthetic route occurs at the TGN, where apical and basolateral proteins are sorted into different post-Golgi carriers that are transported to either of the two plasma membrane domains. This differential sorting is dependent on the presence of apical and basolateral sorting signals in cargo proteins which meet different cargo sorting and carrier formation machineries. The endocytic sorting system functions

independently of the TGN sorting machinery and consists of two separate endosomal systems connected with the apical and basolateral surfaces. Membrane proteins are internalized into apical and basolateral sorting endosomes and transferred to common REs. From there, they are sorted into different recycling routes to the apical or basolateral plasma membrane domains.

In an alternative model, basolateral and apical proteins may leave the TGN in large tubulo-saccular structures (Polishchuk et al., 2000). Sorting occurs within these organelles on the way to the plasma membrane by the removal of basolateral proteins in clathrin-coated vesicles. Alternatively, a large fraction of cargo from the TGN may be transferred to common recycling endosomes (Futter et al., 1995) from where it is sorted into separate routes towards the apical membrane, basolateral membrane or to LEs and lysosomes. The transversal of the endosomal sorting systems by newly synthesized proteins on the way from the TGN to the plasma membrane has first been shown for transferrin and asialglycoprotein receptors (Futter et al., 1995) and later confirmed and extended to polymeric immunoglobulin A (IgA) receptor (Orzech et al., 2000), vesicular stomatitis virus glycoprotein (VSVG) (Ang et al., 2004; Folsch et al., 2003) and E-cadherin (Lock and Stow, 2005). In fact, experiments indicate that over 85% of the biosynthetic transport of some basolateral proteins (e.g. VSVG) occurs through a trans-endosomal route, whereas other basolateral proteins (e.g. TfR) follow a direct route from the TGN to the plasma membrane (Gravotta et al., 2007).

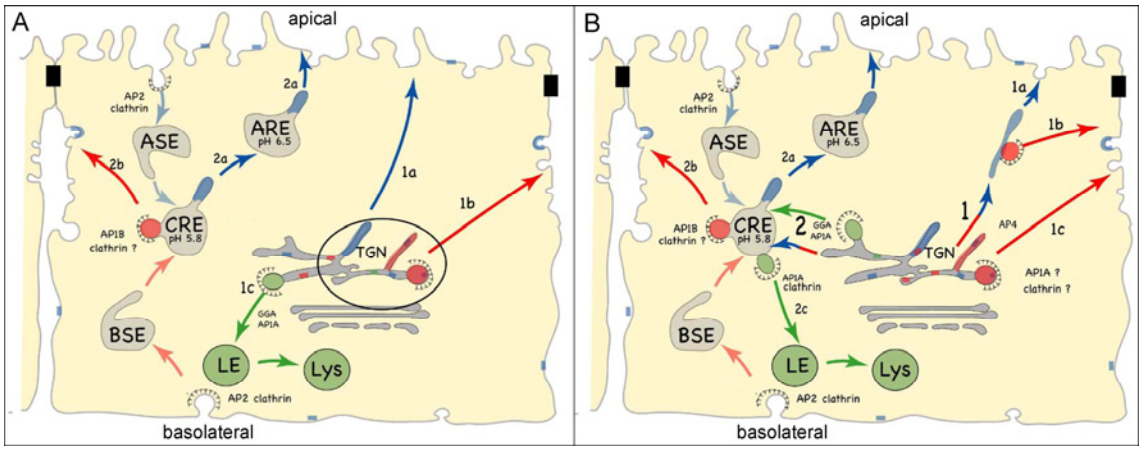

Figure 1-4: Polarized protein sorting in epithelia involves TGN, post-Golgi carriers and endosomes
In the conventional model **(A)** protein sorting in the biosynthetic route occurs only at the TGN where apical and basolateral proteins are incorporated into different post-Golgi transport carriers (routes 1a and 1b). In a third route from the TGN, lysosomal hydrolases are sorted to the LE/ lysosomal compartments (route 1c). The endosomal system serves as sorting station for proteins coming from the two plasma membrane domains, which are internalized into apical and basolateral sorting endosomes (ASE, BSE)

and then mixed in common recycling endosomes (CRE). From there, apical and basolateral proteins are sorted into different recycling routes towards the two plasma membrane domains (routes 2a and 2b).
The alternative model **(B)** proposes that sorting in the biosynthetic route also occurs in tubular structures that leave the Golgi and contain a mixed population of apical and basolateral proteins (route 1). Basolateral cargo is segregated from these structures by clathrin-coated vesicle formation and transported to the basolateral surface (route 1b), whereas the tubules with the enriched apical proteins are targeted to the apical surface (route 1a). Some basolateral sorting vesicles form directly at the TGN (route 1c). The endosomal sorting system is directly connected to the TGN and some apical, basolateral as well as lysosomal proteins are transported from the TGN to REs (route 2). Sorting into separate routes to the apical membrane (2a), basolateral membrane (2b) or to LEs/ lysosomes (2c) occurs at the level of the CRE. The apical sorting route may involve an intermediate stage called apical recycling endosome (ARE). Figures modified from Rodriguez-Boulan and Musch, 2005.

1.4.2 Sorting signals and adaptors

The sorting of apical and basolateral proteins at various stages of intracellular membrane transport is mediated by sorting signals present within cargo molecules. Apical sorting signals include glycosylphosphatidylinositol anchors (Brown et al., 1989; Lisanti et al., 1989), specialized transmembrane domains (Kundu et al., 1996; Scheiffele et al., 1997; Skibbens et al., 1989), N- and O-glycans (Fiedler and Simons, 1995; Yeaman et al., 1997) and determinants present in the cytoplasmic tails of cargo proteins (Rodriguez-Boulan et al., 2005; Tai et al., 1999). These signals mediate apical sorting through interactions with lipid rafts, lectins or cytoplasmic motor proteins (Ellis et al., 2006; Rodriguez-Boulan et al., 2005). Basolateral sorting is mediated by tyrosine-based sorting motifs present for example in low density lipoprotein receptor (LDLR) and VSVG (Matter et al., 1992; Thomas and Roth, 1994), mono- and dileucine based motifs (Deora et al., 2004; Hunziker and Fumey, 1994; Wehrle-Haller and Imhof, 2001) or pleiomorphic sequences for example in polymeric Ig receptor (pIg-R) (Casanova et al., 1991), TfR (Odorizzi and Trowbridge, 1997) and neuronal cell adhesion molecule (N-CAM) (Le Gall et al., 1997). All these signals mediate sorting by interactions with adaptor complexes or alternative adaptors dependent or independent of clathrin (Rodriguez-Boulan et al., 2005).
The recognition of sorting signals by adaptor proteins facilitates the incorporation of cargo into specific carriers. Up to now two basolateral sorting adaptors are known: AP-1B (Ohno et al., 1999) and AP-4 (Simmen et al., 2002). AP-1 exists in two variants: An ubiquitous isoform termed AP-1A, and an epithelial-specific variant termed AP-1B

which differ in their μ1-subunit (μ1A and μ1B respectively). AP-1B is implicated in the sorting of at least some basolateral proteins including Tf and LDL receptors in epithelial cells (Folsch et al., 1999; Gan et al., 2002; Roush et al., 1998) and localizes predominantly to REs of Madin-Darby canine kidney (MDCK) cells, where it functions in both the biosynthetic (VSVG) and recycling (TfR) route. In contrast, the biosynthetic delivery of TfR to the cell surface might be mediated by an AP-1B-independent route directly from the TGN (Gravotta et al., 2007).

1.5 Neuronal polarity and trafficking

One of the most prominent cases of polarized cells is exemplified by neurons (Arimura and Kaibuchi, 2007; Horton and Ehlers, 2003). Neurons exhibit morphologically and physiologically distinct membrane domains, termed the axonal and the somatodendritic compartment. Axons are typically long and thin with an uniform width, whereas dendrites are relatively short and appear thicker as they emerge from the cell body, but become thinner with increased distance. Axons contain synaptic vesicles filled with neurotransmitters that are released at nerve terminals in response to electrical signals from the cell body. Dendrites contain receptors that bind these neurotransmitters thereby receiving the signal from the neighboring neuron. The establishment of the two distinct compartments is fundamental for neuronal function, as they segregate the signal receiving (dendrites) from the signal transmitting (axon) part. Hence, these domains differ with regard to morphology, protein and organelle composition, signaling properties, cytoskeletal organization and physiological functions. Once established, different sets of cell surface proteins within these two domains have to be maintained throughout neuronal life. However, the mechanisms underlying the establishment of neuronal polarity, the maintenance of distinct axonal and somatodendritic domains, and the differential sorting of integral membrane proteins to dendrites and axons were completely unknown until a decade ago.

1.5.1 Development of neuronal polarization

Cultured hippocampal neurons prepared from pre-natal rat embryos have routinely been used to study the establishment of neuronal polarity. The morphological changes that occur during polarization of neurons in such cultures have been described in detail by

Banker and colleagues (Dotti et al., 1988). They can be divided into five stages: In stage 1, shortly after dissociation from embryonic rat brains and attachment to the substrate, hippocampal neurons form several thin filopodia. Already after several hours, a number of immature, morphologically equal neurites, so-called minor processes, are formed from the initial protrusions (stage 2). These neurites undergo repeated rounds of random growth and retraction regulated by a balance between positive and negative signals, thereby keeping their overall length. At stage 3, one neurite breaks the morphological symmetry, starts to extend rapidly and becomes much longer than the other neurites. This extended process finally develops into the axon, all the minor processes maintain their net length while still undergoing spurts of growth and retraction. After a few days, they also elongate and become mature dendrites (stage 4). They are now thicker, but shorter than the axon and begin to establish dendritic components and premature dendritic spines. After maturation, axons and dendrites from synaptic contacts through dendritic spines and axon terminals, and form a neuronal network (stage 5). The early asymmetric neurite outgrowth and axon specification is tightly regulated by a balance of positive and negative signaling activities influencing many cellular functions such as cell adhesion, cytoskeletal rearrangements and polarized protein trafficking (Arimura and Kaibuchi, 2007).

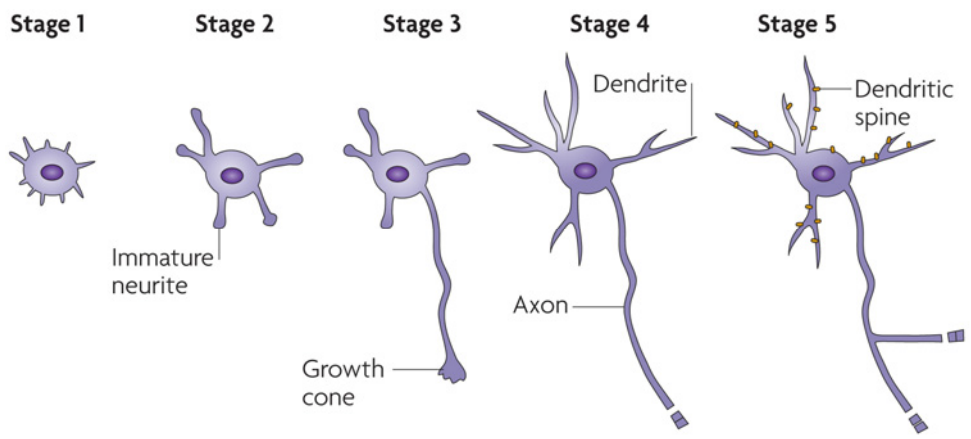

Figure 1-5: Stages of neuronal development and polarization in culture

Schematic representation of the establishment of polarity by hippocampal neurons in culture. The events of neuronal development can be divided into five stages: Shortly after plating of the cells (stage 1), neurons form small protrusions (filopodia). At stage 2, these protrusions develop into several immature neurites. Axons develop first by rapid growth of one of these initially equal immature neurites, thereby establishing the polarity (stage 3). After a few days, dendrites are formed by the remaining neurites (stage 4). Finally, synaptic contacts are formed between axon terminals and dendritic spines and a neuronal network is established (stage 5). Taken from Arimura and Kaibuchi, 2007.

1.5.2 Polarized protein sorting in neurons

Based on sorting in epithelial cells it seems likely that sorting may occur within the secretory (Golgi/ TGN) and endosomal pathways (Craig and Banker, 1994; Winckler and Mellman, 1999). However, it is still under intense investigation whether one pathway dominates over the other in sorting neuronal proteins, whether different mechanisms are required for targeting of axonal versus dendritic proteins and which signals direct protein trafficking in neurons. Different models have been put forward to explain the polarized sorting of proteins to the axonal or somatodendritic compartments (Bradke and Dotti, 2000; Horton and Ehlers, 2003). In the **selective delivery model**, axonal and somatodendritic cargo is segregated at the TGN and/ or REs and packaged into distinct carriers that are selectively targeted to the corresponding membrane domain. This mechanism is, at least in part, responsible for the somatodendritic targeting of TfR, which is excluded from the axonal plasma membrane (Burack et al., 2000). Such exclusive delivery to one of the domains might be aided by the different organization of microtubule polarity. Axonal microtubules are oriented with their plus end towards the periphery as also seen in non-polarized cells, whereas dendrites contain microtubules with mixed polarity (Baas et al., 1988). Thus, exclusive somatodendritic delivery could be achieved by minus end-directed motor proteins. However, according to that model, axonal targeting might be more complex. The compartmental identity of the transport carriers are unknown so far, but, as seen for polarized MDCK cells, might correspond to both TGN-derived tubular carriers as well as REs (Schmidt and Haucke, 2007). The **selective fusion model** postulates that carriers containing axonal cargo initially traffic to both axons and dendrites, but are only capable of fusing with the axonal plasma membrane. This model has originally been proposed for the axonal targeting of neuron-glia cell adhesion molecule (NgCAM)/ L1 (Burack et al., 2000; Sampo et al., 2003), which can be transported into both axons and dendrites. Finally, the **selective retention model** suggests that axonal carriers can fuse with both plasma membrane domains resulting in a transient delivery of axonal proteins to all neurites. As developing neurons mature, selective retrieval of axonal cargo from the somatodendritic membrane via endocytosis generates a non-uniform axonal protein distribution. The formation of a diffusion barrier within the axon initial segment (Winckler et al., 1999), paired with selective retention mechanisms, may finally result in the selective enrichment of axonal proteins in the axon (Kennedy and Ehlers, 2006; Winckler, 2004). This mechanism has been shown to be important for the axonal targeting of the sodium

channel $NA_v1.2$ (Garrido et al., 2001) and the synaptic vesicle SNARE (soluble *N*-ethylmaleimide-sensitive fusion protein-attachment protein receptor) synaptobrevin/ vesicle-associated membrane protein 2 (VAMP2) (Sampo et al., 2003). After endocytic retrieval, cargo could be delivered to the axon through REs by a process called transcytosis. Indeed, endocytosis signals have been shown to be important for axonal targeting of synaptobrevin/ VAMP2, $Na_v1.2$ and NgCAM. However, the latter molecule might reach the axonal membrane via both transcytosis and direct axonal sorting pathways (Wisco et al., 2003). Thus, the endosomal sorting system is used extensively to target proteins to the correct plasma membrane domain.

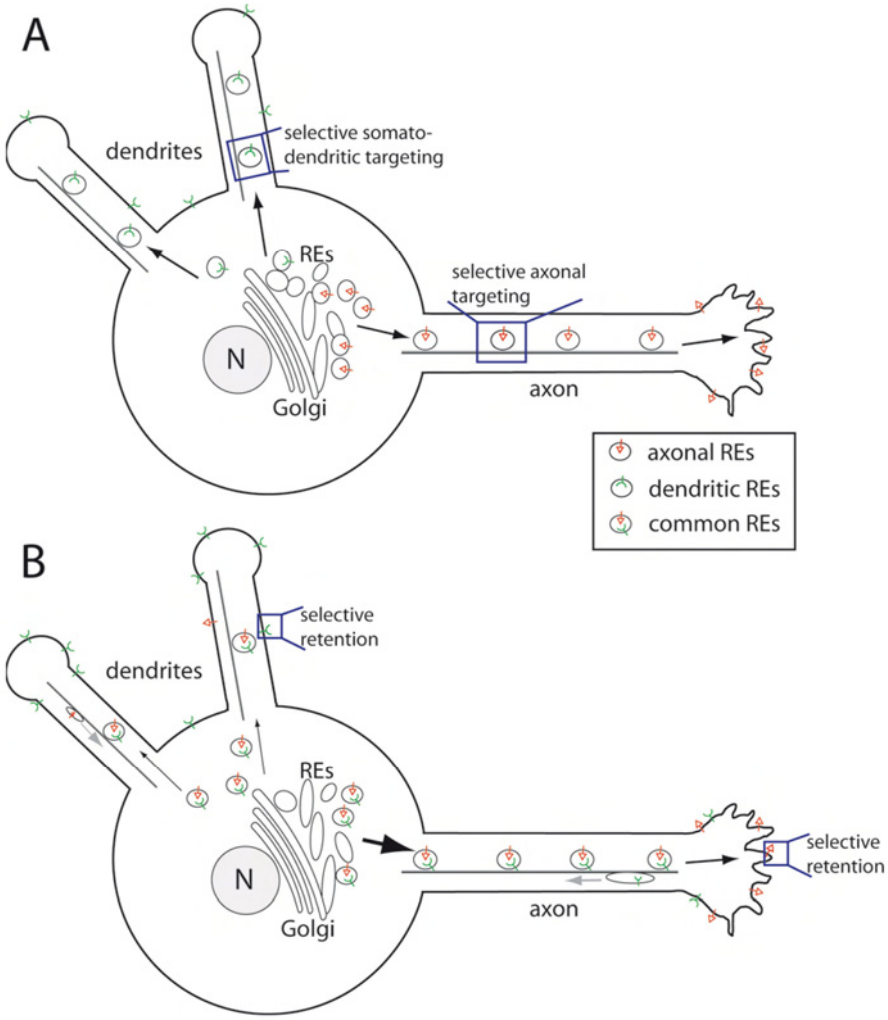

Figure 1-6: Polarized protein sorting in neurons

(A) Selective delivery: Dendritic and axonal proteins are differentially sorted into distinct carriers at the TGN (Golgi) or in REs and selectively transported to the corresponding membrane surface. Differential interactions with motor proteins may contribute to the sorting process. Additionally, certain carriers may only be capable of fusing with either of the two plasma membrane domains (**selective fusion**).

(B) Selective retention: A single population of transport vesicles carrying both axonal and dendritic cargo is generated and transported to axons and dendrites. Different transport rates may favour axonal

over dendritic delivery. Correctly targeted proteins are retained at their site of action, whereas incorrectly targeted proteins are selectively endocytosed from the plasma membrane and transported to the proper surface by transcytosis. This mechanism depends on sorting steps within the endosomal system probably involving REs.
RE, recycling endosomes; N, nucleus; Taken from Schmidt and Haucke, 2007.

1.5.3 Recycling endosomes in neuronal membrane traffic

As mentioned above, differential sorting to axons and dendrites in neurons involves the formation of transport carriers leaving the TGN/ endosomal sorting system. However, the membrane identity of the transported organelles is not really clear. It might be Golgi/ TGN derived, of recycling endosomal origin or most probably a mixture of both. There is evidence that different axonal cargo molecules travel to the axon in distinct carriers originating from the TGN/ recycling endosomal area (Kaether et al., 2000; Zhai et al., 2001), including RE vesicles. For example, NgCAM is found in TfR-positive EEs and REs, from where it is sorted to the axon (Wisco et al., 2003). REs are also involved in the synaptic plasticity-induced delivery of AMPA receptors to dendritic spines, the regions within dendrites where excitatory synapses are formed with axons of communicating neurons (Park et al., 2004). Furthermore, membrane trafficking from REs is required for the activity-dependent growth and maintenance of dendritic spines during long-term potentiation (LTP) of synaptic strength (Park et al., 2006). Thus, REs may be important for receptor up- and down-regulation during activity dependent LTP or long-term depression (LTD) of synaptic transmission and membrane remodeling events during synapse modification.
Based on these and other recent results, REs may play a much more crucial role in neuronal morphogenesis and polarization than previously thought (Schmidt and Haucke, 2007). As already suggested by studies in non-neuronal cells, REs may have a general role in plasmalemmal growth by regulating processes such as membrane trafficking, actin remodeling and membrane delivery to the cleavage furrow during cytokinesis (Riggs et al., 2003; Skop et al., 2001; Wilson et al., 2005). Given that one of the most striking cellular examples of plasmamlemmal membrane growth is the extension of axons and dendrites during neuronal development, one could assume that endosomal membranes, including REs, serve as a main source of membrane addition in developing neurons. Indeed, initial evidence accumulates that points towards a role of REs in neurite extension. First, Golgi-endosomal elements are asymmetrically confined

near the centrosome in early post-mitotic neurons and this determines the position of the future axon as the fastest growing neurite (de Anda et al., 2005). Second, the Rab11-binding protein protrudin regulates Rab11-dependent membrane recycling to promote the directional membrane trafficking required for neurite formation (Shirane and Nakayama, 2006). Third, several components of the recycling endosomal system including the exocyst complex (Vega and Hsu, 2001), the endosomal SNARE syntaxin 13 (Hirling et al., 2000) and the small GTPase Arf6 (Albertinazzi et al., 2003; Hernandez-Deviez et al., 2004) have been shown to localize to growth cones of developing neurites and to regulate plasma membrane shape changes during neuronal morphogenesis. Additionally, tetanus neurotoxin-insensitive VAMP (TI-VAMP), another endosomal SNARE involved in recycling processes in neurons, has been implicated in neurite extension (Alberts et al., 2003). Taken together, recycling endosomal trafficking may operate in parallel to the action of the Golgi apparatus (Horton and Ehlers, 2004) and may accompany additional mechanisms, including local changes in actin dynamics (Bradke and Dotti, 1999), to facilitate neuronal morphogenesis and neurite extension.

1.6 Motor proteins

Motor proteins drive the transport of vesicles and organelles within the cell and thus are the molecular players that facilitate intracellular membrane trafficking events (Caviston and Holzbaur, 2006). All these events depend on the active transport along the cytoskeleton, which is formed by actin filaments, microtubules and intermediate filaments. Transport along such filaments is mediated either by myosin motors (along actin filaments) or kinesin/ dynein motors (along microtubules). Being more relevant for the work presented here, I will focus on the kinesin-driven transport along microtubules.

1.6.1 Microtubule based transport

Microtubules form a dynamic cytoskeleton consisting of polarized filaments with a plus and a minus end. In most cell types, microtubules grow out from the microtubule-organizing center (MTOC) with their plus ends, whereas the minus ends are tethered to the MTOC. There are two major superfamilies of microtubule motor proteins: kinesins and dyneins. Kinesins are a superfamily of proteins with at least 45 members in mammalian cells (Miki et al., 2005). They are grouped in 14 families (named kinesin-1 to -14) based on structure and phylogenetic analysis (Lawrence et al., 2004). All kinesins share a homologous globular motor domain that binds to microtubules and is necessary as well as sufficient to drive the movement along microtubules in an ATP-dependent fashion. In most cases, the motor domain is fused to a neck linker domain that actively participates in force production, a coiled-coil domain that mediates association with other subunits, and a cargo-binding tail domain. The cargo binding tail domains and the accessory subunits of kinesins differ considerably among the different family members (Vale, 2003). This extensive variability allows functional specificity of a certain kinesin family member for the transport of individual cargos.

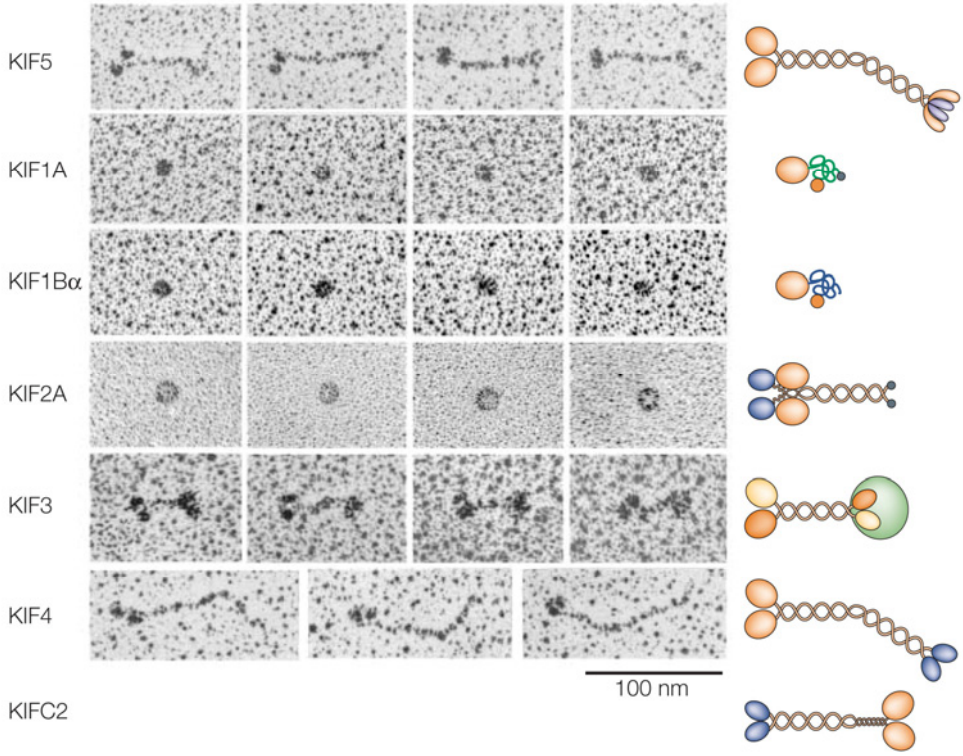

Figure 1-7: Structures of principle members of kinesin superfamily proteins
Different members of the kinesin superfamily proteins (KIFs) were observed by low-angle rotary shadowing (left part) and represented schematically on the basis of electron microscopy or predictions from the analysis of their primary structures (right part). The large orange ovals in each representation indicate the motor domains. KIF5 forms a heterotetramer composed of two heavy and two light chains. KIF1A and KIF1Bα are monomeric and globular. KIF2A is a homodimer with the motor domains in the middle. KIF3 is a heterodimer composed of KIF3A and KIF3B and associates with kinesin superfamily-associated protein 3 (KAP3; green). KIF4 and KIFC2 form homodimers with the motor domains on opposite ends of the molecules. Taken from Hirokawa and Takemura, 2005.

Most kinesin superfamily members, such as kinesin-1, move unidirectionally towards the plus end of microtubules and thus facilitate anterograde transport processes directed towards the cell periphery, for example from the Golgi to the plasma membrane. However, there are also minus end-directed kinesins (for example the kinesin-14 family member KIFC2) that contribute to intracellular trafficking events such as the transport of early endosomes (Bananis et al., 2000). Kinesins are processive motors that mediate long range movements along microtubules before they detach, which leads to a highly efficient transport of cargo. Additionally, relatively few motors are necessary to move cargo effectively (Gross, 2004). This enables a precise regulation of motor activity and rapid changes in the direction of transport.

Cytoplasmic dyneins, the second class of microtubule motor proteins, are implicated in the transport of many different cargos (Pfister et al., 2006). Most dynein-mediated transport processes require an accessory complex called dynactin which functions in cargo binding and motor processivity (Schroer, 2004). Dyneins drive the minus end-directed transport of vesicles and organelles towards the cell center, and are implicated for example in trafficking from the ER to the Golgi complex.

1.6.2 Motor-cargo interactions and their regulation

Initially, it was thought that motor-cargo interactions might simply be mediated by a direct association between a motor protein and a membrane-bound receptor. This simple model has not held up, since many motors seem to interact with their cargo through indirect associations mediated by one or even several adaptors or scaffolding proteins. For example, the kinesin-3 family member KIF13A transports vesicles containing mannose-6-phosphate receptors from the TGN to the plasma membrane (Nakagawa et al., 2000) by direct interaction with the clathrin adaptor complex AP-1 which binds to the cytoplasmic tail of the MPRs and facilitates their packaging into clathrin-coated vesicles (Bonifacino and Traub, 2003; Le Borgne et al., 1993). Thus, AP-1 serves as an adaptor for both the motor and the clathrin coat. Another example for the use of scaffolding proteins is the interaction of the kinesin-2 family member KIF17 with its cargo vesicles containing N-methyl-D-aspartic acid (NMDA) receptors. This interaction is mediated by a tripartite protein complex formed by three adaptor proteins (LIN10, LIN2 and LIN7) (Setou et al., 2000), which serves as a scaffolding complex for NMDA receptors and directly binds to KIF17.

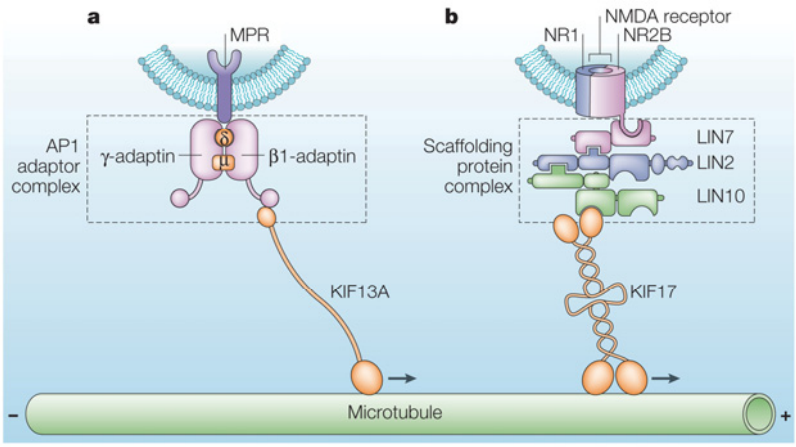

Figure 1-8: Kinesins interact with their cargo through adaptor or scaffolding protein complexes

(a) Mannose-6-phosphate receptor (MPR)-containing vesicles are connected to KIF13A by the adaptor complex AP-1. AP-1 binds sorting signals present in the cytoplasmic tail of MPRs. The β1-adaptin ear domain binds to the carboxy-terminal tail of KIF13A.

(b) The carboxy-terminal tail of KIF17 binds to LIN10 which forms a tripartite scaffolding protein complex together with LIN2 and LIN7. The latter binds to the NR2B subunit of NMDA receptors.

Taken from Hirokawa and Takemura, 2005.

Rab proteins have been identified as potent regulators of motor protein recruitment to organelles (Deneka et al., 2003). They can actively recruit molecular motors and therefore regulate transport between donor and acceptor compartments. This role of Rab proteins has first been identified in studies on myosin-V, an actin-based motor protein which is specifically recruited to melanosomes by the adaptor melanophilin and activated Rab27a (Seabra and Coudrier, 2004). Rab5 has been shown to facilitate the recruitment of the kinesin-3 family member KIF16B to endosomes (Hoepfner et al., 2005), but this mechanism is indirect. Instead of binding directly to Rab5, KIF16B is recruited to the membrane by binding phosphatidylinositol-3-phosphate [PI(3)P] through a PhoX homology (PX) domain present in its tail region. The generation of PI(3)P is driven by the localized stimulation of PI-3-kinase by activated Rab5. Other examples of Rab mediated regulation of motor protein activity involves the recruitment of dynein/ dynactin to the TGN by Rab6 (Short et al., 2002), myosin-Vb recruitment to REs by Rab11 (Hales et al., 2002), the Rab4 and Rab5 mediated co-ordination of kinesin and dynein association with early endosomes (Bielli et al., 2001; Nielsen et al., 1999) and the recruitment of dynein to late endosomes by Rab7 and its effector RILP (Rab7-interacting lysosomal protein) (Jordens et al., 2001). Since each Rab protein

localizes to a specific intracellular compartment and may recruit a certain type of motor protein to the membrane, a precise spatial regulation of transport processes becomes possible. Additionally, a temporal regulation of such recruiting events is provided by Rab proteins, as binding to effector molecules is governed by the cycling between GTP- and GDP-bound states (Zerial and McBride, 2001). There are also other regulators of adaptor/ scaffolding protein mediated motor-cargo interactions including other small GTPases, as for example the Rho-like GTPase Miro (Glater et al., 2006; Guo et al., 2005). Furthermore, certain signal transduction pathways, such as mitogen activated protein (MAP) kinase cascades have been shown to be involved in such regulatory events. For example, Jun N-terminal kinase (JNK)-binding scaffolding proteins (JIPs) interact with kinesin-1 and might regulate kinesin-dependent transport (Verhey et al., 2001).

1.6.3 The kinesin-1 protein family

The kinesin-1 protein family includes the first member of the kinesin superfamily, also called conventional kinesin, which was identified to generate microtubule-based motility (Vale et al., 1985). Conventional kinesins form heterotetramers composed of two heavy (KHC) and two light chains (KLC). Up to now, the family contains three mammalian heavy chain members, KIF5A, KIF5B and KIF5C. KIF5B is expressed ubiquitously, whereas KIF5A and KIF5C are neuron specific (Kanai et al., 2000). There are also three light chain genes known (Junco et al., 2001; Rahman et al., 1998) which undergo alternative splicing (Cyr et al., 1991). Thus, the association of the different heavy and light chains in various permutations potentially creates a variety of different motors.

The KIF5 heavy chains are composed of an amino-terminal motor domain, a neck domain, a long coiled-coil stalk, and a globular tail domain (Hirokawa et al., 1989). At the end of the stalk domain, two kinesin light chains are associated to form fan like ends (Diefenbach et al., 1998). Kinesin light chains contain several tetratricopeptide repeat (TPR) motifs that have been reported to interact with cargo or adaptor/ scaffolding proteins, e.g. JIPs or APP (amyloid precursor protein). Conventional kinesins have been reported to bind numerous membrane cargos including mitochondria (Tanaka et al., 1998), lysosomes (Nakata and Hirokawa, 1995), endoplasmic reticulum, certain neuronal transport vesicles for transport along axons and dendrites (Hirokawa and Takemura, 2005) as well as nonmembranous cargo such as mRNA granules (Kanai et

al., 2004), tubulin oligomers (Terada et al., 2000) and intermediate filaments (Prahlad et al., 1998). The interaction with cargo molecules can be mediated by either the heavy chain tails or the associated light chains. In neurons, binding to KLC tends to be used for axonal transport (Kamal et al., 2000), whereas binding to KIF5 tail is used for directing cargo to dendrites (Setou et al., 2002).

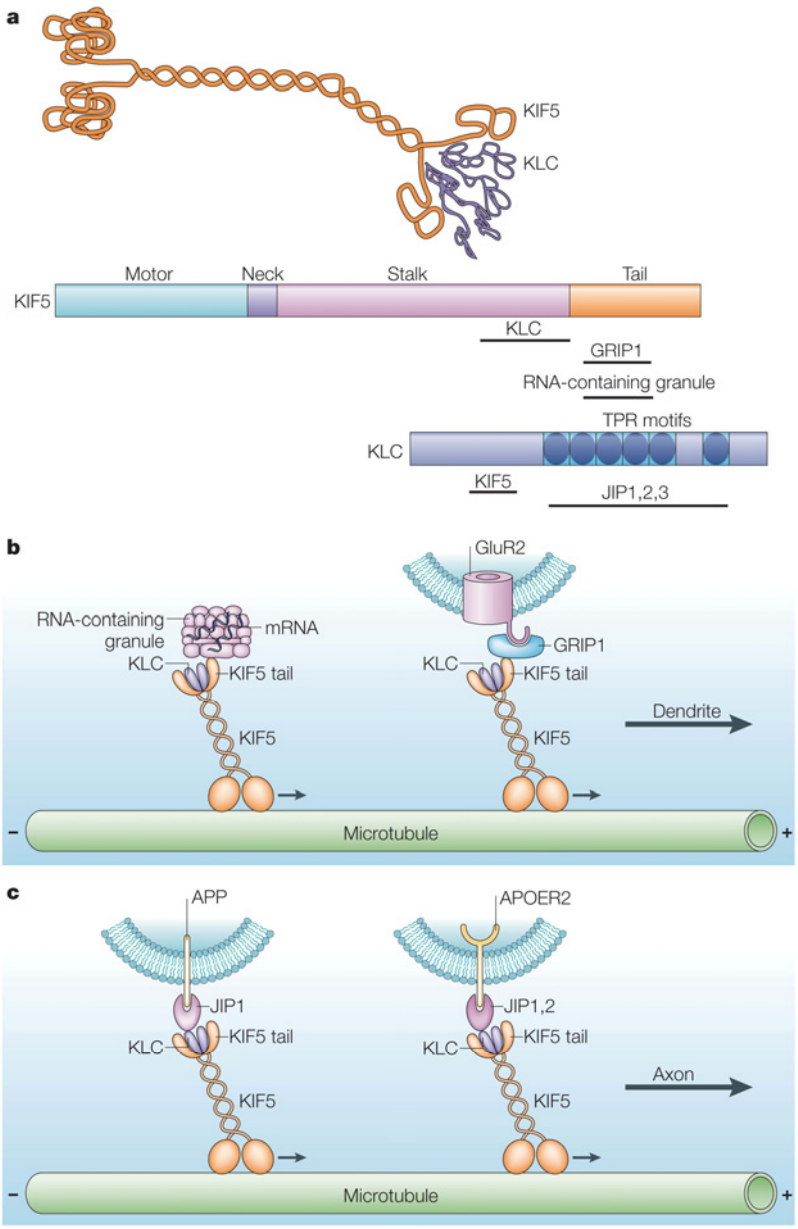

Figure 1-9: Kinesin superfamily protein 5 (KIF5) structure and selective transport mechanisms

(a) Schematic model of the kinesin heavy chain (KIF5) and light chain (KLC) structure and their association. Two heavy and two light chains form a heterotetramer. KIF5 is composed of a globular motor domain at the amino-terminus, a central neck and stalk domain and a carboxy-terminal tail. KLC associates with the carboxy-terminal end of the stalk region of KIF5 and contains tetratricopeptide repeat (TPR) motifs that mediate binding to cargo adaptor or scaffolding proteins.

(b) The carboxy-terminal tail of KIF5 binds cargo or adaptor proteins, like RNA-containing granules or GRIP1 (glutamate receptor interacting protein) associated with AMPA-receptor subunits (GluR2) containing vesicles and facilitate their transport to dendrites in neurons.
(c) Alternatively, the TPR motifs of KLC bind cargo adaptors, like JIPs, and transport APP (amyloid precursor protein) or APOER2 (apolipoprotein E receptor 2)-containing vesicles to axons.
Taken from Hirokawa and Takemura, 2005.

1.7 γ-BAR, an AP-1 interacting protein involved in post-Golgi trafficking

γ-BAR represents a recently identified Golgi associated, peripheral membrane protein that specifically interacts with the ear domain of the γ-adaptin subunit of the AP-1 adaptor complex (Neubrand et al., 2005) and thus constitute a member of the AP-1 associated family of accessory proteins. Its initial identification was based on a visual screen employing GFP-tagged full length cDNAs (Liebel et al., 2003; Wiemann et al., 2001) in order to find novel proteins that are associated with the late secretory pathway and thus potentially regulate post-Golgi membrane trafficking (Simpson et al., 2000). Several proteins that localize to the Golgi apparatus have been selected for further analysis, one of them being the cDNA clone DKFZp564C182 abbreviated '2c18', later named γ-BAR. When expressed as a carboxy-terminally tagged eGFP fusion protein in Vero cells, γ-BAR localizes to the juxta-nuclear Golgi region as well as to smaller discrete structures throughout the cytoplasm. Time-lapse microscopy studies revealed that these vesicular and tubular structures are highly mobile and cycle between the Golgi and the cell periphery, sometimes reaching the plasma membrane. Endogenous γ-BAR co-localizes in part with late Golgi markers (e.g. TGN46) and AP-1, but no overlap was observed with ERGIC53, a membrane protein that cycles between the ER and the cis-Golgi region or the cis-Golgi marker GM130. Furthermore, in immunogold electron microscopic studies, γ-BAR was found in close proximity to the TGN and post-Golgi membranes including membrane structures with early and late endosomal character as well as at the plasma membrane.
Sequence analysis of the cDNA encoding γ-BAR identified a protein of 302 amino acids with a molecular weight of 34.2 kDa and an isoelectric point (pI) of 4.6. Sequence alignments and BLAST searches did not reveal any significant homologies to other known proteins or domains.

In yeast two-hybrid screens using γ-BAR (aa 1-151) as a bait and a human fetal brain library as prey, γ-adaptin was found to interact directly with γ-BAR (Neubrand et al., 2005). However, no interacting clones could be found that corresponded to the subunits of other adaptor complexes such as AP-2, AP-3, AP-4 and GGAs or to components of COPI and COPII complexes. Further characterization of this interaction using direct binding assays indicated that the binding of γ-adaptin to γ-BAR occurs via its ear domain. Furthermore, both endogenous and overexpressed γ-BAR are able to co-immunoprecipitate γ-adaptin from HeLa cell extracts, but not α-adaptin (AP-2), δ-adaptin (AP-3) or GGA3. Altogether, these results suggest a direct and specific interaction of γ-BAR with AP-1.

Characterization on the functional level revealed that the intracellular levels of γ-BAR are critical for membrane association of AP-1. Overexpression of γ-BAR was found to enhance the association of AP-1 with membranes. Conversely, siRNA-mediated depletion of γ-BAR has been reported to decrease the level of AP-1 on membranes. Vice versa, in cells lacking functional AP-1 complexes by genetic deletion of μ1A (Meyer et al., 2000) or by treatment with siRNAs, endogenous γ-BAR seems no longer associated with Golgi or endosomal membranes and is instead spread diffusely throughout the cytoplasm. Furthermore, γ-BAR is not only required for the proper membrane localization of AP-1, but is also necessary for normal AP-1-dependent transport between the TGN and endosomes. Changes in the intracellular level of γ-BAR affect trafficking between the TGN and endosomes as seen by a dramatic change in the distribution of MPRs in cells overexpressing γ-BAR-eGFP. In line with that, elevated levels of γ-BAR cause missorting of MPR cargo such as the lysosomal enzyme cathepsin D.

When treating cells with brefeldin A (BFA), a drug that specifically inhibits the activation of the Golgi-localized small GTPase Arf1, thereby reversibly blocking membrane traffic at the Golgi (Donaldson et al., 1992; Klausner et al., 1992; Zeghouf et al., 2005), both AP-1 and the COPI coat complex rapidly dissociate from membranes (Robinson and Kreis, 1992). However, when overexpressing γ-BAR in Vero cells and treating these cells with BFA, AP-1, but not COPI, is largely retained at a juxta-nuclear location that persisted treatment much longer than in non-transfected cells. Thus, the protein has been named γ-BAR, for γ-adaptin brefeldin A resistance (Neubrand et al., 2005).

Initial studies in neurons done by Carlos Dotti and colleagues revealed that endogenous γ-BAR shows a peri-nuclear accumulation similar to that in HeLa and Vero cells. Occasionally, γ-BAR was found to localize to axonal vesicle clusters and also shows axonal localization when overexpressed in hippocampal neurons. Further studies revealed that overexpression of γ-BAR leads to re-routing of transferrin receptor to the axon where it co-localizes with overexpressed γ-BAR as well as endogenous AP-1 in vesicle clusters along the axon and to growth cones.

1.8 Aims of the studies

The focus of this work was to dissect the functions of the protein γ-BAR in membrane trafficking events in non-neuronal cells as well as primary neurons. To analyze its function in endomembrane traffic, we aimed at the identification of additional γ-BAR-interacting partners followed by the dissection of these interactions and their functional relevance using biochemical as well as cell biological approaches. In addition, we aimed at elucidating the precise molecular mechanism by which γ-BAR associates with membranes and whether this depends on its interaction with AP-1.

2 Materials and Methods

2.1 Materials

2.1.1 Chemicals and Disposables

Chemicals were purchased from GE Healthcare, Invitrogen, Merck, Pierce, Roth, Serva and Sigma. Disposables were obtained from Amersham, Greiner, Millipore, Sarstedt, Schott and Whatman.

2.1.2 Enzymes

Enzymes were purchased from the following companies:

New England Biolabs (NEB): Restriction enzymes, T4 DNA polymerase, VENT polymerase, Alkaline phosphatase, calf intestinal (CIP), Klenow fragment

Roche: T4 DNA ligase

Genaxxon: Taq polymerase

2.1.3 Molecular Biology Kits

Promega : Wizard Plus SV miniprep kit

Qiagen : Plasmid midi prep kit (standard and endotoxin free)

PeqLab: E.Z.N.A. Cycle pure and gel extraction kits

2.1.4 Synthetic oligonucleotides

Custom designed synthetic DNA and siRNA oligonucleotides were purchased from MWG Biotech. A list of primers can be found in the appendix. We used the following siRNAs for the knockdown of certain genes in mammalian cells by RNA interference (RNAi):

Name	Sequence	Target gene
γ-BAR 27mer #2	CGA AGU AGU AGA CUC UCA UCA GAU GCU	human γ-BAR
rat γ-BAR#1	GUA GUA GAC UCU CAU CUG ATT	rat γ-BAR
rat γ-BAR#3	AUC GUU GAC UUA CAA GAG ATT	rat γ-BAR, human control
scrambled	GCU GAU ACG CUA UAC UGA UTT	rat control

For the knockdown of human KIF5B in HeLa cells, pre-designed and validated siRNAs were purchased from Qiagen (GeneSolution siRNA, Cat. No. 1027416), on which no sequence information is available.

2.1.5 Markers and loading dyes

DNA markers were purchased from Fermentas (λ-DNA/ EcoRI+HindIII marker, GeneRuler 1kb DNA ladder, GeneRuler 50bp DNA ladder) and Genaxxon (100 bp + 1.5 kb ladder). Protein markers were purchased from NEB (broad range protein marker, pre-stained broad range protein marker) or self-made. 6x DNA loading dye solution was purchased from Fermentas or self made (0.05% bromphenol blue, 0.05% xylene cyanol, 30% glycerol in ddH_2O). 6x sample buffer for SDS-PAGE was prepared in a total volume of 50 ml containing 375 mM Tris, 60% (v/v) glycerin, 30% (v/v) β-mercaptoethanol, 18% (w/v) SDS and a "tip of a spatula" bromphenol blue (no water added).

2.1.6 Antibodies

2.1.6.1 Primary antibodies

The following primary antibodies were used for immunoblotting (IB), immunofluorescence (IF) and immunoprecipitation (IP):

Mouse monoclonal antibodies

AP-1 (γ-adaptin)	clone 88	BD Biosciences	IB 1:2000, IF 1:100
AP-2 (α-adaptin)	clone AP6	purified (hybridoma)	IF 1:100 (4 mg/ml stock)
β-actin	clone AC-15	Sigma	IB 1:10,000
BERP	clone 27	BD Biosciences	IB 1:250
clathrin HC	clone TD-1	P. de Camilli	IB 1:10 (tissue culture sup)
clathrin HC	clone X22	Affinity Bioreagents	IF 1:500
clathrin LC	clone 57.1	Synaptic Systems	IB 1:400
Cytochrome C	clone 6H2.B4	BD Biosciences	IF 1:100
EEA1	clone 14	BD Biosciences	IF 1:100
FLAG-tag	clone M2	Sigma	IB 1:2000, IF 1:1000, IP
GAPDH	clone 71.1	Sigma	IB 1:1,000,000
GFP	clone 1E4	Stressgen	IB 1:1000

GM130	clone 35	BD Biosciences	IF 1:100
HA-tag	clone HA.11	Babco (Covance)	IB 1:1000, IF 1:1000, IP
His_6-tag		Novagen	IB 1:1000
kinesin HC	clone H2	Chemicon	IB 1:500, IF 1:200
LAMP1	clone H4A3	S. Höning	IF 1:250
MPR46	clone 10C6	S. Höning	IF 1:400
myc-tag	clone 9E10	Sigma	IF 1:200
p21-Arc/ ARPC3	clone 24A6	Synaptic Systems	IB 1:1000
synapsin I	clone 46.1	Synaptic Systems	IB: 1:5000
transferrin receptor	clone H68.4	Zymed Laboratories	IB 1:200, IF 1:100

Rabbit polyclonal antibodies

γ-BAR	#11	this study, purified	IF 1:100, IP
γ-BAR	#13	this study, purified	IB 1:500
HA-tag	Y11	Santa Cruz	IB 1:500
Klc2		Xiao-Jiang Li	IB 1:1000
p34-Arc/ ARPC2		Upstate	IB 1:1000
Rab11		Zymed Laboratories	IF 1:25
TGN46 (sheep polyclonal)		Serotec	IF 1:1000

2.1.6.2 Secondary antibodies

Secondary antibodies for immunoblotting, conjugated with horseradish peroxidase (HRP) or alkaline phosphatase (AP), were purchased from Dianova. For immuno-fluorescence, we used Alexa Fluor (488, 568, 594 and 647) labeled secondary antibodies from Molecular Probes.

2.1.7 Bacterial strains

Strain	Description	Source
E. coli TOP 10	strain for high-efficiency cloning and plasmid propagation, allows blue/white colour screening	Invitrogen
E. coli BL 21 – CodonPlus™	strain for efficient high-level expression of heterologous proteins in *E. coli*, contains extra copies of tRNA genes that most frequently limit translation	Stratagene

2.1.8 Plasmids

Plasmid	Description	Source
pGex 4T-1	prokaryotic expression vector to produce N-terminal GST-tagged fusion proteins, ampicillin resistance	Amersham - Pharmacia
pET-28a(+)	prokaryotic expression vector to produce N-terminal His-tagged fusion proteins, kanamycin resistance	Novagen
pEGFP-N1, 2, 3	eukaryotic expression vector for production of C-terminal eGFP-tagged fusion proteins, CMV promoter, pUC origin of replication for propagation in *E.coli*, SV40 origin for replication in mammalian cells, kanamycin resistance, neomycin resistance	BD Biosciences Clontech
pcDNA3	eukaryotic expression vector (no tag), CMV promoter, T7 promoter, ampicillin resistance, neomycin resistance	Invitrogen
pcHA2	modified eukaryotic expression vector based on pcDNA3, N-terminal HA-tag, ampicillin resistance, neomycin resistance	Yasuo Nemoto (Yale University, USA)
pcFLAG	modified eukaryotic expression vector based on pcDNA3, N-terminal FLAG-tag, ampicillin resistance, neomycin resistance	Yasuo Nemoto (Yale University, USA)
pcMYC	modified eukaryotic expression vector based on pcDNA3, N-terminal MYC-tag, ampicillin resistance, neomycin resistance	custom made

2.1.9 Mammalian cell lines

Cos7: African green monkey kidney cells (fibroblasts)

HeLa: Human cervix carcinoma cells (epithelial-like cells)

HEK293: Human embryonal kidney cells (fibroblasts)

NIH-3T3: Swiss mouse embryo (fibroblasts)

PC12: Rat adrenal pheochromocytoma

2.1.10 Media, Buffers and Solutions

Ampicillin stock: 50 mg/ml in ddH_2O sterile filtered

Chloramphenicol stock: 34 mg/ml in ethanol sterile filtered

Gentamicin stock: 15 mg/ml in ddH_2O sterile filtered

Kanamycin stock: 10 mg/ml in ddH_2O sterile filtered

LB medium: 1% (w/v) yeast extract
0.5% (w/v) trypton
0.5% (w/v) NaCl

2xYT medium:	1.6% (w/v) trypton 1% (w/v) yeast extract 0.5% (w/v) NaCl pH 7.4
5x TE buffer:	50 mM Tris pH 8.0 5 mM EDTA pH 8.0
10x TBE (for 1l):	108 g Tris base 55 g borate acid 7.4 g EDTA
4x SDS-PAGE separating gel buffer:	0.4% SDS 1.5 M Tris pH 8.8
4x SDS-PAGE stacking gel buffer:	0.4% SDS 0.5 M Tris pH 6.8
10x SDS running buffer:	246 mM Tris 1.92 M Glycin 10% SDS
Coomassie stain (1l):	1 g Coomassie G250 100 ml Acetic acid 250 ml Methanol
Coomassie destain (1l):	100 ml Acetic acid 250 ml Methanol
10x TBS:	200 mM Tris 1.4 M NaCl pH 7.6
TSM:	100 mM Tris 100 mM NaCl 5 mM $MgCl_2$ pH 9.5
2x Bradford reagent:	70 mg CoomassieG250 100 ml 85% H_3PO_4 50 ml Ethanol in 500 ml, filtered
10x PBS:	1.37 M NaCl 27 mM KCl 43 mM Na_2HPO_4 14 mm NaH_2PO_4 pH 7.4
high-salt PBS (for IF):	20 mM Na_3PO_4 0.5 M NaCl (0.3% Triton-X 100

2.2 Molecular Biology Methods

2.2.1 Polymerase chain reaction (PCR)

PCR was performed for the amplification of DNA fragments from existing plasmids for subsequent cloning, for PCR-based site directed mutagenesis (overlap extension PCR) and for screening of *E. coli* colonies after transformation with newly generated plasmid constructs (colony PCR). A standard PCR was performed in a final volume of 50 µl containing template DNA (100 ng-1 µg), reaction buffer, 200 µM of each dNTP, 1 µM of each primer and 1 U of Vent-polymerase (NEB). For colony PCRs, Taq polymerase was used (0.25 U per reaction).

For a standard PCR, the following programme was run in a T3 Thermocycler (Biometra):

2’	94°C		initial denaturation
30’’	94°C	|	denaturation
30’’	55°C	| → 20-30 cycles	annealing
30-90’’	72°C	|	elongation
5’	72°C		final elongation

The time for the synthesis step (72°C) in each cycle depends on the length of the PCR product. As a rule of thumb, the DNA polymerase synthesizes 1000 bp in one minute.

2.2.2 Analytical and preparative agarose gel electrophoresis

Agarose gels were prepared in a concentration of 0.7, 1, 1.5 or 2% agarose (w/v) in 1x TBE buffer. DNA solutions were mixed with the appropriate volume of 6x loading dye prior to loading onto the gel. Electrophoresis was performed in 1x TBE buffer at 90 to 100 V and the DNA was stained in an ethidium bromide (EtBr) containing water bath. The stained DNA was visualised by illumination of the gel with UV light.

2.2.3 Isolation and purification of DNA fragments from agarose gels

After preparative gel electrophoresis, the DNA band of the desired size was cut out of the gel. DNA fragments were isolated from the gel slice using the E.Z.N.A. Gel extraction kit (PeqLab) following the manufacturer’s instructions. Elutions were done in 30 µl of ddH_2O.

2.2.4 Analytical and preparative DNA restriction digest

We used restriction enzymes and recommended buffers form NEB. Varying DNA amounts ranging from 500 ng - 1 µg (analytical scale) up to 5 µg (preparative scale) of plasmid DNA or isolated PCR products were added to NEBuffer (10x stock), BSA (100x stock), 10 to 50 U of restriction enzymes (approx. 10 U per 1 µg of DNA) and

adjusted with ddH_2O to a final volume of 10 to 50 µl. The reaction mixtures were incubated at 37°C for 2 to 6 hours.

2.2.5 Vector DNA dephosphorylation

Linearized plasmid DNA was 5'-dephosphorylated prior to ligation in order to prevent re-ligation of the vector backbone. We used 0.5 units alkaline phosphatase (NEB) for 1 µg of vector DNA in any NEB buffer and incubated for 60 min at 37°C. Afterwards, the DNA was purified using the E.Z.N.A. Cycle Pure kit (PeqLab).

2.2.6 Oligonucleotide annealing and phosphorylation

For the generation of small inserts (less than 50 bp) to be ligated into a vector backbone, we purchased oligonucleotides (MWG Biotech) corresponding to the forward and reverse complement DNA sequence of the desired insert. Oligos had to be annealed and phosphorylated prior to ligation. For annealing, 5 µl of 10x annealing buffer (100 mM Tris pH 7.4, 1 M NaCl), 20 µl of each oligo (100 µM stock) and 5 µl ddH_2O were mixed and heated up to 95°C for 5 min. The temperature was gradually reduced in 5°C steps (each step 5 min) until 2°C above the T_M of the oligos. Then, the temperature was reduced in 1°C steps down to 2°C below the T_M (each step 10 min) and further reduced in 5°C steps (5 min) down to room temperature.

For the phosphorylation of the annealed oligos, we used T4 polynucleotide kinase (PNK) from NEB. A typical reaction mix consists of 2 µl annealed oligos, 0.3 µl of 100 µM ATP, 1 µl PNK, 2 µl 10x PNK buffer and 14.7 µl ddH_2O. The reaction was incubated for 30 min at 37°C and the PNK was heat inactivated for 20 min at 65°C. 180 µl ddH_2O were added after the incubation (1:10 dilution) and 2µl of the phosphorylated duplex was used for the ligation reaction using 50-100 ng of digested and dephosphorylated vector DNA.

2.2.7 Ligation of DNA fragments into linearized vectors

Prior to ligation, both insert and vector DNA had to be digested with the corresponding restriction enzymes and the vector DNA was dephosphorylated.

For ligation, the vector and insert DNA were combined in a 1:3 molar ratio, reaction buffer and 1 U T4-DNA ligase (Roche) were added and adjusted to a final volume of 20

µl with sterile ddH_2O. Samples were incubated at 16-20°C for 1 to 3 hours or at 12°C overnight. Then, the ligation mix was used for transformation of chemically competent *E. coli* TOP10 cells.

2.2.8 Preparation of chemically competent *E. coli* cells

50 ml of LB medium were inoculated with *E. coli* TOP10 or BL21 cells and grown at 37°C until the OD_{600} was at about 0.4 (2 x 10^8 cells/ml). The cells were harvested by centrifugation for 10 min at 2500x g and 4°C, the medium was removed and the cells were resuspended in 10 ml of 0.1 M $CaCl_2$ solution. Then, the cell suspension was incubated on ice for at least 15 to 30 min up to 3 hours, centrifuged (10 min, 2500x g, 4°C) and resuspended in 2 ml of 0.1 M $CaCl_2$ solution. 100 µl of the cell suspension was either used immediately for one transformation reaction or 50% glycerol solution was added to a final concentration of 10%. Aliquots of 100 µl were frozen in liquid nitrogen and stored at -80°C until use.

2.2.9 Transformation of chemically competent *E. coli* cells

100 µl aliquots of competent *E. coli* cells (TOP10 or BL21) were thawed on ice and mixed with either 10 µl of a ligation reaction mix or 10 to 100 ng of purified vector DNA. After incubation for 30 min on ice, cells were incubated at 42°C for 90 sec (heat shock) and chilled on ice. Afterwards, 900 µl of LB medium were added and cells were incubated for 45 to 60 min at 37°C while shaking. After recovery, cells were plated on LB-agar plates containing the appropriate antibiotic for selection. Plates were incubated at 37°C overnight.

2.2.10 Colony PCR to screen for positive clones

Colonies that had grown on LB-plates had to be checked for integration of the correct insert using the colony PCR technique. For this purpose, PCR reactions were set up containing some cell material from a single colony and a set of primers that are specific for the flanking vector regions upstream and downstream of the insert. In the first denaturation step of the PCR, the cells get disrupted and the plasmid DNA is set free. Then, the region between the two primers is amplified and should correspond to the desired insert size plus the flanking vector regions.

Single clones were picked from a plate with a sterile pipette tip, some material was transferred to a PCR tube, some to a new LB-agar plate (to have the picked clone on a plate for further usage). For the PCR, a master mix was prepared containing reaction buffer, 2.5 mM $MgCl_2$ 0.2 mM of each dNTP, 25 pmol of each primer and 0.25 U of *Taq* DNA polymerase (Genaxxon) per reaction and filled up with ddH_2O to 25 µl per reaction. 25 µl of the master mix were added to each of the PCR tubes. For the PCR, a standard programme was run in a thermocycler as described above. Afterwards, the PCR reactions were analyzed by agarose gel electrophoresis.

2.2.11 Overnight cultivation of *E. coli* cells

Single clones from LB-agar plates or some material from frozen glycerol stocks were transferred into LB-medium supplemented with the appropriate antibiotics using a sterile pipette tip. Liquid cultures were grown overnight at 37°C and shaken at 200 rpm.

2.2.12 Plasmid DNA isolation from *E. coli* cultures for mini-screens

1.5 ml of *E. coli* overnight cultures were transferred to an 1.5 ml tube, pelleted (13.000 rpm, 1 min) and resuspended in 100 µl of 5xTE buffer pH 8 + P1-buffer (contains RNase). Then 200 µl of 0.2 M NaOH + 1% SDS were added and mixed by inverting the tube several times (cell lysis). For stopping the cell lysis, 150 µl of 3 M K-acetate pH 4.8 were added and mixed (invert tube). The mixture was centrifuged for 10 min at 13.000 rpm and the supernatant was transferred to a new 1.5 ml tube. For DNA precipitation 800 µl of -20°C cold isopropanol were added and centrifuged for 10 to 20 min at 14.000 rpm and 4°C. The supernatant was removed completely, the pellet was washed with 500 µl of 70% ethanol and centrifuged again for 10 min. Supernatant was removed again, the pellet was dried at 50°C and resuspended in 30 µl of ddH_2O. 3 µl of this DNA solution was used for restriction digest in a final volume of 10 µl and analyzed in an agarose gel to screen for positive clones.

2.2.13 Plasmid DNA preparation (mini prep and midi prep)

Mini preparations of plasmid DNA from 10 ml of *E. coli* overnight cultures were performed using the *Wizard Plus* DNA mini preparation kit (Promega) following the manufacture's instructions. For the preparation of larger DNA amounts with higher

quality (e.g. for transfection of mammalian cells) from 100-150 ml of *E. coli* overnight cultures we used the QIAGEN Plasmid Midi Kit with a Qiagen-tip 100 following the manufacture's instructions. For DNA used in transfections of primary neuron cultures, the endotoxin-free version of the kit was used.

2.2.14 Spectrophotometric determination of DNA concentration

DNA solutions were diluted 1:100 in a final volume of 100 µl with dH_2O. The absorption at λ = 260 nm was measured in a special plastic cuvette using an Eppendorf Biophotometer. The DNA concentration was calculated using the following formula:

$c = A_{260}$ x dilution factor x 50 ng/µl 1 OD_{260} = 50 ng/µl

2.2.15 DNA sequencing

Sequencing of plasmid DNA was performed by MWG Biotech. For that, 1-2 µg of purified plasmid DNA (mini-prep) were air dried at 60°C.

For sequence analysis we used the DNASTAR software package and the NCBI Blast tools (Align two sequences) available under http://www.ncbi.nlm.nih.gov/BLAST/.

2.3 Protein Biochemical Methods

2.3.1 Overexpression of recombinant proteins in *E. coli*

Overnight cultures of *E. coli* expression strains (BL21) that carry an expression vector were usually diluted 1:20 in 2xYT-medium containing the appropriate antibiotic and grown to an OD_{600} of 0.7 to 0.8. Protein expression was induced by adding a final concentration of 0.5 mM IPTG. Usually, protein expression cultures were grown for 3 hours at 30°C. However, in order to increase the solubility of the produced proteins, the expression temperature was sometimes lowered to 25°C or the expression time was shortened. Alternatively, expression was performed at 15°C overnight. After expression of the proteins, the bacteria were harvested by centrifugation at 4000x g for 15 min, the medium was removed and the cell pellets were frozen at -80°C.

Small aliquot of the cultures were taken before induction with IPTG and after expression of the protein in order to determine the cell densities (OD_{600}) and for SDS-PAGE analysis of the protein extracts.

2.3.2 Purification of recombinant GST and His_6-fusion proteins

2.3.2.1 Batch technique

Frozen cell pellets from bacterial expression cultures were resuspended in ice cold 1x PBS (usually 10 ml for a pellet from a 250 ml expression culture). 1 mM PMSF, 100 units of Benzonase endonuclease (Sigma) and a "tip of a spatula" lysozyme were added. For the purification of His_6-tagged proteins, NaCl was added to a final concentration of 200-500 mM. The mixture was incubated on ice for 10 min and sonicated for 90 sec with 60% power and 50% duty cycle to break up the cells. If necessary, detergent (1% Triton X-100 or 2% Chaps) was added. After incubation on ice (10 min), the mixture was transferred to centrifugation tubes and centrifuged for 20 to 30 min at 40,000x g and 4°C. The supernatant was recovered and incubated with the appropriate pre-washed binding resin. We used GST-bind resin from Novagen for GST fusion proteins or Ni-NTA Agarose from Qiagen or Sigma for His_6-tagged proteins. We usually used 250 µl of a 50% slurry for the supernatant from a 250 ml expression culture. For His_6-tagged proteins, 10 mM imidazole was added to the supernatant prior to mixing with the beads. The mixture was incubated for 1-2 hours at 4°C under end over end rotation to allow binding of the tagged proteins to the beads. The binding resin was pelleted by centrifugation at 1000x g for 3 min, the supernatant was removed and the beads were washed three times with the corresponding binding buffer (1x PBS for GST; supplemented with the appropriate concentration of NaCl and imidazole for His_6-tagged proteins). For GST-fusion proteins to be used in pulldown assays, the washing solution was removed and the beads were resuspended in 1x PBS. The protein concentration on the beads was determined by Bradford assay. For elution of the protein, the beads were resuspended in an appropriate volume (usually 1 ml) of elution buffer (for GST-fusions: 20 mM Tris-HCl pH 8.0 plus 100 mM NaCl or PBS, supplemented with 20 mM reduced glutathione; for His_6-tagged proteins: 20 mM Tris-HCl pH 7.4 plus 500 mM NaCl or PBS plus 200-500 mM NaCl, supplemented with 300-400 mM imidazole) and incubated for 1 hour at 4°C (His_6) or at room temperature (GST) under end over end rotation. After centrifugation, the supernatant was recovered, the protein concentration was determined and the samples were subjected to dialysis in order to remove supplements (imidazole, glutathione), change buffer or reduce salt concentration.

2.3.2.2 Fast protein liquid chromatography (FPLC)

We used the Äkta liquid chromatography system (Amersham Biosciences) for the purification of larger amounts of recombinant proteins, gel filtrations and affinity purification of antibodies. All steps were performed at 4°C using commercially available columns (HisTrap, GSTrap, HiTrap protein G, HiTrap desalting) and commonly recommended buffers for column loading, washing and protein elution.

2.3.3 Protein quantification (Bradford assay)

The protein stock solution was usually diluted 1:10 and 5, 10 and 20 µl were mixed with 1x PBS to a final volume of 500 µl. Then, 500 µl of 2x Bradford reagent was added and the mix was incubated for 5 to 10 min. The optical density at 595 nm was determined using 1x Bradford reagent (500 µl 2x Bradford reagent and 500 µl 1xPBS) as blank. The protein content was calculated from a reference curve determined with BSA as standard.

2.3.4 Cross-linking of GST-fusion proteins to beads

For large scale pulldown experiments and affinity purification of polyclonal antibodies from rabbit antisera, GST-fusion proteins were covalently crosslinked to GST-bind resin upon purification. We used the water-insoluble, non-cleavable, homobifunctional N-hydroxysuccinimide ester (NHS-ester) Disuccinimidyl Suberate (DSS, from Pierce) as a cross-linker. NHS-esters react with primary amines (free α-amine groups at the N-termini of proteins or ε-amine groups of lysine residues) and produce a amide bond thereby releasing N-hydroxysuccinimide. For the crosslinking reaction, approximately 3-4 mg of protein bound to GST-bind resin (500 µl bed volume) were incubated with 3.5 mg DSS dissolved in 250 µl DMSO and mixed with 375 µl PBS before adding to the beads. The mixture was incubated for 1 hour at room temperature. Remaining cross-linking activity was blocked (50 mM Tris-HCl pH 7.3, 150 mM NaCl, 10 min at room temperature) and the beads were extensively washed (three to four times with 50 mM Tris-HCl pH 7.3, 150 mM NaCl, 50 mM glutathione for 10 min at room temperature). Finally, the beads were washed in buffer without glutathione, packed into disposable 5 ml polyethylene columns (Pierce) and stored in buffer containing 0.02% Na-azide until use.

2.3.5 Preparation of protein extracts from rat brain

All steps were performed at 4°C. Frozen rat brain tissue (one brain for approx. 10 ml of buffer) was homogenized in ice-cold homogenization buffer (320 mM sucrose, 4 mM Hepes pH 7.4), supplemented with 1 mM PMSF and mammalian protease inhibitor cocktail (Sigma; 5 µl for 1 ml of buffer) using a Teflon homogenizer with ten to twelve strokes at 900 rpm. The homogenate was centrifuged at 1000x g for 10 min to remove unbroken cells, large cell debris and nuclei. The supernatant containing the cytosol and membrane fraction was immediately transferred to centrifugation tubes and supplemented with 5x buffer (final concentration: 20 mM Hepes pH 7.4, 100-150 mM KCl, 2 mM $MgCl_2$) and 1% Triton X-100 to solubilize membrane associated proteins. The extract was incubated on ice for 15 min and centrifuged at 40,000x g for 20 min. The supernatant was recovered and ultracentrifuged at 180,000x g for 15 min. The last two centrifugation steps remove all unsolubilized membranes and other debris; solubilized proteins are found in the supernatant. The protein concentration in the extract was determined by Bradford assay.

2.3.6 Affinity purification from rat brain extract ("Pulldown")

2.3.6.1 Small scale affinity purification for immunoblotting

Rat brain extract was prepared as described above and mixed with an appropriate amount of GST fusion protein or GST alone bound to glutathione coupled beads. Usually, approximately 2 to 5 mg of rat brain extract with a protein concentration of 2-5 mg/ml and 50 to 100 µg of GST-fusion protein were mixed in a volume of 1 ml. The mixture was incubated for 2 hours at 4°C by end over end rotation. After centrifugation at 1000x g for 3 min and 4°C, the supernatant was removed and the beads were washed three times with 1x pull down buffer (100-150 mM KCl, 20 mM Hepes pH 7.4, 2 mM $MgCl_2$) containing 1% Triton X-100 and twice with 1x buffer without detergent. The washing buffer was completely removed and the beads were eluted by incubation at 95°C for 3 min in 1x sample buffer. The eluates were subjected to SDS-PAGE analysis and immunoblotting.

2.3.6.2 Large scale affinity purification for mass spectrometry analysis

Large scale pulldowns were performed for the identification of putative binding partners by mass spectrometry. For that, purified GST-fusion proteins bound to glutathione coupled beads were covalently cross-linked to the matrix prior to incubation with protein extracts. Affinity purifications were performed essentially as described above using 25-30 mg rat brain extract loaded onto a disposable column. After incubation for 2 hours at 4°C with end over end rotation, the columns were extensively washed with buffer first with and then without Triton X-100. Bound proteins were eluted by high salt (binding buffer plus 1 M NaCl), precipitated with trichloroacetic acid (TCA) and pooled prior to SDS-PAGE.

2.3.7 *In vitro* binding experiments

In order to test whether proteins directly interact with each other, we performed GST-pulldown assays using purified or *in vitro* translated proteins. GST-fusion proteins were purified as described and kept bound to the beads. Usually, 50 µg GST-fusion proteins were incubated with 20 µg purified (His_6-tagged) protein or with ultracentrifuged *in vitro* translated proteins in 1 ml binding buffer (20 mM Hepes pH 7.4, 150 mM NaCl, 2 mM $MgCl_2$, 1% Triton X-100). Incubation, washing and elution were done as described above.

2.3.8 *In vitro* transcription/ translation

We used the TNT Coupled Reticulocyte Lysate System (Promega) for combined *in vitro* transcription/ translation and radioactive labelling of proteins. Transcription of mRNA from DNA templates (vectors) was driven by a T7 or SP6 promoter. The reaction mix was assembled according to the manufacture's instruction and contained rabbit Reticulocyte Lysate, reaction buffer, the respective RNA polymerase (T7 or SP6), amino acids, [^{35}S] labelled methionine (GE Healthcare), ribonuclease inhibitor and the DNA template. The reaction was incubated at 30°C for 90 min and ultracentrifuged at 180,000x g before it was used for direct binding assays as described above.

2.3.9 Immunoprecipitation

For the isolation of native protein complexes, co-immunoprecipitation experiments have been performed using rat brain extracts or protein extracts from transfected mammalian cells (usually Cos7 or HEK293). Commonly, 50 µl protein A/G PLUS agarose beads (Santa Cruz Biotechnology) were washed twice with 1 ml PBS + 0.1% Triton X-100. Beads were pelleted by centrifugation at 1000x g for 3 min at 4°C. Afterwards, the beads were incubated with the appropriate amount of antibodies in 1 ml PBS + 0.1% Triton X-100 for either 1 hour at room temperature or overnight at 4°C and washed twice with 1 ml binding buffer (20 mM Hepes pH 7.4, 80-150 mM NaCl, 2 mM $MgCl_2$) containing 1% Triton X-100. Protein extracts from rat brain tissue or mammalian cells were prepared in binding buffer with 1% Triton X-100 and added to the beads. Usually, we used 2-4 mg of rat brain extract or 500 µg to 1 mg of cell extracts in a volume of 1 ml. The reaction was incubated at 4°C for 4 hours under end over end rotation. Afterwards, beads were washed 3 times for 5 min with binding buffer containing 1% Triton X-100 and once quickly without detergent. The supernatant was completely removed using a Hamilton pipette and 40-50 µl 1x sample buffer supplemented with 5% fresh β-mercaptoethanol (to ensure complete separation of the antibody heavy and light chains) were added. Samples were incubated at 95°C for 5 min before subjection to SDS-PAGE and immunoblotting.

2.3.10 SDS polyacrylamide gel electrophoresis (SDS-PAGE)

Polyacrylamide gels were prepared with a concentration of 7, 8, 10, 12 or 14% acrylamide for the separating gel and 3% for the stacking gel in separating or stacking gel buffer, respectively. Protein samples were prepared for electrophoresis in 1x sample buffer, denatured at 95°C and loaded onto the gel. Electrophoresis was performed in 1x SDS-PAGE running buffer with 20 to 25 mA per gel. Afterwards, the gels were either processed for immunoblotting or the protein bands were visualized with Commassie blue staining solution. Unspecific staining was removed by incubation with destaining solution.

2.3.11 Immunoblotting

After SDS-PAGE, the proteins were transferred from the polyacrylamide gel to a nitrocellulose membrane by semi-dry blotting. For that, three layers each of Whatman paper soaked with blotting buffer (80% 1x SDS-PAGE running buffer, 20% methanol) were placed underneath the membrane and above the gel in a blotting chamber. Electrotransfer of the proteins from the gel onto the membrane was performed at 1 mA/ cm^2 (45 mA per gel). After that, the protein bands on the membrane were reversibly stained with Ponceau S (0.3% in 1% acetic acid), unspecific staining was removed with 1% acetic acid and the blot was scanned for documentation. The membrane was washed once with TBS and incubated with blotto (3% w/v skimmed milk powder in TBS) for 1 hour at room temperature to block all binding sites on the membrane. After washing twice with TBS, the blot was incubated with primary antibody solution (appropriate dilution in 2% BSA and 0.02% NaN_3 in TBS) either for 2 hours at room temperature or overnight at 4°C. Next, the membrane was washed three times with TBS. Horseradish peroxidase (HRP)- or alkaline phosphatase (AP)-coupled goat anti-mouse or goat anti-rabbit secondary antibodies (Dianova) freshly diluted in blotto (1:5000 for HRP-, 1:1000 for AP-coupled) were added and incubated for 1 hour at room temperature. The blot was washed three times with TBS and visualization of the bound antibodies was performed according to the type of secondary antibody.

For HRP-coupled secondary antibodies, ECL detection reagent (Amersham Biosciences) was applied to the membrane, the luminescence signals were detected by overlaying the blot with a chemiluminescence film (Hyperfilm™ ECL, Amersham Biosciences) and the film was developed by incubation in developer and fixation solution.

For AP-coupled secondary antibodies, the blot was washed in TSM buffer and incubated in developing solution (84 µl of 20 mg/ml BCIP, 61 µl of 50 mg/ml NBT in 70% DMF, in 10 ml TSM). The reaction was stopped by washing with dH_2O.

2.3.12 Sample preparation for mass spectrometry

For the identification of unknown protein bands on Coomassie stained protein gels by mass spectrometry, we excised the relevant bands and subjected them to in gel digest with trypsin. For the Coomassie staining of the gels, we used freshly prepared colloidal Coomassie staining and destaining solutions according to manufacturer's instructions

(Roth). Gel bands were excised and cut into 1x1 mm pieces. Gel fragments were transferred to 500 µl reaction tubes, 20 µl of a 1:1 mixture of acetonitrile : 100 mM NH_4HCO_3 were added and the tubes were incubated in a shaker for 15 min. Samples were briefly centrifuged, the supernatant was exchanged to 100% acetonitrile and incubated for 5 min until the gel pieces turned white. Acetonitrile was removed and the gel pieces were dried for 10 min using a speed vac. For reduction of disulfide bonds, the lyophilized gel pieces were incubated in 20 µl 100 mM DTT in 100 mM NH_4HCO_3 for 30 min at 56°C. Samples were briefly centrifuged, the supernatant was removed with a pipette and its volume was measured. Gel pieces were again dehydrated twice by the addition of 20 µl of 100% acetonitrile. Free cysteine residues were covalently modified (carbamidomethylation) by addition of 20 µl of 55 mM iodacetamide in 100 mM NH_4HCO_3 and incubation for 20 min at room temperature in the dark. The supernatant was removed, exchanged for 100 mM NH_4HCO_3 and the samples were incubated for 15 min at room temperature. Afterwards, gel pieces were incubated in 20 µl 100% acetonitrile until they turned white and dried for 10 min. 12.5 µg/ml trypsin (sequencing grade, Roche) in 25 mM NH_4HCO_3 was prepared and added to the dried gel pieces (volume: 20 µl minus the volume of the supernatant measured after reduction in DTT + 3 µl). Samples were placed on ice for 30 min before incubation at 37°C overnight. Samples were briefly centrifuged and again incubated at 37°C for 30 min before the supernatant was removed (around 3 µl) and subjected to mass spectrometric analyses. MALDI-TOF (matrix-assisted laser desorption and ionization – time of flight) mass sprectrometry was performed by Dr. Peter Franke at the Institute of Chemistry and Biochemistry of the Freie Universität Berlin. Proteins were identified by peptide mass fingerprinting analysis. Relevant peaks from the recorded spectrum were selected and used for database searches. The database search engine (Matrix Science - Mascot Peptide Mass Fingerprint) is available under http://www.matrixscience.com/.

2.3.13 Polyclonal antiserum production

We raised antibodies against γ-BAR using purified His-tagged γ-BAR aa 52-302 as antigen which was dialyzed twice against PBS + 50 mM NaCl. Animal immunisation and bleeding experiments were performed at the Charité FEM, Campus Benjamin Franklin together with Dr. M. Ladeburg. We immunized 3 female rabbits (Chinchilla Bastard; Charles River Germany) with 150 µg antigen in 100 µl PBS mixed with 100 µl complete Freund's adjuvant (Sigma) by subcutaneous injection at two to three sites in

the back of the animals. Rabbits were boosted three to four times by injection of 150 µg antigen in 250 µl PBS plus 250 µl incomplete Freund's adjuvant. The first boost was done four weeks after the first injection, all following boosts every ten to twelve days until the final bleed. Test bleeds were taken before the first injection and together with each boost to analyze the reactivity against the antigen. The serum was recovered from the bleeds by centrifugation at 10,000x g and stored at -20°C

2.3.14 Affinity purification of polyclonal antibodies from rabbit antiserum

Polyclonal rabbit antibodies were affinity purified on an antigen column to remove unspecific cross-reactivity. Therefore, GST-tagged γ-BAR aa 52-302 was purified, cross-linked to the GST-bind resin as described above and packed into disposable 5 ml polyethylene columns (Pierce).

Rabbit antiserum was heat inactivated for 30 min at 56°C, supplemented with binding buffer (50 mM Tris pH 7.4, 150 mM NaCl final concentration), applied to the pre-equilibrated column and incubated for 2 hours at room temperature. The column was washed three times with 50 mM Tris pH 7.4/ 500 mM NaCl and antibodies were eluted with 100 mM Glycine-HCl buffer pH 2.7 in 1 ml fractions which were immediately neutralized by adding 100 µl of 1 M Tris-HCl pH 9.0. The protein concentration in the eluted fractions was determined, fractions with the highest protein content were pooled, dialyzed against PBS and concentrated. The purified antibodies were stored at -20°C after addition of 50% glycerol. The specificity of the antibodies was verified in immunoblots and by immunofluorescence staining of cultured mammalian cells.

2.3.15 Cultured mammalian cell fractionation

Cultured mammalian cells were separated into soluble and membrane bound protein fractions to analyze the proteins that are associated with one or the other part. Cells were harvested by trypsinization, pelleted and resuspended in 1 ml buffer (20 mM Hepes pH 7.4, 2 mM $MgCl_2$, 100 mM NaCl) supplemented with 1 mM PMSF and mammalian protease inhibitor cocktail. The cell suspension was passed about 15 times through a 27G canuelae and centrifuged at 700x g for 3 min to remove large cell debris, unbroken material and nuclei. The supernatant was recovered and ultracentrifuged at 180,000x g. The supernatant of the last centrifugation step contained soluble proteins and the pellet contained the membrane protein fraction. The soluble fraction was

recovered, Triton X-100 was added and samples were again ultracentrifuged. The membrane fraction (pellet) was rinsed twice with buffer, resuspended in buffer containing Triton X-100, incubated for 15 min on ice to solubilize membrane proteins and centrifuged at 20,000x g for 15 min. The supernatants of the soluble and membrane protein fractions were recovered and the protein content was determined before mixing with 6x sample buffer for SDS-PAGE.

2.4 Cell Biological Methods

2.4.1 General mammalian cell culture

Mammalian cell lines were cultured in humidified incubators at 37°C and 5% CO_2. Media were purchased from Invitrogen. We used Dulbecco's modified Eagle's medium (D-MEM) containing glutamine or glutamax, sodium pyruvate, pyridoxine and either 1 g/l (Cos7, Hela) or 4.5 g/l glucose (HEK293, NIH-3T3, PC12). Media were supplemented with 10% heat inactivated fetal calf serum (FCS) and antibiotics (50 units/ml penicillin, 50 µg/ml streptomycin). For PC12 cells, the medium was supplemented with 10% horse serum and 5% FCS. Cells were generally passaged every 3-5 days using trypsin/EDTA solution (Invitrogen) and plated at 1:5-1:20 dilutions onto new culture dishes.

2.4.2 Transfection of plasmid DNA and siRNAs

Mammalian cells were transfected with vectors for eukaryotic expression at 80-90% confluency using Lipofectamine 2000 transfection reagent (Invitrogen) according to the manufacture's instructions with changes in the amount of DNA and Lipofectamine 2000 used (2.5 µg DNA and 5 µl Lipofectamine per 9.5 cm^2 well). DNA/ Lipofectamine complexes were prepared in Opti-MEM (Invitrogen) and added to the cells cultured in antibiotics free medium. Cells were incubated for 4 hours before the medium was changed. Cells were further processed 24 hours after transfection.

For siRNA transfections, Oligofectamine (Invitrogen) was used and cells were transfected at 30-50% confluency. For efficient knockdowns (>90%) two rounds of transfections were done with an interval of 48 hours. We used 5 µl Oligofectamine and 300-400 pmol siRNA per 9.5 cm^2-well prepared in Opti-MEM. Medium was exchanged to antibiotics free medium (half the normal volume) prior to addition of the complexes.

Cells were incubated for 3 hours and full medium was added up to the normal volume. The cells were usually passaged between the first and second transfection. Experiments with siRNA treated cells were usually performed 48 hours after the second transfection. When vector DNA and siRNAs were co-transfected in the second round of transfection, Lipofectamine 2000 was used and transfections were performed 24 hours before the experiment.

2.4.3 Generation of stable cell lines

Cell lines stably expressing a certain gene were generated by selection with geneticin, an analog of neomycin. Eukaryotic expression vectors usually contain a neomycin resistance cassette, which allows transfected cells to grow in medium containing geneticin. Cells were transfected as described above and passaged in different dilutions 24 hours after transfection using medium containing 500 µg/ml geneticin (Invitrogen). Medium was changed every 2 days until all non-transfected control cells had died and single colonies could be observed (between 1-3 weeks). Single colonies were picked, dissociated and transferred to 48- or 96-well plates. Cells were expanded in selective medium and checked for gene expression by immunoblotting. Several positive clones were chosen and aliquots were stored in liquid nitrogen.

2.4.4 Immunofluorescence staining

Cells seeded on glass coverslips were fixed either with 4% PFA (para-formaldehyde), 4% sucrose in PBS pH 7.4 for 20-30 min at room temperature or in pre-cooled 100% methanol for 10 min at -20°C. Afterwards, coverslips were washed 3 times in PBS and cells were permeabilized and blocked in PBS containing 30% goat serum and 0.3% Triton X-100 (blocking solution). Primary antibodies were diluted in blocking solution, applied to the coverslips in a humidity chamber (30-50 µl per coverslip upside down onto parafilm) and incubated for 1 hour at room temperature. Coverslips were washed 3 times with PBS and incubated with Alexa Fluor labeled secondary antibodies (1:100 – 1:200 dilutions) for 1 hour at room temperature. Afterwards, coverslips were washed again 3 times in PBS and mounted onto glass slides using Immumount mounting solution (Thermo Electron) supplemented with 1 µg/ml DAPI.

In order to reduce background by unspecific binding of antibodies, in some cases high-salt PBS (containing 500 mM NaCl) was used instead of PBS. For some antibodies (e.g

LAMP-1), it was necessary to leave out the detergent in all steps after fixation with methanol.

2.4.5 Fluorescence microscopy and quantification

For fluorescence image acquisitions and analysis we used a Zeiss Axiovert 200M Digital Research Microscopy System equipped with a special light source and the Slidebook Digital Microscopy software package provided by Intelligent Imaging Innovations. This setup allows quasi-confocal imaging by deconvolution of the acquired images. The deconvolution algorithm used by the software reverses the optical distortion that takes place in a microscope, thus greatly improving z-resolution.
For quantification of fluorescence intensities we made use of the mask creation and statistics functions provided by the software. Details about quantification procedures can be found in the respective figure legends.
Alternatively, images were acquired using a confocal spinning disc microscopy system (Ultra VIEW ERS Rapid Confocal Imager) and the Image Suite software (Perkin Elmer).

2.4.6 Transferrin uptake and recycling assays

2.4.6.1 Microscopy-based transferrin assays

Transfected cells were seeded on matrigel coated glass coverslips and starved the next day for at least 1 hour in serum free medium before the assay. Alexa Fluor 594 labeled Tf (Molecular Probes) was diluted to a concentration of 25 µg/ml in serum free medium containing 0.2% BSA and centrifuged for 10 min to remove precipitates. The solution was added to the coverslips (100 µl per coverslip) in a humidity chamber and incubated for 20 min at 37°C in a humidified incubator to allow internalization of the Tf ("pulse"). The humidity chamber was immediately placed on ice and the coverslips were washed three times with ice-cold Hank's balanced salt solution (HBSS) supplemented with 20 mM Hepes. Alternatively, PBS supplemented with 0.5 mM $CaCl_2$ and 0.5 mM $MgCl_2$ was used for washing. For the analysis of Tf-uptake, coverslips were fixed with 4% PFA, 4% sucrose in PBS pH 7.4 for 30 min at room temperature. For recycling ("chase"), 100 µl of pre-warmed medium containing 10% FCS and 1 mg/ml unlabelled holo-Tf (Sigma) were added to the coverslips and incubated at 37°C (humidified

incubator). Coverslips were removed after different periods of time (15, 20, 30 min), dipped twice into ice-cold HBSS + Hepes (or PBS + 0.5 mM $CaCl_2$ + 0.5 mM $MgCl_2$) and fixed as described. After fixation, coverslips were washed 3 times in PBS and mounted on glass slides or processed for immunofluorescence staining.

2.4.6.2 Quantitative transferrin assays

Cells were seeded on 12-well plates after transfection with siRNAs as described above and starved the next day for at least 2 hours in serum free medium. Plates were chilled on ice and 250-300 µl medium containing 20 µg/ml unlabeled holo-Tf and 300 ng/ml [^{125}I]-labeled Tf (Perkin Elmer; specific activity: 0.3-1.0 µCi/µg) were added to each well. Plates were incubated at 37°C in a humidified incubator and removed after several periods of time (5, 10, 20 and 30 min for the uptake assay) or complete internalization of Tf was allowed for 30 min (for the recycling assay). As a control for unspecific binding, one plate was kept on ice. Afterwards, plates were chilled on ice and washed 3 times with ice-cold 0.5% BSA in PBS. For uptake assays, plates were kept on ice in PBS + 0.1% BSA. For recycling, pre-warmed medium containing 100-fold excess of Tf (2 mg/ml) was added and the plates were incubated at 37°C (incubator). They were removed at several time points (3, 6, 9 and 12 min), chilled on ice and the medium was changed to 0.1% BSA in PBS. Plates were kept on ice until all plates were ready for further processing. Washing was done alternating with 0.1% BSA in PBS and 0.1% BSA in PBS + 25 mM acetic acid pH 4.2 three times for three min each (everything on ice) to remove surface bound Tf. After the last short washing step (0.1% BSA in PBS), the solution was completely removed and 1 ml PBS containing 1% Triton X-100 was added. Plates were incubated for 10 min at room temperature to solubilize the cells, the solution of each well was transferred to liquid scintillation tubes containing 10 ml Ultima-Gold liquid scintillation cocktail (Perkin Elmer) and the counts per minute (CPM) were measured in a scintillation counter.

2.4.7 Low density primary hippocampal neuron cultures

Primary hippocampal neurons from embryonic day E18 rat embryos were prepared and cultivated in low density cultures essentially as described by Goslin, Asmussen and Banker (in: Culturing Nerve Cells, 2nd edition, 1998). Briefly, hippocampi were dissected from the brains of E18 rat embryos, treated with 0.25% trypsin for 15 min at

37°C, washed in Ca^{2+} and Mg^{2+} free Hanks' balanced salt solution (HBSS), and dissociated by repeated passage through a constricted Pasteur pipette. Cells were plated in horse serum-containing cell culture medium at a density of 150.000 cells per 6 cm tissue culture dish containing six 15 mm poly-L-lysine coated coverslips with wax dots at their surface. After cells had attached to the substrate (>5 hours after preparation), coverslips were transferred upside down to dishes with glial cell monolayers containing serum-free medium. Glial cells were prepared separately from embryonic rat brains and plated in the appropriate density or "left-over" cultures on dishes in which neurons have been plated were used. Details for preparation of coverslips, media composition, dissection, plating and culturing of neurons and astroglial cells can be found in the chapter "Rat Hippocampal Neurons in Low-Density Culture" of the book mentioned above.

2.4.8 Transfection of primary hippocampal neurons

Primary hippocampal neurons were transfected at day *in vitro* (DIV) 8 to 10 using the Effectene transfection reagent (Qiagen) essentially as described by the manufacture's instructions. We used 0.3 µg DNA, 2.4 µl Enhancer and 6 µl Effectene per coverslip placed in one well of a 12-well plate. We used conditioned medium from the culture dish were neurons had grown in and incubated with the transfection mix overnight. Cells were fixed 20-24 hours after transfection and processed for immunofluorescence staining and microscopy.

Alternatively, primary neurons were transfected directly after preparation using the Amaxa Nucleofector II system with the Rat Neuron Nucleofector Kit following the manufacture's instructions. We used $5x10^5$ cells in 100 µl transfection solution and 3 µg DNA per transfection. After transfection, 500 µl of pre-warmed plating medium (containing horse serum) were added and the cells were plated onto two 6 cm tissue culture dishes with coverslips. Coverslips were transferred to the glial cell culture dishes the next day. Cell were fixed after different periods of time as described above and processed for immunofluorescence staining.

2.4.9 Immunofluorescence staining of cultured neurons

For immunofluorescence staining of cultured neurons grown on glass coverslips we used a modified protocol. Cell culture medium was removed from the coverslips and the

cells were fixed immediately in 4% PFA, 4% sucrose in PBS pH 7.4 for 15 min or in -20°C methanol for 5-10 min. After fixation, cells were washed 3 times with PBS. PFA-fixed cells were quenched for 10 min in 50 mM NH_4Cl and washed 3 times with PBS. Cells were permeabilized in PBS + 0.1% Triton X-100 for 3 min and washed again three times in PBS. Coverslips were transferred onto parafilm in a wet chamber, immediately covered with 100 µl blocking solution (2% FCS, 2% BSA, 0.2% Fish Gelatin in PBS) and incubated for 1 hour at room temperature. The blocking solution was aspirated and 100 µl primary antibody solution (diluted in 10% blocking solution in PBS) were applied for 1 hour. After three washes with PBS, 100 µl secondary antibody solution (in 10% blocking/ PBS) were added and incubated for 30 min. Coverslips were washed three times in PBS, the wax dotes were removed, the coverslips were briefly dipped into water and mounted onto glass slides in a drop of Gelmount mounting solution (Sigma).

2.4.10 Quantification of neurite lengths

Images were acquired with an inverted microscope (Zeiss) using the freely available software Scion Image (Scion Corporation). Neurite lengths were quantified by drawing a freehand line along the longest neurite of each neuron and calculating the length in µm from the length of the line in pixels using the appropriate factor for the objective that had been used for image acquisition.

3 Results

3.1 Interaction between γ-BAR and AP-1

3.1.1 γ-BAR exclusively interacts with the ear domain of γ-adaptin

AP-1 has been identified in a yeast-2-hybrid screen to directly interact with γ-BAR (Neubrand et al., 2005). The interaction site within the AP-1 complex resides within the ear-domain of the γ-adaptin subunit (γ-ear). We wanted to further analyze, whether γ-BAR interacts with γ-ear only or might also be able to bind the ear-domains of other AP large subunits. We therefore purified His-tagged β1- and γ-ears of AP-1, β2- and α-ears of AP-2, as well as the β3A-ear of AP-3 and incubated them with purified GST-tagged γ-BAR Δ51 (aa 52-302) or a mutant thereof (WENDF-mutant; ^{260}WENDF^{264}→LENDL) that has been shown to lack the ability to bind to AP-1 *in vitro* (Kukhtina et al., unpublished data). We found that γ-BAR interacts solely with the ear domain of γ-adaptin.

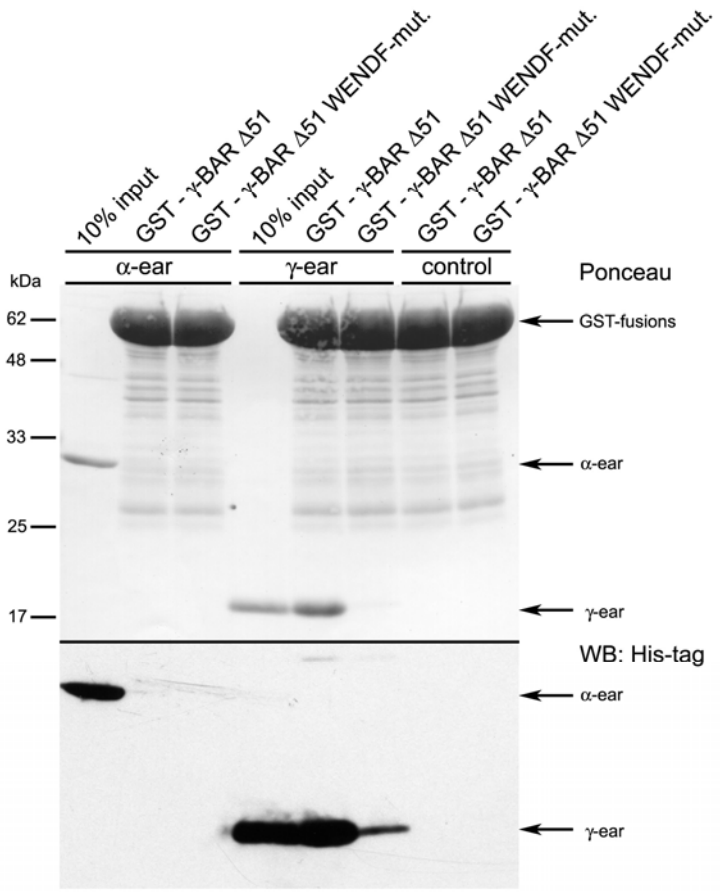

Figure 3-1: γ-BAR selectively binds to the γ-ear of AP-1 but not the α-ear of AP-2 *in vitro*

20 µg GST-fusion proteins (γ-BAR Δ51 and the WENDF mutant thereof) and GST as a control were purified, coupled to beads and incubated with 40 µg purified His-tagged γ-adaptin or α-adaptin ear domains. Samples were subjected to SDS-PAGE and immunoblotting. The upper part shows the Ponceau stained blotting membrane, the lower part the immunoblot decorated with antibodies against the His_6-tag. γ-BAR selectively binds to purified γ-ears. Binding is drastically reduced in the WENDF mutant of γ-BAR.

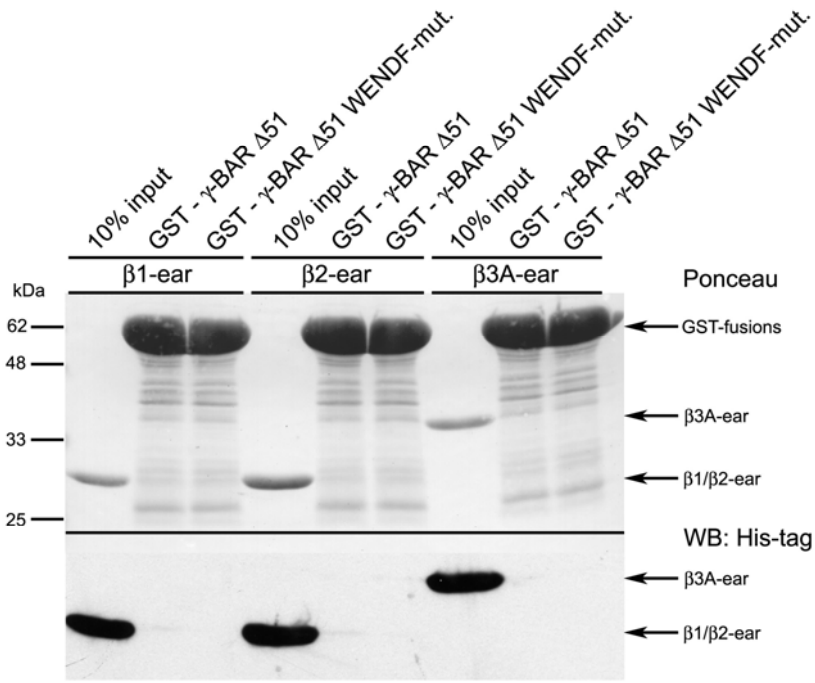

Figure 3-2: γ-BAR does not bind to β-adaptin ear domains of AP-1, AP-2 and AP-3

20 µg GST-fusion proteins (γ-BAR Δ51 and the WENDF mutant thereof) and GST as a control were purified, coupled to beads and incubated with 40 µg purified His-tagged β1-, β2- and β3A ear domains. Samples were subjected to SDS-PAGE and immunoblotting. The upper part shows the Ponceau stained blotting membrane, the lower part the immunoblot decorated with antibodies against the His_6-tag. γ-BAR does not bind any of the purified β-ear domains.

3.2 Membrane association and anchoring of γ-BAR

It has already been described that γ-BAR is a peripherally associated membrane protein lacking any transmembrane domains (Neubrand et al., 2005). The association of γ-BAR with membranes could thus be mediated by posttranslational modifications or by binding to other membrane associated proteins (e.g. AP-1). We therefore aimed at further dissecting the mechanisms by which γ-BAR associates with membranes.

3.2.1 The majority of γ-BAR is associated with membranes

First, we analyzed the extent of membrane association of γ-BAR by subcellular fractionation of cultured HeLa-cells into membrane and cytosolic fractions (Figure 3-3). The integral membrane protein TfR was exclusively found in the membrane fraction, whereas the cytosolic marker protein glyceraldehyd-3-phosphate dehydrogenase (GAPDH) was mostly cytoplasmic. γ-BAR almost entirely associated with the membrane fraction. This raises the question of how membrane association of γ-BAR is achieved.

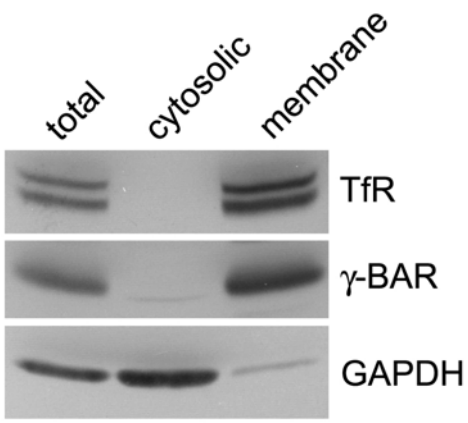

Figure 3-3: Subcellular distribution of γ-BAR
HeLa cells were separated into cytosolic and membrane protein fractions and subjected to SDS-PAGE (50 µg each lane) and immunoblotting. Total cell lysates were used for comparison. Antibodies against γ-BAR, transferrin receptor (TfR, an integral membrane protein) and glyceraldehyd-3-phosphate dehydrogenase (GAPDH, a cytosolic protein) were used as controls. γ-BAR is almost completely associated with the membrane fraction.

3.2.2 Membrane recruitment of γ-BAR is independent of AP-1 interaction

Recently, it has been suggested that γ-BAR and AP-1 are reciprocally required for their association with membranes (Neubrand et al., 2005). γ-BAR was shown to control the membrane association/ dissociation of AP-1 by direct interaction with the ear domain of γ-adaptin. Furthermore, it was suggested that γ-BAR can bind to membranes independently of AP-1 but fails to do so in cells lacking a functional AP-1 complex. In

order to test whether AP-1 binding activity is required and/ or sufficient for the association of γ-BAR with membranes, we performed GST-pulldown analyses using truncated GST-fused γ-BAR variants. Additionally, γ-BAR-eGFP chimeras were expressed in HeLa cells and their subcellular distribution was analyzed (Figure 3-4).

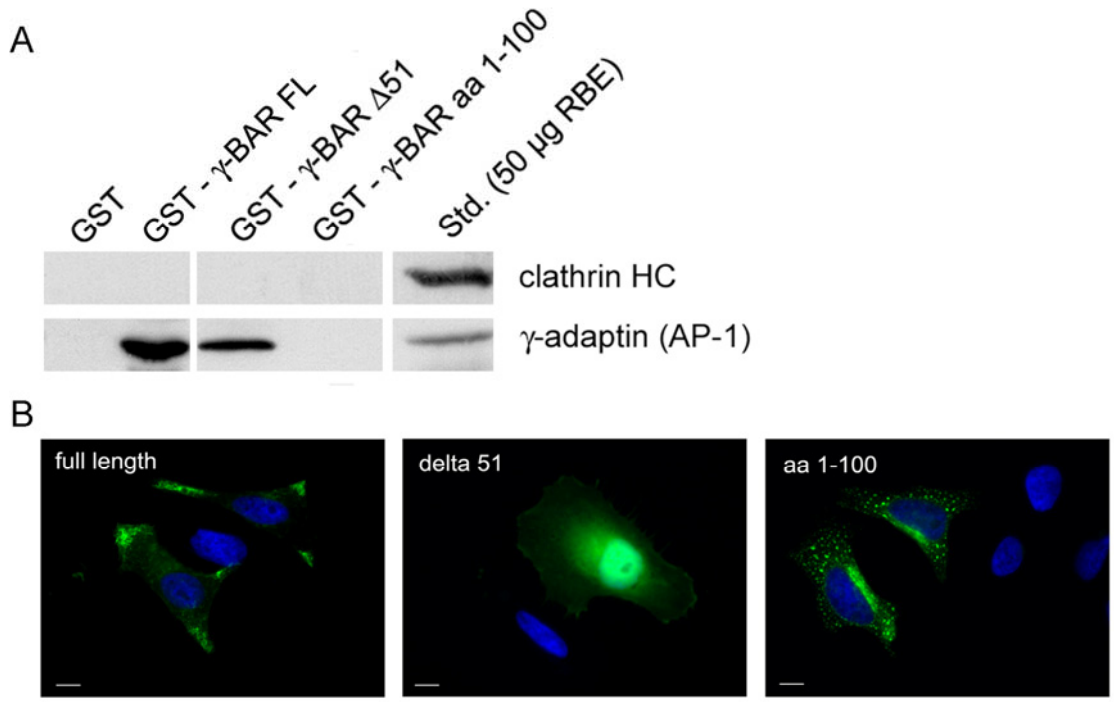

Figure 3-4: Membrane association of γ-BAR does not depend on its AP-1 binding activity

(A) GST-pulldown assay: GST (control), GST-tagged γ-BAR full length (FL) and the two truncation mutants aa 52-302 (Δ51) and aa 1-100 were purified from *E.coli* expression cultures and 20 µg of each protein bound to beads were incubated with Triton X-100 protein extracts prepared from rat brain tissue (1.5 mg total protein for each sample). Bound proteins were analyzed by SDS-PAGE and immunoblotting using antibodies against γ-adaptin (AP-1) and clathrin heavy chain (HC) as a control. Std., standard corresponding to 50 µg rat brain extract (RBE).

(B) Subcellular distribution of γ-BAR-eGFP chimeras in HeLa-cells: HeLa cells were transiently transfected with plasmids encoding eGFP-tagged γ-BAR (full length, delta 51 and aa 1-100) and the subcellular distribution was analyzed by fluorescence microscopy (green). DAPI-stained nuclei are shown in blue. The scale bar is 10 µm.

Full length γ-BAR binds AP-1 in pulldowns and associates with membranes in the cell periphery. A construct lacking the first 51 amino acids (delta 51) is still able to bind to γ-adaptin *in vitro*, but fails to associate with membranes upon expression in HeLa-cells, where it displays an entirely cytosolic expression pattern. A construct comprising the amino-terminal 100 amino acids (aa 1-100) does not bind to γ-adaptin but still localizes

to membranes with a perinuclear and scattered endosomal-like distribution. These observations suggest that γ-BAR harbors membrane binding activity within its amino-terminal 100 amino acids independent of its AP-1 binding activity.

3.2.3 γ-BAR membrane recruitment is due to palmitoylation

The membrane binding activity of γ-BAR could be mediated by direct binding to lipid bilayers [as seen for example for epsin amino-terminal homology (ENTH) domains], through binding to other membrane associated proteins (e.g. Arf proteins) or by inserting a lipid anchor into the membrane. Recombinant γ-BAR failed to bind liposomes of different lipid composition *in vitro* (data not shown). Thus, we analyzed the amino-terminal sequence of γ-BAR with respect to residues that could be potential targets for posttranslational lipid modifications. We identified such residues within the first nine amino acids and a construct lacking these nine amino acids (γ-BAR aa 10-100) fused to eGFP indeed remained completely cytosolic (Figure 3-5). The glycine residue at position 2 of the γ-BAR sequence could be modified by myristoylation. To test this we mutated glycine 2 to alanine (γ-BAR aa 1-100 G2A), but no effect on the cellular distribution could be observed. Several cysteine residues at positions 4, 5 and 9 could be targets for palmitoylation. In fact, mutating all three cysteines to serines caused γ-BAR to remain entirely cytoplasmic.

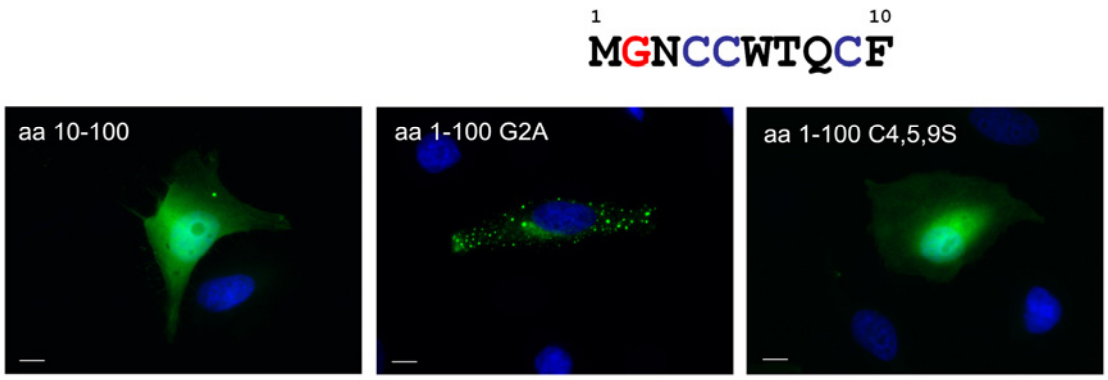

Figure 3-5: Three amino-terminal cyteines are critical for γ-BAR membrane association

Localization of mutants of γ-BAR (aa 1-100) either lacking the first nine amino acids (aa 10-100), or containing a glycine to alanine mutation at position 2 (red in the sequence; aa 1-100 G2A) or three cysteine to serine mutations at positions 4, 5 and 9 (blue; aa 1-100 C4,5,9S). HeLa cells were transiently transfected with constructs encoding indicated eGFP-tagged γ-BAR fragments. The cubcellular localization of γ-BAR chimeras was analyzed by fluorescence microscopy (green). DAPI-stained nuclei are shown in blue. The scale bar is 10 µm.

To verify the role of the cysteine residues for membrane association, we analyzed the subcellular distribution of full length γ-BAR constructs (wild type or carrying the corresponding mutations) biochemically and by fluorescence microscopy.

Whereas transfected wild type γ-BAR is fully associated with membranes at the cell periphery (Figure 3-6, panel A upper part and B lane 3), the C4,5,9S mutant remains largely cytosolic as seen by immunofluorescence (panel A lower part) and biochemical analysis (panel B, lane 5). A small fraction of mutant γ-BAR appeared to be associated with membranes (lane 6). This might be due to its binding to membrane bound AP-1 complexes.

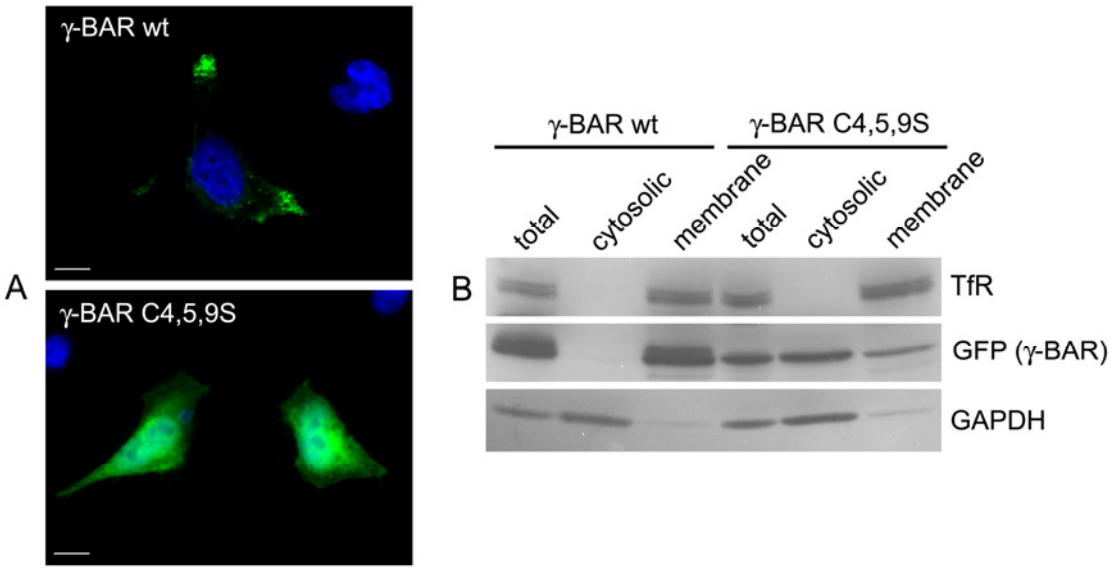

Figure 3-6: The γ-BAR C4,5,9S mutant becomes largely cytosolic

HeLa cells were transiently transfected with plasmids encoding eGFP-tagged γ-BAR wild type or its C4,5,9S mutant. The subcellular distribution of chimeric proteins was analyzed by: **(A)** fluorescence microscopy (scale bar = 10 µm) and **(B)** biochemically. For the latter, cytosolic, membrane and total protein fractions were prepared from transiently transfected HeLa cells und 50 µg total protein was used for SDS-PAGE and immunoblotting using antibodies against the GFP-tag of the γ-BAR constructs, as well as TfR and GAPDH as controls for membrane and cytosolic proteins, respectively.

In order to address whether the cysteine residues are indeed subject to palmitoylation, we treated cells with the known palmitoylation inhibitor 2-bromopalmitate (2-BrP) (Fang et al., 2006; Webb et al., 2000) prior to and during transfection with γ-BAR-encoding plasmids.

As seen from Figure 3-7, γ-BAR (aa 1-100) is membrane associated in mock-treated cells, but becomes cytosolic upon incubation with 2-bromopalmitate. This strongly suggests that palmitoylation is involved in the proper association of γ-BAR with membranes.

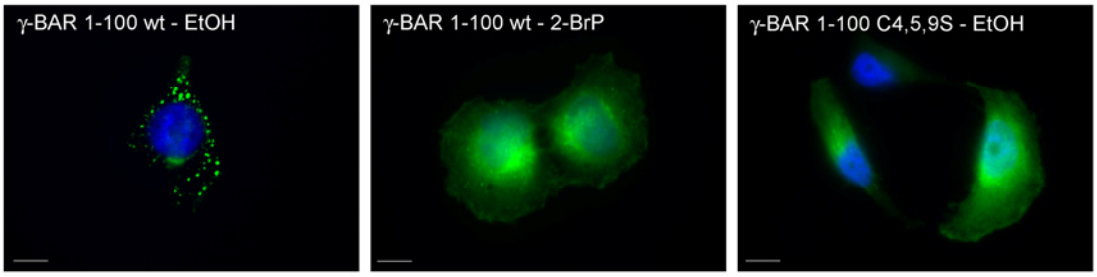

Figure 3-7: 2-bromopalmitate treatment inhibits γ-BAR membrane association
HeLa cells were pre-incubated with 50 µM 2-bromopalmitate (2-BrP, dissolved in ethanol) or the same volume of ethanol (EtOH) for 2 hours, transiently transfected with plasmids encoding the indicated eGFP-tagged γ-BAR constructs and the treatment was continued for another 20 hours. Afterwards, the cells were fixed and the subcellular distribution of the transfected constructs was analyzed by fluorescence microscopy. DAPI-stained nuclei are shown in blue. The scale bar is 10 µm.

3.3 Search for additional interaction partners of γ-BAR

3.3.1 Affinity purifications from rat brain extracts

We aimed at the identification of additional binding partners of γ-BAR besides the known interaction with the AP-1 adaptor complex. The γ-adaptin subunit has been identified in a yeast-2-hybrid screen using an amino-terminal γ-BAR fragment (aa 1-151) as bait (Neubrand et al., 2005). The carboxy-terminal half of γ-BAR was found to be autoactivating in that screen. Previous results showed that γ-BAR not only localizes to the TGN and regulates AP-1 localization and function, but, upon overexpression, is also found in smaller, highly mobile structures throughout the cytosplasm. We therefore speculated that there might be additional interacting partners besides the AP-1 complex that facilitate post-Golgi transport processes. Thus, we tried to identify putative binding partners of γ-BAR using affinity purifications from Triton X-100 extracted rat brain homogenates. A GST-tagged version of human γ-BAR lacking the first 51 amino acids was used, because this construct displayed much better solubility compared to full length γ-BAR when expressed in *E. coli*. GST was used as a control. Recombinant

proteins were covalently crosslinked to the affinity matrix using DSS. Immobilized proteins were then incubated with rat brain extracts, extensively washed and bound proteins were eluted under high salt conditions. After SDS-PAGE and Coomassie staining, bands specifically present in the γ-BAR containing samples were subjected to tryptic in-gel digest and analyzed by MALDI-TOF mass spectrometry to identify the corresponding proteins (Figure 3-8).

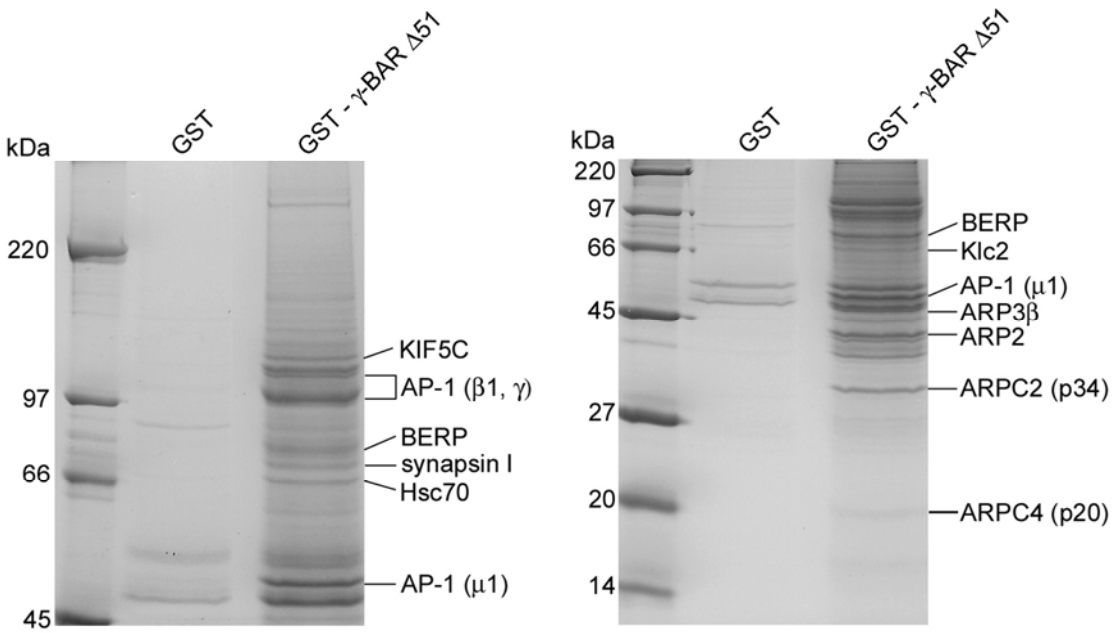

Figure 3-8: Affinity purification of potential γ-BAR binding partners from rat brain extracts
Recombinant GST-γ-BAR and GST as a control (1.5 mg each) were purified, cross-linked to glutathione agarose beads and incubated with Triton X-100 extracted rat brain homogenates (12.5 mg total protein). Binding was performed in the presence of 50 mM KCl, washing with 150 mM KCl and elution in 1M NaCl. The indicated bands were cut from the gels (left: 7%; right: 13%), subjected to tryptic digestion and the containing proteins were identified by MALDI-TOF mass spectrometry-based peptide mass fingerprint analysis.

We could identify several putative binding partners for γ-BAR. First, we found several subunits of the known interactor AP-1 (β1, γ and μ1) confirming that GST-tagged γ-BAR Δ51 maintains its binding activity after cross-linking. Furthermore, we identified both subunits of a conventional kinesin of the KIF5 family (kinesin-1): the heavy chain KIF5C and its associated light chain Klc2. Other identified proteins include: (i) The ring finger protein BERP (ring finger protein 22, also called Trim3), which interacts with the actin based motor protein myosin V (El-Husseini and Vincent, 1999), (ii) synapsin I, a member of a class of synaptic vesicle associated proteins that play a critical role in

vesicle clustering and actin dynamics within the synaptic vesicle pool at synapses (Ferreira and Rapoport, 2002), and (iii) several of the seven subunits of the Arp2/3 complex (ARP2, ARP3β, ARPC2/ p34 and ARPC4/ p20). Arp2/3 is a downstream target of several signaling pathways (including Cdc42 signaling), stimulates actin polymerization and branching and is involved in processes such as cellular motility and growth (Goley and Welch, 2006). Lastly, we found the heat shock protein Hsc70, the significance of which remains unclear.

In order to confirm the identity of these proteins, we performed immunoblotting using specific antibodies against ubiquitous kinesin heavy chains, γ-adaptin (AP-1), BERP, synapsin I and the p34 subunit of the Arp2/3 complex. All proteins that were found in the mass spectrometric analysis could also be verified by immunoblotting of the affinity purified material (Figure 3-9).

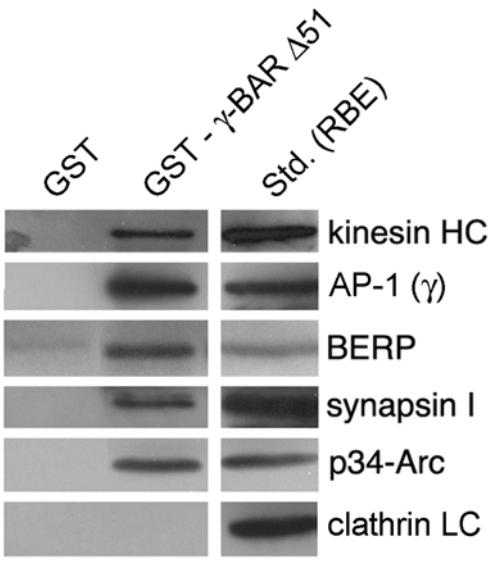

Figure 3-9: Verification of potential γ-BAR interacting partners

GST and GST-γ-BAR Δ51 bound to glutathione agarose beads were used for affinity purifications from rat brain extracts. Bound proteins were eluted and subjected to SDS-PAGE and immunoblotting using antibodies against the indicated proteins. Clathrin light chain (LC) antibodies were used as a negative control. Std., standard corresponding to 50 µg rat brain extracts (RBE) used for the affinity purification.

3.4 γ-BAR directly interacts with conventional kinesins

3.4.1 Several γ-BAR versions can associate with conventional kinesin

For the identification of putative binding partners shown above, a truncated version of γ-BAR (missing the first 51 amino acids) was used. However, we wanted to confirm that full length γ-BAR is also able to bind to kinesin in affinity purification experiments (pull down assays). To this aim, we prepared GST-fusion proteins comprising full length rat γ-BAR, a splice variant missing exon 6 (aa 92-124) or human γ-BAR Δ51. All three GST-γ-BAR fusion proteins were able to pull down conventional kinesin heavy chains as well as AP-1 (γ-adaptin), but not clathrin light chains used as a negative control (Figure 3-10).

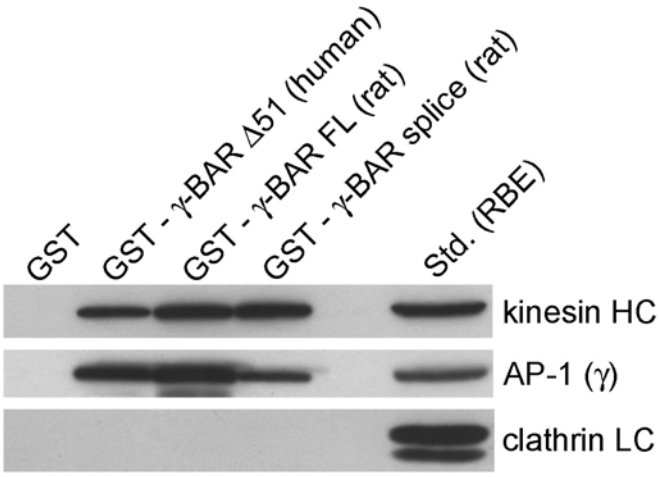

Figure 3-10: Several γ-BAR versions are able to pull down kinesin heavy chains (kinesin HC) and γ-adaptin (AP-1) from rat brain extracts

GST-tagged human γ-BAR Δ51 as well as rat γ-BAR full length (FL) and a splice variant thereof were purified and 20 µg of each fusion protein were used for pull down assays from Triton X-100 extracted rat brain homogenates (1.4 mg total protein each). Kinesin HC and γ-adaptin (AP-1) binding was confirmed by immunoblotting. Clathrin light chain (LC) antibodies were used as negative control. Std., standard (50 µg rat brain extract)

3.4.2 γ-BAR directly interacts with the light chains of conventional kinesins

In order to analyze whether the interaction between γ-BAR and conventional kinesins is direct, we performed *in vitro* binding assays using *in vitro* translated kinesin heavy chains (mouse KIF5C) and light chains (mouse Klc2) in GST pull down experiments.

As a positive control for binding, we used translated "ear" domains of AP-1γ. [^{35}S]-methionine labeled proteins were offered to GST-γ-BAR Δ51 or GST as a control. Samples were analyzed by autoradiography.

Kinesin light chain Klc2 but not the KIF5C heavy chain directly interacted with γ-BAR in this assay. However, it should be noted that the kinesin heavy chain was subject to partial degradation.

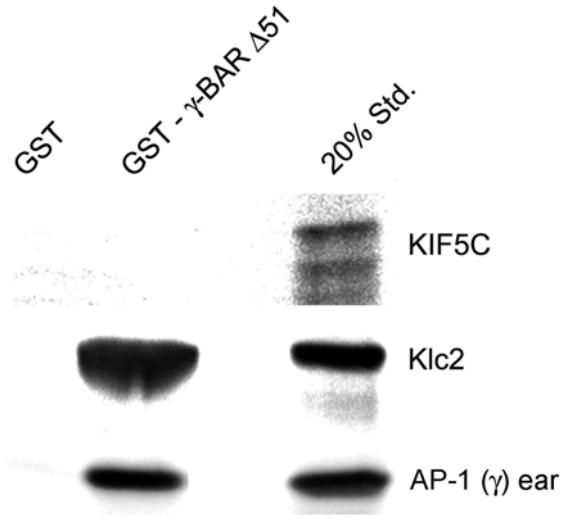

Figure 3-11: γ-BAR directly binds kinesin light chains

In vitro synthesized, [^{35}S]-labeled kinesin heavy chains (KIF5C), light chains (Klc2) and γ-adaptin ear domains (positive control) were incubated with 12.5 µg GST or GST-γ-BAR Δ51 bound to beads. Samples were analyzed by SDS-PAGE followed by autoradiography. 20% Std, 1/5 of total amount of *in vitro* translated proteins used for affinity chromatography.

3.4.3 γ-BAR and kinesin light chains form complexes *in vivo*

To confirm the interaction between γ-BAR and the light chains of conventional kinesins, we analyzed whether the two proteins are present as a complex in cells as well as in native protein extracts by performing co-immunoprecipitation experiments.

First, HEK293 cells were co-transfected with HA-tagged Klc2 and FLAG-tagged γ-BAR. Protein extracts were prepared and used for immunoprecipitation using antibodies against the FLAG epitope tag.

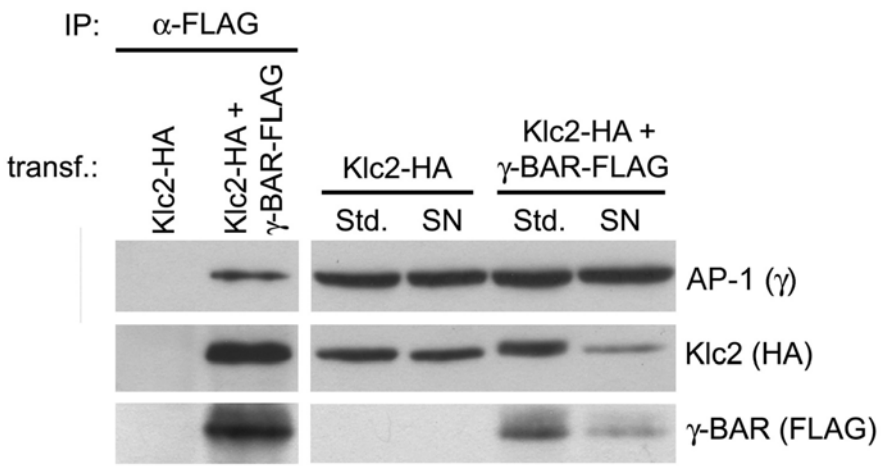

Figure 3-12: γ-BAR and Klc2 can be co-immunoprecipitated from transfected fibroblasts
HEK293 cells were co-transfected with plasmids encoding HA-tagged Klc2 and FLAG-tagged γ-BAR and harvested 24 hours after transfection. Triton X-100 cell lysates (700 µg total protein) were prepared and incubated with anti-FLAG tag antibodies bound to protein A/G agarose beads. Immunoprecipitated proteins were detected by immmunoblotting using antibodies against the protein tags (anti-HA and anti-FLAG tag) or endogenous γ-adaptin. Std., standard: 25 µg of the cell lysate used for immunoprecipitation; SN, supernatant corresponding to 25 µg cell lysate after immunoprecipitation.

FLAG-tagged γ-BAR was precipitated by the anti-FLAG tag antibody (Figure 3-12, lane 2) together with co-transfected HA-Klc2 and endogenous γ-adaptin (AP-1). Klc2 was not precipitated from cells transfected with HA-tagged Klc2 alone (lane 1). Co-immunoprecipitation of the co-transfected proteins was quite efficient since both proteins were partially depleted from the extract after incubation with antibodies (comparison of lane 5 and 6, each corresponding to an aliquot of the input and the supernatant recovered after the IP, respectively).

We also analyzed the subcellular localization of co-transfected γ-BAR-eGFP and HA-Klc2 expressed in HeLa cells by immunofluorescence microsccopy (Figure 3-13). When transfected alone, HA-tagged Klc2 showed mostly cytosolic staining pattern with a moderate perinuclear accumulation. However, when co-overexpressed with γ-BAR-eGFP, the distribution of HA-Klc2 changed dramatically. It was found in peripheral accumulations where it completely co-localized with γ-BAR-eGFP. The observed redistribution of Klc2 towards the cell periphery will be discussed in more detail later on.

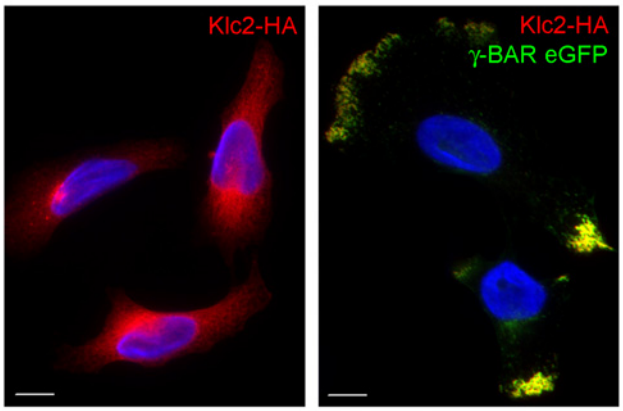

Figure 3-13: Klc2-HA is redistributed by co-transfected γ-BAR-eGFP in HeLa cells

HeLa cells were transfected with constructs encoding HA-tagged Klc2 alone or together with γ-BAR-eGFP and analyzed by immunostaining with an antibody against the HA-tag. When co-overexpressed, γ-BAR-eGFP caused a re-distribution of Klc2-HA to the cell periphery and a complete co-localization of the two proteins. DAPI-stained nuclei are shown in blue. The scale bar represents 10 µm.

Furthermore, we wanted to analyze whether native γ-BAR and Klc2 can be co-immunoprecipitated from tissue extracts. We used Triton X-100 extracted brain homogenates from neonatal rat embryos. Immunoprecipitation experiments were performed using affinity purified polyclonal antibodies against γ-BAR and nonspecific rabbit IgGs as a control.

Our polyclonal anti γ-BAR antibodies were able to efficiently immunoprecipitate endogenous γ-BAR, as the protein was almost completely depleted from the protein extract (compare lanes 5 and 3 in Figure 3-14). Klc2 and γ-adaptin (AP-1) were found together with γ-BAR in these immunoprecipitates. Nonspecific rabbit IgG did not precipitate any of these proteins. The amount of precipitated Klc2 was low compared to the amount of γ-adaptin being co-precipitated together with γ-BAR. Comparably low efficiencies have also been observed for other kinesin-binding partners (see for example Konecna et al., 2006).

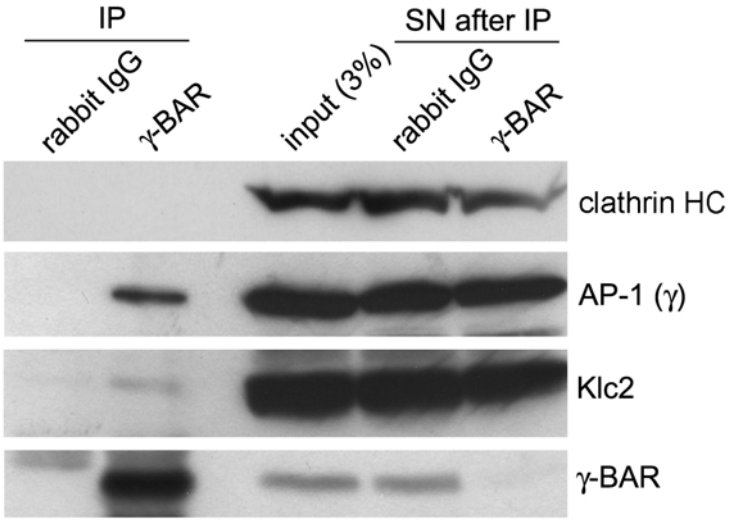

Figure 3-14: Native γ-BAR and Klc2 can be co-immunoprecipitated from brain extracts
Affinity purified polyclonal anti γ-BAR antibodies or non-specific rabbit IgGs (control) were coupled to protein A/G agarose beads and incubated with Triton X-100 protein extracts prepared from fresh neonatal rat (P1) embryonic brains (2 mg total protein each sample). Bound proteins were analyzed by immunoblotting using antibodies against γ-BAR, Klc2 as well as γ-adaptin (AP-1) and clathrin heavy chain (HC) as positive or negative control, respectively. Input, 3% (66 µg) of the total material used for IP; SN, supernatant corresponding to 3% of the lysate after immunoprecipitation.

3.4.4 Kinesin binding by γ-BAR is independent of its membrane association

As shown above, γ-BAR associates with membranes via palmitate lipid anchors attached to cysteine residues at its amino-terminal end. Membrane association might in turn influence binding to conventional kinesins. To investigate this possibility, we transfected Cos7 cells with FLAG-tagged γ-BAR wild type as well as the palmitoylation-defective mutant C4,5,9S and performed co-IPs using anti-FLAG tag antibodies. Then, we analyzed the samples for the presence of endogenous proteins associated with transfected γ-BAR by immunoblotting.

Binding of γ-BAR to conventional kinesins and AP-1 seems to be independent of its membrane association. When expressed in fibroblasts, the palmitoylation-defective mutant of γ-BAR bound to endogenous Klc2 and γ-adaptin to the same extent as the wild type protein (Figure 3-15, lane 2 and 3). None of the proteins was precipitated by the antibody using protein extracts from non-transfected cells (lane 1).

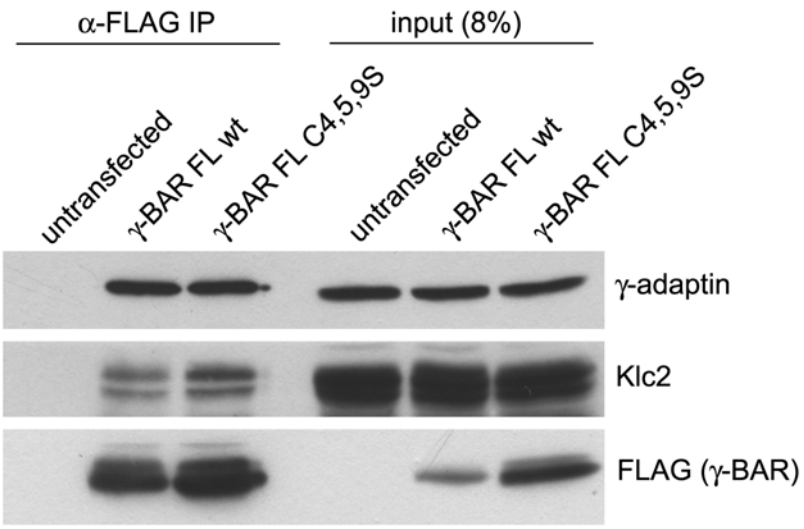

Figure 3-15: Transfected γ-BAR FL and the C4,5,9S mutant bind Klc2 and γ-adaptin

Cos7 cells were transiently transfected with expression plasmids encoding FLAG-tagged γ-BAR or the palmitoylation-defective mutant (C4,5,9S) and Triton X-100 cell extracts (350 µg total protein) were used for co-immunoprecipitation using anti-FLAG tag antibodies immobilized on beads (α-FLAG IP). Endogenous proteins that bound to γ-BAR were analyzed by subjecting the samples to SDS-PAGE and immunoblotting using antibodies against FLAG-tag, Klc2 and γ-adaptin (AP1). Input corresponds to 30 µg (8%) of the cell lysates used for immunoprecipitation.

3.4.5 The carboxy-terminal domain of γ-BAR is required for kinesin binding

We further analyzed which part of γ-BAR is required for kinesin binding. To this aim, two γ-BAR truncation mutants fused to the FLAG-epitope tag were generated. The first mutant comprised amino acids 1 to 140, the second amino acids 140 to 302 of human γ-BAR. Constructs expressing either protein were transfected in Cos7 cells, cell extracts were prepared and used for co-IPs as before. Full length γ-BAR was expressed as a control.

As expected, full length γ-BAR bound to both Klc2 and γ-adaptin (AP-1), whereas the carboxy-terminal fragment of γ-BAR (aa 140-302) was able to bind to Klc2 only (Figure 3-16, lane 2 and 4). In contrast, the amino-terminal fragment (aa 1-140) associated only with γ-adaptin but not Klc2 (lane 3). We conclude, that the binding sites within γ-BAR for AP-1 and Klc2 are distinct.

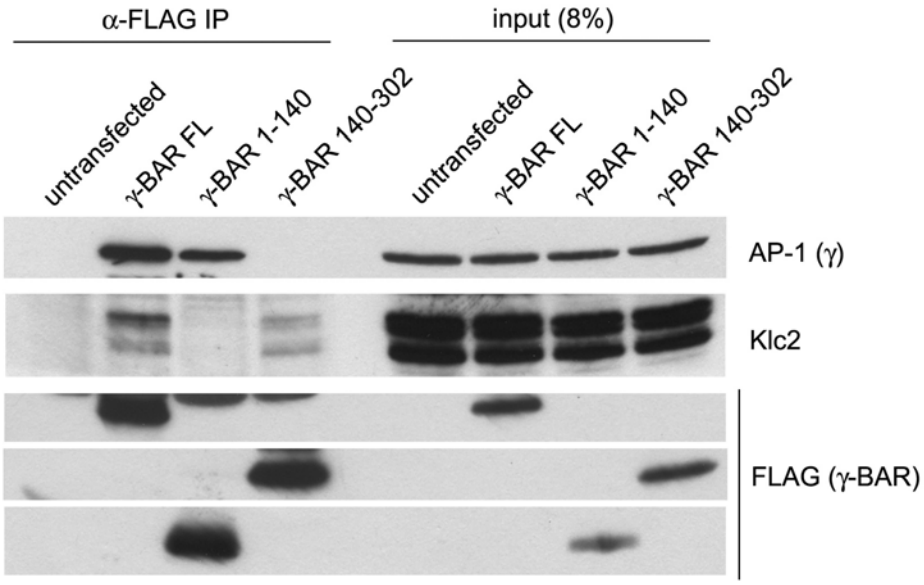

Figure 3-16: AP-1 and Klc2 bind different parts of γ-BAR

Expression plasmids encoding FLAG-tagged γ-BAR full length (FL), aa 1-140 and aa 140-302 constructs were transfected into Cos7 cells. Triton X-100 extracted cell lysates (300 µg total protein) were incubated with anti-FLAG tag antibodies coupled to beads (α-FLAG IP). Bound proteins were analyzed by SDS-PAGE and immunoblotting using antibodies against γ-adaptin (AP-1), Klc2 and FLAG tag. Input corresponds to 25 µg (8%) of the cell lysates used for immunoprecipitation.

3.4.6 The carboxy-terminal part of γ-BAR harbors a tryptophan-based acidic motif important for kinesin binding

Recently, Calsyntenin-1, a neuronal transmembrane protein of the cadherin superfamily of adhesion molecules, was found to directly interact with the TPR motifs of kinesin light chain 1 (Klc1) via its cytoplasmic domain (Konecna et al., 2006). Calsyntenin-1 was found in a subset of vesicles aligned along microtubules in growth cones of primary cortical neurons and shows dynamic properties typical for kinesin-mediated transport. Thus, it might be a cargo-docking protein for kinesin-1-mediated vesicular transport. The binding of calsyntenin-1 to Klc1 is mediated by two conserved binding motifs, termed KBS1 and KBS2 (kinesin-binding segments 1 and 2). These binding motifs have the consensus sequence L/M-E/D-**W**-D-D-S. Mutation of the tryptophans to alanines in both motifs almost completely abolished the binding to Klc1, whereas single mutations in either of the motifs reduced the binding to about 30%. The carboxy-terminal part of γ-BAR, which binds to Klc2, contains two similar motifs: L-E-**W**-E-D-E (aa 208-213) and L-E-**W**-E-N-D (aa 258-263) with the first motif being more closely related to the

defined consensus sequence. Both motifs are completely conserved between human, mouse and rat γ-BAR. We generated single point mutants of γ-BAR by mutating the tryptophans within either of the two motifs to alanines (γ-BAR W210A and γ-BAR W260A) as well as a double point mutant (γ-BAR W210/260A). GST-tagged γ-BAR Δ51 mutants were then used in pulldown assays from rat brain extracts to analyze their binding to conventional kinesin (Figure 3-17). We found that the first putative kinesin light chain binding motif of γ-BAR (aa 208-213) seems to be important for the association with kinesin, since a tryptophan to alanine exchange at position 210 completely abolished binding (lane 3). Mutation of the tryptophan residue within the second motif (aa 258-263) did not have a major effect on Klc binding, although the binding of kinesin to that mutant construct seemed to be diminished (lane 4). None of the mutations affected binding to AP-1.

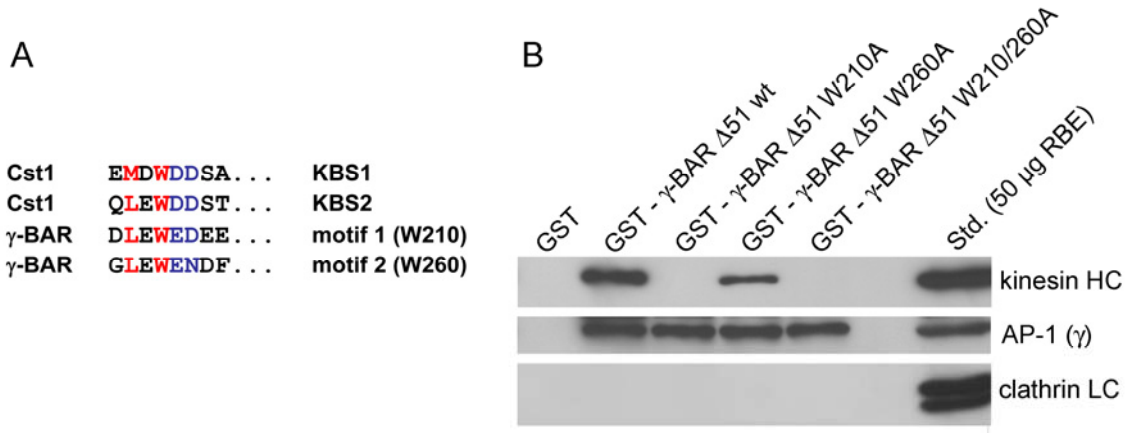

Figure 3-17: Mutation of a single tryptophan to alanine in a putative kinesin light chain binding motif of γ-BAR abolishes binding to conventional kinesin

(A) Sequence comparison between the kinesin-binding segments (KBS) 1 and 2 of Calsyntenin-1 (Cst1) and the two similar motifs found in γ-BAR. Residues shown to be important for kinesin light chain binding (Konecna et al., 2006) are color-coded.

(B) GST, GST-γ-BAR Δ51 and point mutants thereof (W210A, W260A and the double mutant W210/260A) were purified and 20 µg of each fusion protein were incubated with 1.6 mg rat brain extract. Samples were subjected to SDS-PAGE and immunoblotting using antibodies against kinesin heavy chain (HC), γ-adaptin (AP-1) and clathrin light chain as a control. The W210A mutation completely abolishes binding to conventional kinesin, whereas the interaction with AP-1 is unaffected. Std., standard corresponding to 50 µg rat brain extract (RBE).

3.5 γ-BAR localization and function in living cells

3.5.1 Endogenous γ-BAR associates with the endosomal recycling compartment

Published results point towards an association of γ-BAR with AP-1 at the trans-Golgi network (perinuclear compartment) and on vesicular profiles (Neubrand et al., 2005). However, we did not observe a complete co-localization of endogenous γ-BAR with AP-1 in the perinuclear compartment of HeLa cells. Traditionally, the TGN was seen as the major sorting station for cargo proteins traveling along the biosynthetic route (Griffiths and Simons, 1986). Recent data indicate that sorting can also occur from other organelles (Rodriguez-Boulan and Musch, 2005), such as recycling endosomes (REs). Most frequently, REs are found in a perinuclear location adjacent to the TGN. Thus, the localization of specific markers for the two compartments appears largely overlapping when analyzed by immunofluorescence microscopy. We analyzed the localization of the recycling endosomal markers transferrin receptor (TfR) and Rab11 in relation to endogenous γ-BAR in HeLa cells. For immunofluorescence stainings we used an antibody against endogenous TfR. For the analysis of Rab11, we transfected plasmids encoding myc-tagged Rab11a owed to the lack of specific monoclonal antibodies suitable for immunofluorescence analysis that could be used in combination with our polyclonal γ-BAR antisera.

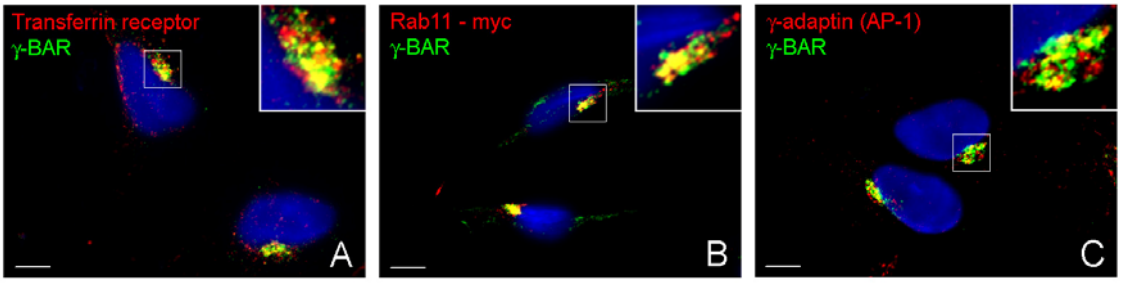

Figure 3-18: Endogenous γ-BAR partially co-localizes with TfR, Rab11 and AP-1

HeLa cells were fixed in methanol und subjected to immunofluorescence stainings for endogenous γ-BAR (green) together with (A) transferrin receptor, (B) transfected myc-tagged Rab11 or (C) AP-1 (all red). DAPI was used to stain nuclei (blue). Deconvolution was used to generate quasi-confocal images. Insets show 3-fold magnified view of boxed areas. The scale bar is 10 µm.

As expected, γ-BAR partially co-localized with AP-1. Furthermore, endogenous γ-BAR also co-localized with endogenous TfR and transfected Rab11 at perinuclear REs. We conclude that γ-BAR might be present at both, the TGN and recycling endosomal membrane profiles. This finding is further supported by the fact that AP-1 is also found at (recycling) endosomes and facilitates anterograde and retrograde transport between the Golgi and endosomes (Hinners and Tooze, 2003).

3.5.2 γ-BAR overexpression re-localizes the recycling endosomal compartment in HeLa cells

Published data on overexpression of eGFP-tagged γ-BAR in Vero cells (Neubrand et al., 2005) show a perinuclear accumulation together with AP-1. We overexpressed the same construct in HeLa cells. To our surprise, a large proportion of the transfected cells displayed a peripheral accumulation of γ-BAR-eGFP labeled membrane structures underneath the plasma membrane. In order to analyze the identity of these organelles, we performed co-stainings in γ-BAR-eGFP overexpressing HeLa cells using antibodies against marker proteins.

AP-1 as well as the RE marker proteins TfR and Rab11 co-localized with overexpressed γ-BAR-eGFP in organellar clusters at the cell periphery. This indicates that upon γ-BAR overexpression, the recycling endosomal compartment is re-located. This activity of γ-BAR might be due to its direct interaction with microtubule associated motor proteins (kinesins) which will be discussed later.

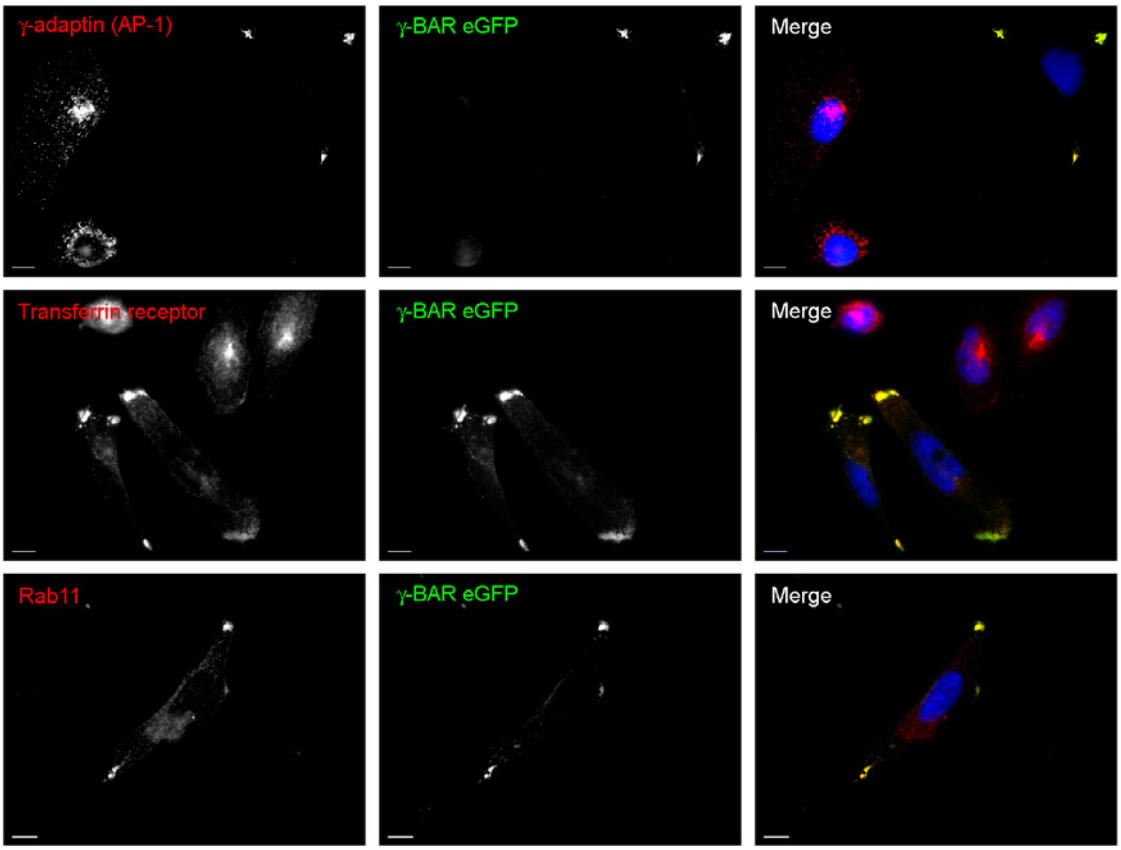

Figure 3-19: γ-BAR overexpression drags the recycling endosomal compartment towards the cell periphery

HeLa cells were transfected with plasmids encoding γ-BAR-eGFP, fixed and processed for immunofluorescence stainings using antibodies against γ-adaptin (top panel), transferrin receptor (middle panel) and Rab11 (lower panel). DAPI-stained nuclei are shown in blue. The scale bar is 10 µm.

To further investigate the nature of the compartment relocalized in γ-BAR-eGFP overexpressing cells, we analyzed a number of additional marker proteins.

A partial co-localization of overexpressed γ-BAR with clathrin was observed, which seemed to selectively affect the perinuclear but not the plasmalemmal pool of clathrin (Figure 3-20, panel A). The TGN/ endosomally localized cation-dependent mannose-6-phosphate receptor MPR46 (panel B) and the trans Golgi marker TGN46 (panel C) also displayed a partial relocation. It should be noted here that TGN46 does not exclusively localize to the trans-Golgi network, but continuously cycles between the TGN and the plasma membrane thereby traveling also through endosomal compartments. No co-localization was observed with the cis-Golgi matrix protein GM130 (panel D). Furthermore, γ-BAR-eGFP at the cell periphery did not overlap with the distribution of the adaptor complex AP-2, which marks coated pits at the plasma membrane (Figure

3-21, panel A), early endosomal antigen 1 (EEA1), a marker for early endosomes (panel B), the late endosomal/ lysosomal marker LAMP-1 (panel C), or the mitochondrial protein cytochrome C (panel D).

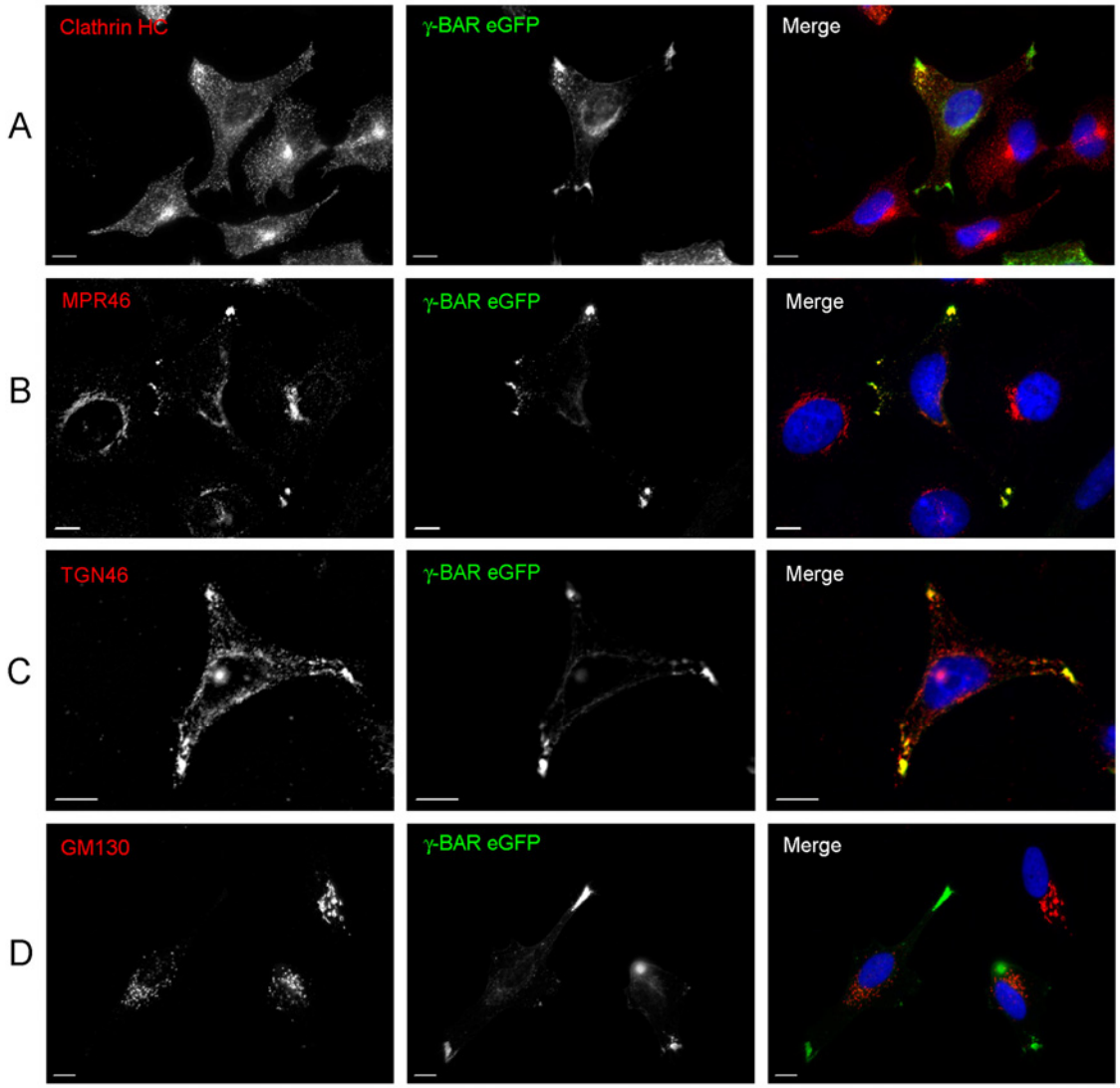

Figure 3-20: Localization of organellar marker proteins in γ-BAR-eGFP expressing HeLa cells
γ-BAR-eGFP expressing HeLa cells were fixed and processed for immunofluorescence microscopy using antibodies against the following marker proteins: **(A)** clathrin heavy chain (HC), **(B)** mannose-6-phosphate receptor (MPR46), **(C)** TGN46 (a non resident trans-Golgi marker) and **(D)** GM130 (cis-Golgi). DAPI-stained nuclei are shown in blue. The scale bar is 10 µm.

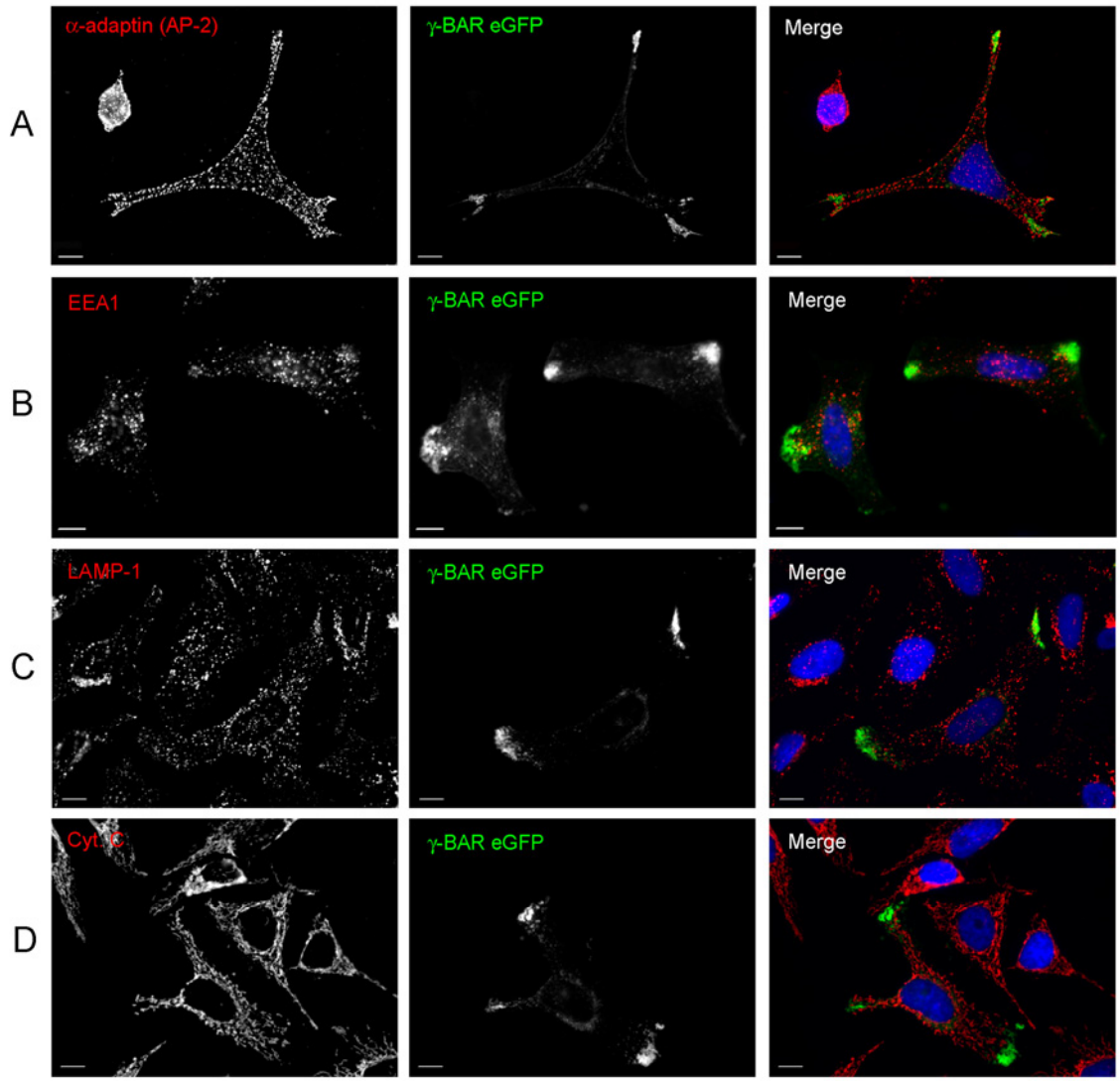

Figure 3-21: Localization of organellar marker proteins in γ-BAR-eGFP expressing HeLa cells
γ-BAR-eGFP expressing HeLa cells were fixed and processed for immunofluorescence stainings using antibodies against the following marker proteins: **(A)** α-adaptin (AP-2, coated pits at plasma membrane), **(B)** EEA1 (early endosomes), **(C)** LAMP-1 (late endosomes/ lysosomes) and **(D)** Cytochrome C (Cyt. C, mitochondria). DAPI-stained nuclei are shown in blue. The scale bar is 10 µm.

3.5.3 The γ-BAR induced re-localization of recycling endosomes is dependent on intact microtubules and conventional kinesin KIF5

Based on the observations that (i) γ-BAR directly interacts with conventional kinesins (see above), (ii) upon overexpression associates with highly mobile membrane carriers throughout the cell (timelapse movies and (Neubrand et al., 2005)) and (iii) the corresponding shift of perinuclear REs towards the cell periphery, we speculate that γ-BAR is involved in the transport and/ or intracellular positioning of these organelles.

Thus, the accumulation of REs at the cell periphery upon γ-BAR overexpression should depend on microtubules and associated motor proteins like conventional kinesins. To test this, we treated HeLa cells with the microtubule de-polymerizing agent nocodazole and analyzed the distribution of transfected γ-BAR-eGFP and endogenous kinesin.

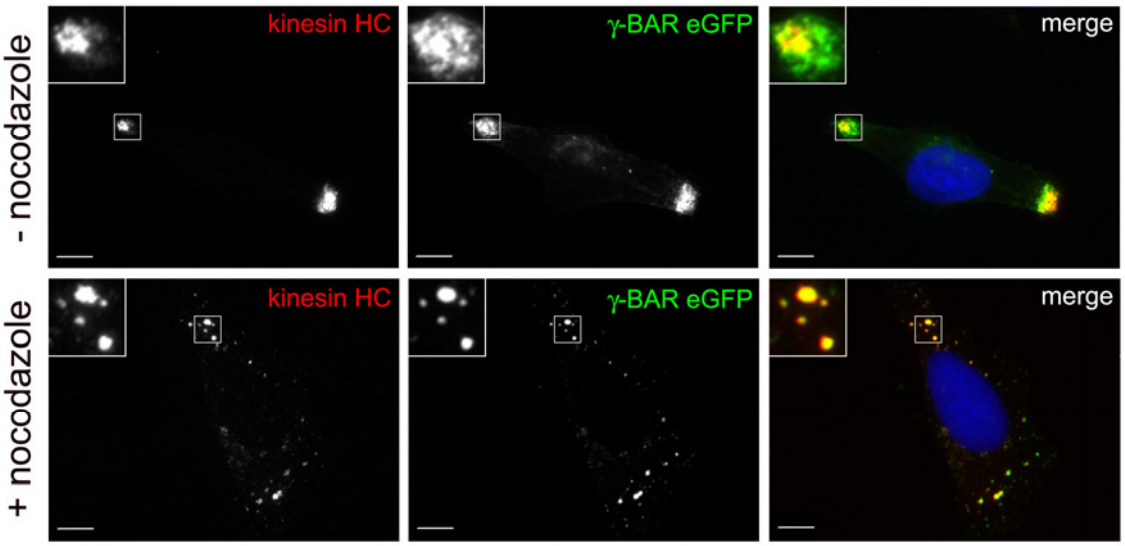

Figure 3-22: Nocodazole treatment disperses the peripherally accumulated compartment
HeLa cells were transfected with constructs encoding γ-BAR-eGFP, treated with 10 µM nocodazole for 1 hour at 37°C (lower panel) or left untreated (control, upper panel), fixed and stained for endogenous conventional kinesin using antibodies against ubiquitous kinesin heavy chains (HC). DAPI-stained nuclei are shown in blue. Insets represent 3-fold magnification of boxed areas. The scale bar is 10 µm.

Conventional kinesin accumulated together with γ-BAR-eGFP in the peripheral compartment (Figure 3-22, upper panel). This accumulation is quite striking since non-transfected HeLa cells did not display a similar staining pattern when using the kinesin antibody at the same dilution (data not shown). Following treatment with nocodazole, the peripheral compartment got dispersed into smaller discrete membrane structures containing γ-BAR-eGFP. Kinesin remained associated with these structures. Additionally, we examined the distribution of AP-1 and TfR in γ-BAR-eGFP expressing cells after nocodazole treatment (Figure 3-23). Also these two marker proteins were associated with the dispersed compartment.

These results demonstrate that the accumulation and positioning of the peripheral compartment is dependent on microtubules and perhaps on the activity of microtubule-associated motor proteins, i.e. conventional kinesins.

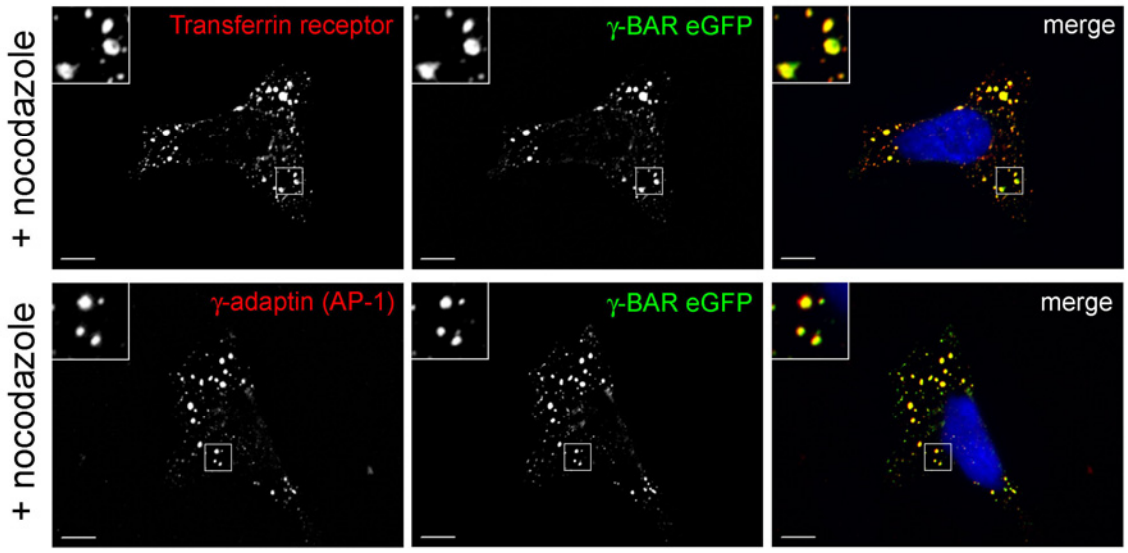

Figure 3-23: TfR and AP-1 stay associated with the dispersed compartment after nocodazole treatment

γ-BAR-eGFP expressing HeLa cells were treated as described in Figure 3-22 and stained for endogenous transferrin receptor (upper panel) and AP-1 (lower panel). Insets show 3-fold magnified view of boxed areas. DAPI-stained nuclei are shown in blue. The scale bar is 10 µm.

In order to analyze whether the γ-BAR driven accumulation of the RE compartment is indeed dependent on conventional kinesin, we treated HeLa cells with two different pre-designed siRNAs (Qiagen) against the ubiquitous kinesin-1 heavy chain family member KIF5B and analyzed the distribution of co-transfected γ-BAR-eGFP in these cells. Knockdown efficiency was controlled by immunostaining for endogenous conventional kinesin heavy chain. Knockdown of KIF5B resulted in a significantly higher degree of perinuclear accumulation of γ-BAR-eGFP-containing organelles. 86% or 90% of the siRNA treated cells displayed a perinuclear accumulation of γ-BAR, whereas only 12% of the control siRNA treated cells contained perinuclear γ-BAR-eGFP (Figure 3-24).

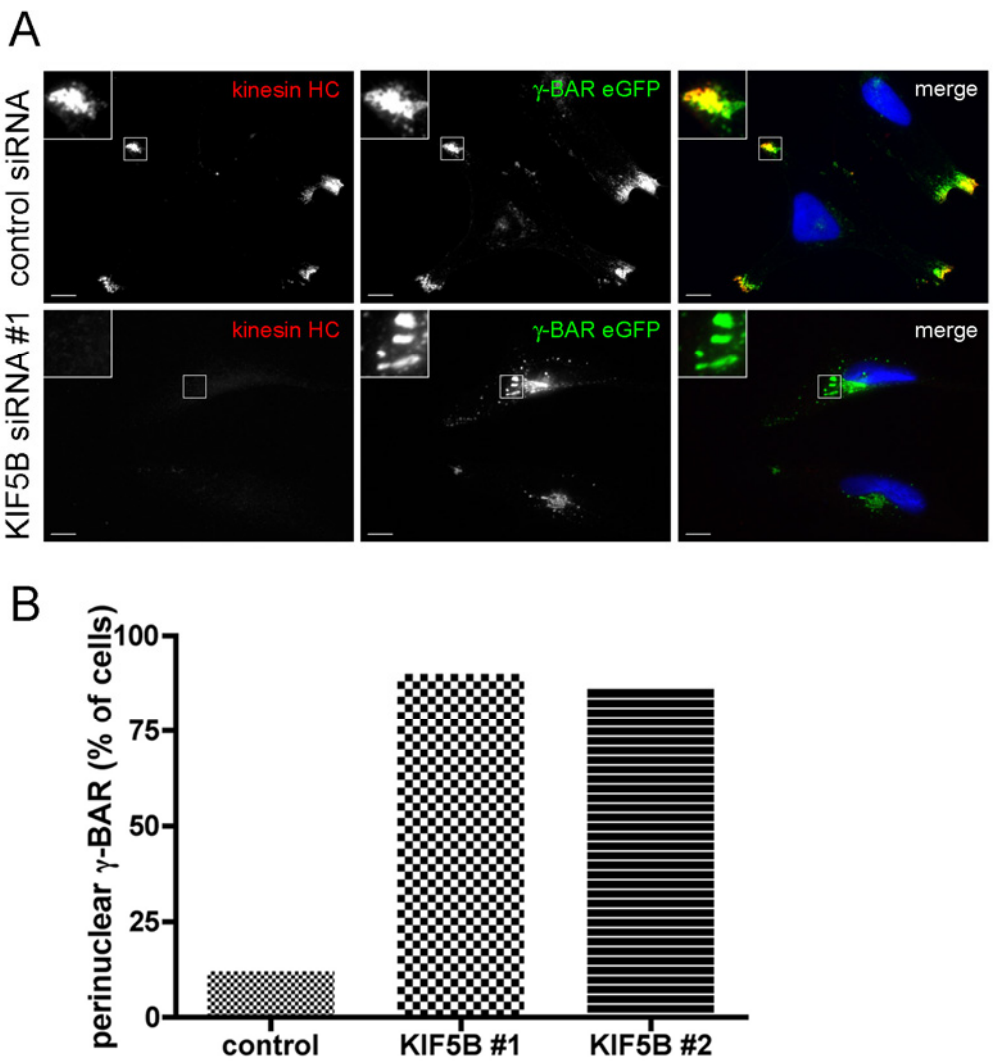

Figure 3-24: Intact kinesin KIF5 is necessary for the γ-BAR induced re-localization of REs

(A) HeLa cells were treated twice with siRNAs against the ubiquitous kinesin heavy chain KIF5B or a control siRNA (day 1 and 4) and co-transfected with expression plasmids encoding γ-BAR-eGFP (day 4). On day 5 cells were fixed and immunostained using antibodies against conventional kinesin heavy chain (HC). KIF5B siRNA-treated cells were devoid of kinesin immunoreactivity and displayed a high degree of perinuclear accumulated γ-BAR-eGFP. Insets represent 3-fold magnification of boxed areas. DAPI-stained nuclei are shown in blue. The scale bar is 10 µm.

(B) Quantification of the effects exemplified in (A). The fraction of γ-BAR-eGFP transfected cells containing perinuclear accumulated γ-BAR was plotted. Two different siRNAs against KIF5B gave almost identical results. 50 cells were scored for each data point.

Using co-immunoprecipitation experiments we could show that an amino-terminal fragment of γ-BAR comprising amino acids 1-140 does not bind to kinesin (see Figure 3-16), but maintains its membrane association due to palmitoylation. We sought to investigate the subcellular distribution of this construct and its effect on the RE marker protein TfR and on conventional kinesin. We therefore transfected HeLa cells with an eGFP-tagged version of γ-BAR (aa 1-140) and analyzed fixed cells with antibodies against endogenous TfR and kinesin HC (Figure 3-25).

The amino-terminal fragment of γ-BAR localized to membranes in a perinuclear compartment but also to discrete endosomally-like structures dispersed throughout the cytoplasm. These structures strikingly resemble the dispersed organelles visible after nocodazole treatment (see Figure 3-22 and Figure 3-23). γ-BAR (aa 1-140)-eGFP containing structures were immuno-positive for TfR but did not contain kinesin. Thus, it appears that the carboxy-terminal domain of γ-BAR facilitates recruitment of conventional kinesin to membranes and that this interaction is crucial for the peripheral accumulation of REs. Disruption of microtubules or transfection of a kinesin binding-deficient γ-BAR mutant led to a dispersed distribution of TfR positive REs.

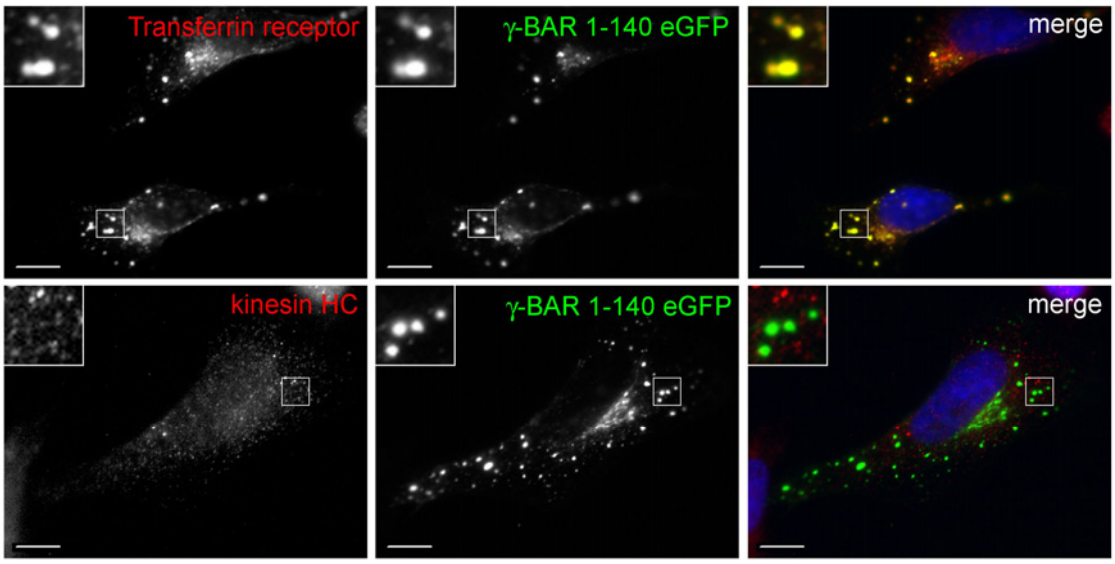

Figure 3-25: γ-BAR (aa 1-140) co-localizes with TfR but not with kinesin

HeLa cells were transfected with plasmids encoding eGFP-tagged γ-BAR (aa 1-140), fixed and processed for immuno-fluorescence staining using antibodies against transferrin receptor (upper panel) and kinesin HC (lower panel). DAPI-stained nuclei are shown in blue. Insets represent 3-fold magnification of boxed areas. The scale bar is 10 µm.

3.5.4 Conventional kinesin KIF5 is necessary for the positioning of transferrin-containing endosomes

Based on our observation that conventional kinesin KIF5 is necessary for γ-BAR induced re-localization of REs to the cell periphery, we hypothesized that KIF5 plays a role in the intracellular transport and positioning of REs. To test this hypothesis, KIF5B was knocked down in HeLa cells as described above and cells were loaded with fluorescently labeled transferrin for one hour. After fixation, the cells were imaged using spinning disc confocal microscopy. Strikingly, cells treated with siRNAs against KIF5B showed enhanced peri-nuclear accumulation of transferrin compared to control treated cells (Figure 3-26). These data can either be explained by enhanced clustering of REs or delayed recycling of Tf from perinuclear endosomes.

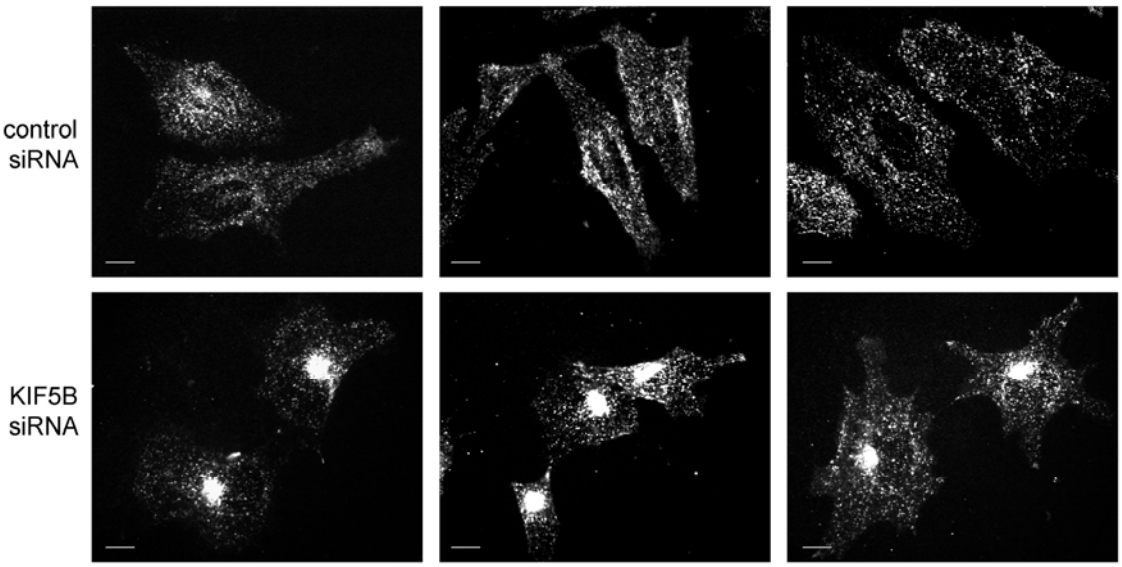

Figure 3-26: KIF5B knockdown promotes peri-nuclear clustering of Tf-loaded endosomes
HeLa cells were treated twice with siRNAs against ubiquitous kinesin heavy chain KIF5B or a control siRNA (day 1 and 3). 48 hours after the 2nd transfection (day 5), cells were allowed to internalize Alexa Fluor 568-labeled transferrin for at least one hour, fixed and imaged by confocal microscopy. Each panel shows three examples of control and siRNA-treated cells. KIF5B knockdown causes a huge peri-nuclear accumulation of Tf-positive endosomes. The scale bar is 10 µm.

3.5.5 γ-BAR knockdown in HeLa cells

We designed blunt 27-mer siRNAs against the human γ-BAR cDNA sequence and verified their efficiency to knock down γ-BAR in HeLa cells. Such blunt 27-mer RNA duplexes have been shown to be more potent effectors of RNAi than traditional 21mer siRNAs (Kim et al., 2005). Using the designed siRNAs, we observed a near complete knockdown of γ-BAR judged from immunoblots (Figure 3-27).

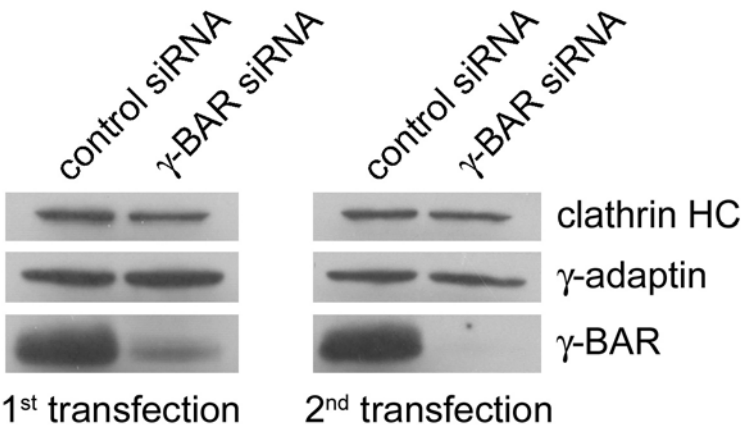

Figure 3-27: siRNA mediated knockdown of γ-BAR in HeLa cells

HeLa cells were transfected twice with a 27-mer siRNA against γ-BAR and a non-targeting control siRNA. Cell extracts were prepared 3 days after each transfection round and subjected to immunoblotting using antibodies against γ-BAR as well as γ-adaptin (AP-1) and clathrin HC as controls.

We analyzed γ-BAR-deficient HeLa cells by indirect immunofluorescence microscopy against different marker proteins. Since knockdown of γ-BAR was highly efficient, we mixed cells separately treated with γ-BAR or control siRNAs after two rounds of transfection before seeding them onto coverslips. This allowed us to analyze knockdown and control cells on the same coverslip using antibodies against γ-BAR (Figure 3-28).

We did not observe any obvious differences in the steady state distributions of AP-1, TfR or the 46 kDa mannose-6-phosphate receptor (MPR46) between γ-BAR knockdown or control siRNA-treated cells. All three markers remained associated with the perinuclear compartment in the absence of γ-BAR as judged from the immunofluorescence images. We could also not confirm the published observation that AP-1 loses its juxta-nuclear localization in HeLa cells lacking γ-BAR (Neubrand et al., 2005).

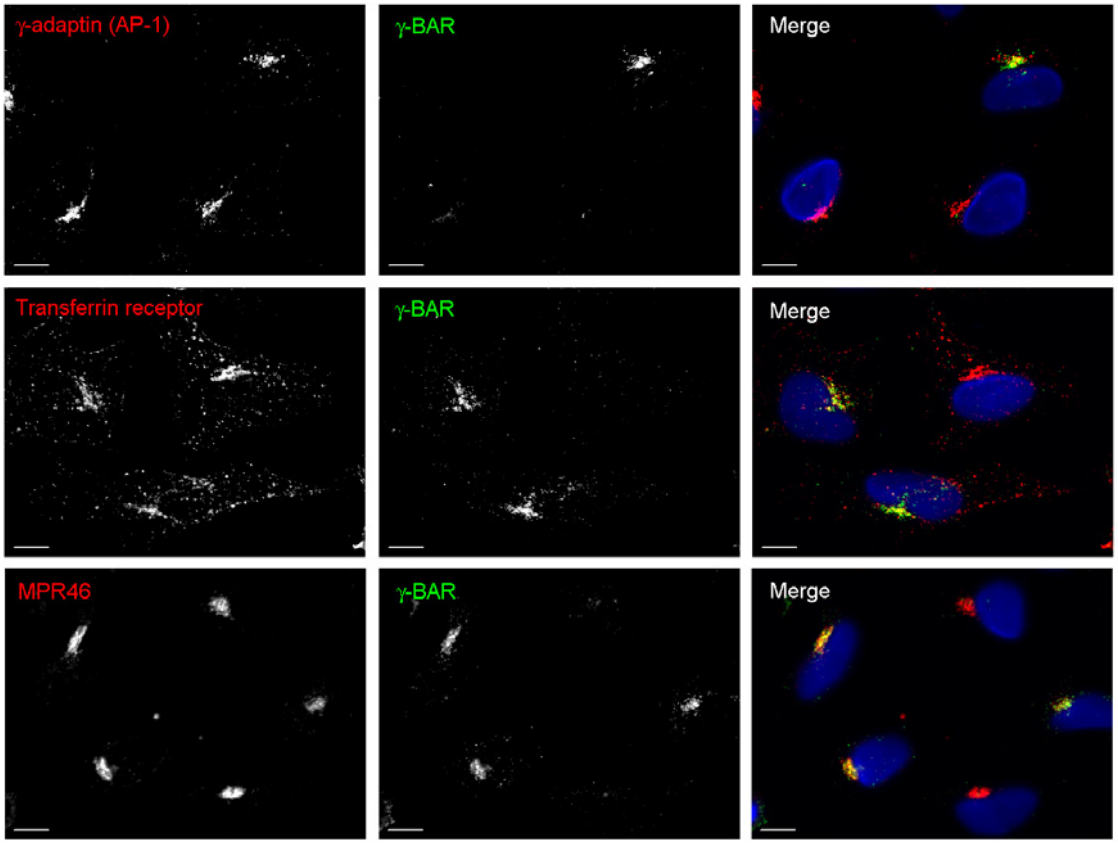

Figure 3-28: γ-BAR knockdown does not influence the steady state distribution of marker proteins
Anti-γ-BAR and control siRNAs were used separately to transfect HeLa cells twice using Oligofectamine (48 hours between the two rounds of transfection). γ-BAR knockdown and control treated cells were mixed before seeding them onto coverslips and fixed 48 hours after the second round of transfection. Immunofluorescence analysis was performed using antibodies against γ-BAR (green) and γ-adaptin/ AP-1 (upper panel), transferrin receptor (middle panel) or mannose-6-phosphate receptor (MPR46, lower panel) in red. DAPI stained nuclei are shown in blue. The scale bar is 10 µm.

3.6 γ-BAR effects the rate of transferrin recycling

3.6.1 γ-BAR overexpression causes retention of internalized transferrin in the peripheral compartment

Based on our observation that γ-BAR overexpression causes an accumulation of recycling endosomal organelles positive for AP-1, TfR and Rab11 in the periphery of HeLa cells, we sought to examine the fate of internalized ligands that are sorted towards recycling endosomes. After binding of iron-saturated transferrin (diferric Tf) to its receptor (TfR), the receptor-ligand complex is rapidly endocytosed into peripheral early endosomes. The acidic pH of this compartment causes the release of iron from transferrin, whereas Tf itself remains bound to TfR and the complex recycles back to the cell surface via two distinct routes: direct sorting from early endosomes to the plasma membrane (fast recycling) or via a slower pathway involving perinuclear Rab11-positive REs.

We allowed γ-BAR overexpressing cells to internalize fluorescently labeled transferrin (pulse). Internalized Tf was then chased for different periods of time to analyze the rate of recycling. After internalization, Tf was found in endosomal structures throughout the cell and in perinuclear REs. In γ-BAR overexpressing cells internalized Tf localized to the peripheral compartment together with its receptor, thus confirming the identity of these organelles as REs. Interestingly, recycling from this peripheral RE compartment was delayed (Figure 3-29). After 30 minutes of recycling, about 55% of the labeled transferrin remained associated with the peripheral compartment in γ-BAR overexpressing cells. By contrast, in non-transfected cells, most of the Tf had recycled back to the cell surface and only 8% of the initial fluorescence was still present inside the cells.

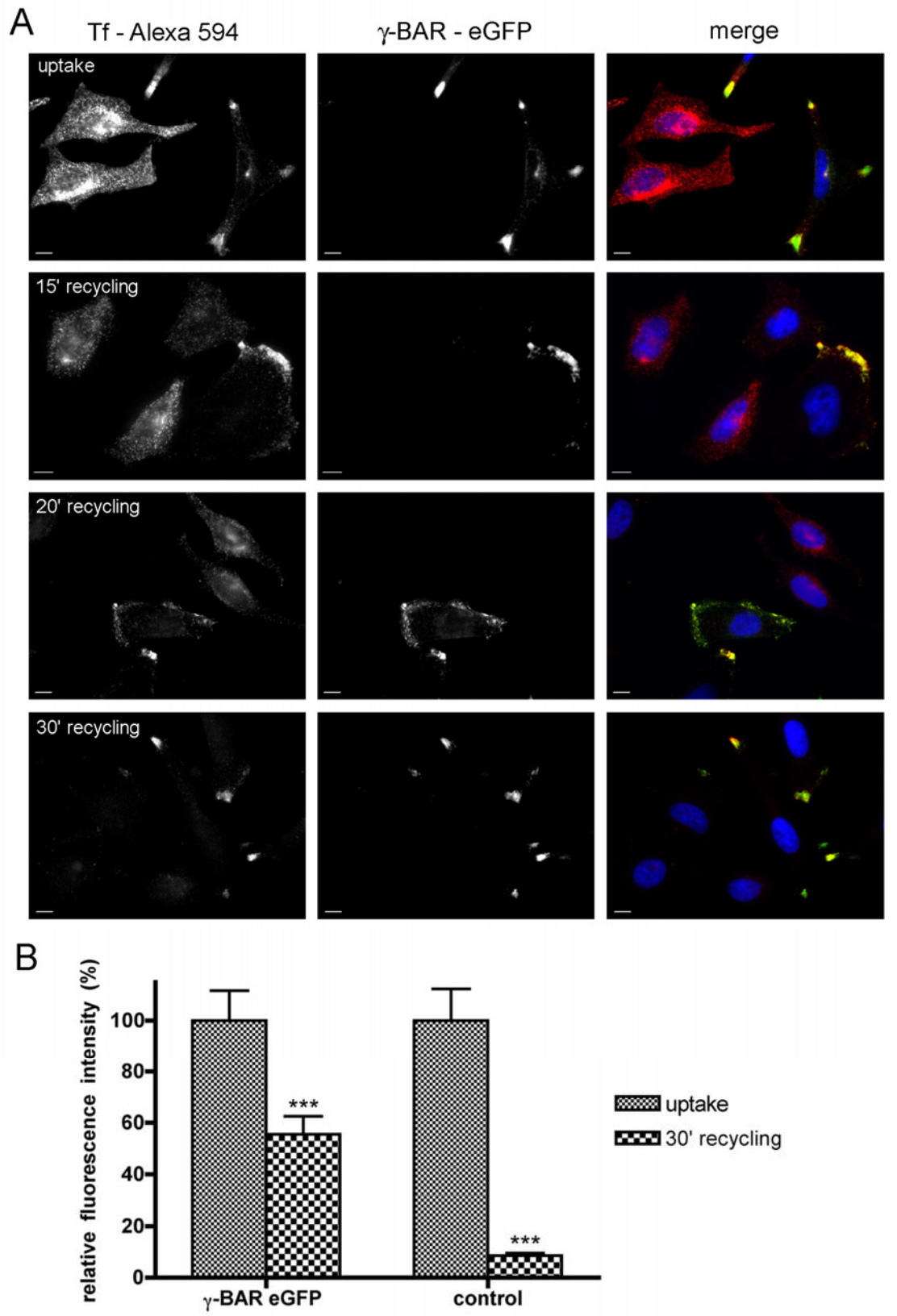

Figure 3-29: Internalized Tf is relocated to peripheral γ-BAR-eGFP-positive REs and its recycling is delayed

(A) HeLa cells were transfected with expression plasmids encoding γ-BAR-eGFP. 24 hours after transfection, cells were serum starved and incubated with medium containing 25 µg/ml Alexa Fluor 594 labeled transferrin (uptake). Cells were washed and incubated with 40-fold excess of unlabeled Tf to

allow recycling of the labeled ligands (chase). Cells were fixed after different periods of time (15, 20 and 30 min of recycling) and processed for fluorescence microscopy. DAPI stained nuclei are shown in blue. The scale bar is 10 µm.

(B) Quantification of the microscopic images (uptake and 30 min recycling) in panel A was achieved using the microscopy software Slidebook 4.1 (Intelligent Imaging Innovations). We determined mean fluorescence values for γ-BAR-eGFP transfected or control cells in the same frame. For transfected cells we defined a mask that covered the areas of the cells were γ-BAR-eGFP is accumulated (green channel) and determined the mean fluorescence intensity of the red channel (Tf - Alexa 594) inside that mask. For control cells, the entire cells were selected (mask drawn by hand) and mean fluorescence intensities were determined. We averaged the values of 25-30 cells analyzed from 13-15 frames for each data point and normalized to the values for the uptake time point. Error bars represent s.e.m.; *** indicates statistically significant differences with $P<0.0001$ (unpaired t test, two-tailed P value).

3.6.2 γ-BAR knockdown accelerates the rate of transferrin recycling

As demonstrated above, γ-BAR overexpression caused a delay in the recycling of Tf back to the cell surface. However, this effect might be non-specific. To further analyze the role of endogenous γ-BAR in Tf recycling we transfected HeLa cells with siRNAs against γ-BAR (27mer) or a non-targeting siRNA as a control. Quantitative Tf-recycling was then assayed using [^{125}I]-labeled Tf and scintillation counting. Recycling of Tf appeared to be accelerated at early time points (up to 12 minutes) in γ-BAR-depleted versus control cells (Figure 3-30). The largest difference was seen after 9 minutes of recycling, where 35% of the internal Tf was left in knockdown compared to 58% in the control cells. However, at later time points of recycling (20-30 minutes) no significant difference was detectable between the two cell populations (data not shown). These data indicate that knockdown of γ-BAR might lead to a shift of Tf recycling towards a fast pathway, perhaps via Rab4-positive early endosomes. A possible explanation could be that loss of γ-BAR results in inhibition of RE function.

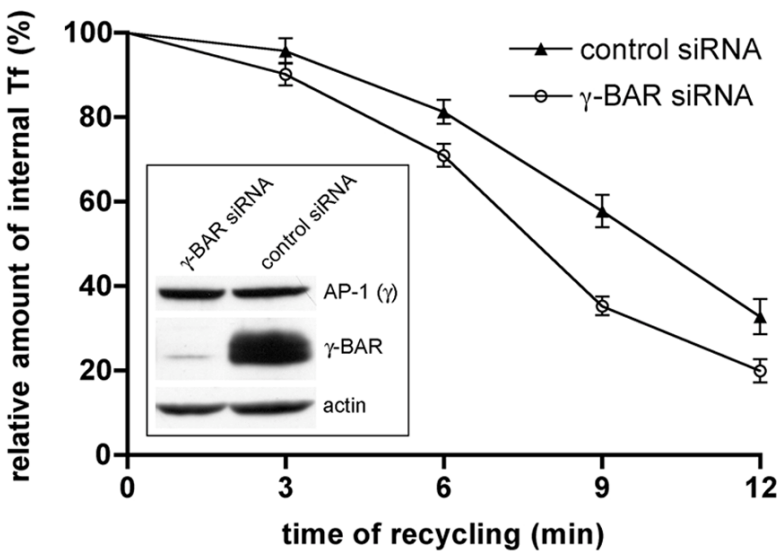

Figure 3-30: γ-BAR knockdown accelerates the rate of Tf-recycling

HeLa cells were transfected twice with a siRNA against γ-BAR or a non-targeting siRNA (see inset for knockdown efficiency), starved for at least 2 hours and used for quantitative Tf-recycling experiments with [^{125}I]-labeled transferrin. Uptake was allowed for 30 minutes in 20 µg/ml holo-Tf supplemented with ~300 ng/ml labeled Tf with a specific activity of 0.3-1.0 µCi/µg. Cells were extensively washed on ice. For recycling, cells were chased in medium containing 100x fold excess (2 mg/ml) of unlabeled Tf for different periods of time, washed to remove surface bound Tf and extracted using 1% Triton X-100 in PBS. The extracts were mixed with liquid scintillation cocktail and counts per minute (CPM) were measured in a liquid scintillation counter. Initial CPM values (uptake) were set to 100%. Each datapoint represents the mean of eleven values from five different experiments. Error bars represent s.e.m.

3.6.3 γ-BAR knockdown has no influence on the rate of transferrin uptake

We further investigated the effect of γ-BAR knockdown on TfR trafficking by analyzing the amount of internalized [^{125}I]-labeled Tf after different periods of time (Tf uptake). Identical amounts of γ-BAR siRNA and control treated Hela cells were seeded onto 12-well plates and used for [^{125}I]-Tf uptake experiments essentially as described for the recycling experiments above. Cells were allowed to internalize Tf for different periods of time and cell lysates were used for liquid scintillation counting. Knockdown of γ-BAR did not have any detectable effect on the amount of internalized Tf in HeLa cells, indicating that γ-BAR is not involved in the endocytosis of membrane proteins, i.e. TfR from the plasmalemma.

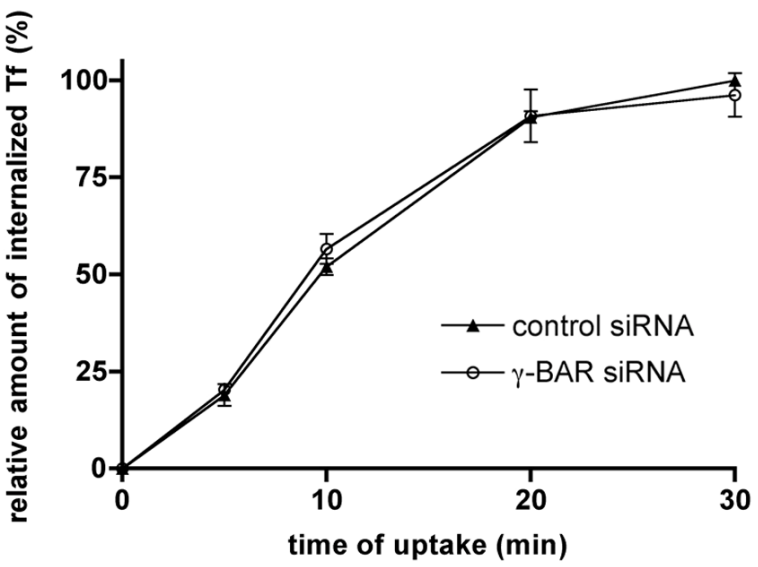

Figure 3-31: γ-BAR knockdown does not influence the amount of internalized Tf

HeLa cells were transfected twice with a siRNA against γ-BAR or a non-targeting siRNA (control), starved for at least 2 hours and used for quantitative Tf-uptake experiments with [^{125}I]-labeled transferrin. Uptake was allowed for the indicated periods of time (5, 10, 20 and 30 minutes) in medium containing 20 µg/ml holo-Tf supplemented with ~300 ng/ml labeled Tf (specific activity of 0.3-1.0 µCi/µg). Cells were extensively washed on ice to remove surface bound Tf and extracted using 1% Triton X-100 in PBS. The extracts were added to liquid scintillation cocktail and counts per minute (CPM) were measured in a liquid scintillation counter. Values were normalized to the 30 minutes uptake value of the control treated cells (100%). Each datapoint represents the mean of four values from two independent experiments. Error bars represent s.e.m. The efficiency of the knockdown was routinely checked by immunoblot analysis as seen in Figure 3-30.

3.7 γ-BAR localization and function in neurons

3.7.1 Localization of endogenous and overexpressed γ-BAR

Endogenous γ-BAR localization was examined by indirect immunofluorescence microscopy against the protein in cultured hippocampal neurons from E18 rat embryos at different time points after preparation. We obtained a specific perinuclear labeling for γ-BAR in the cell body which partly co-localized with γ-adaptin (AP-1) and TfR at different stages of development (data by Carlos Dotti and colleagues and own data, see also Figure 3-34 for γ-BAR labeling). However, a specific labeling in axons or dendrites could not be detected using our purified polyclonal antibodies.

We also expressed a splice variant of rat γ-BAR lacking 33 amino acids in the central domain as an eGFP-fusion protein in primary hippocampal neurons. Cells were transfected at day 9 after preparation (DIV 9) and fixed the next day. Overexpressed γ-BAR accumulated in spots along neurites and in growth cones of growing neurites, presumably axons. These accumulations contained AP-1, TfR and kinesin HC (Figure 3-32), suggesting that they were of RE origin.

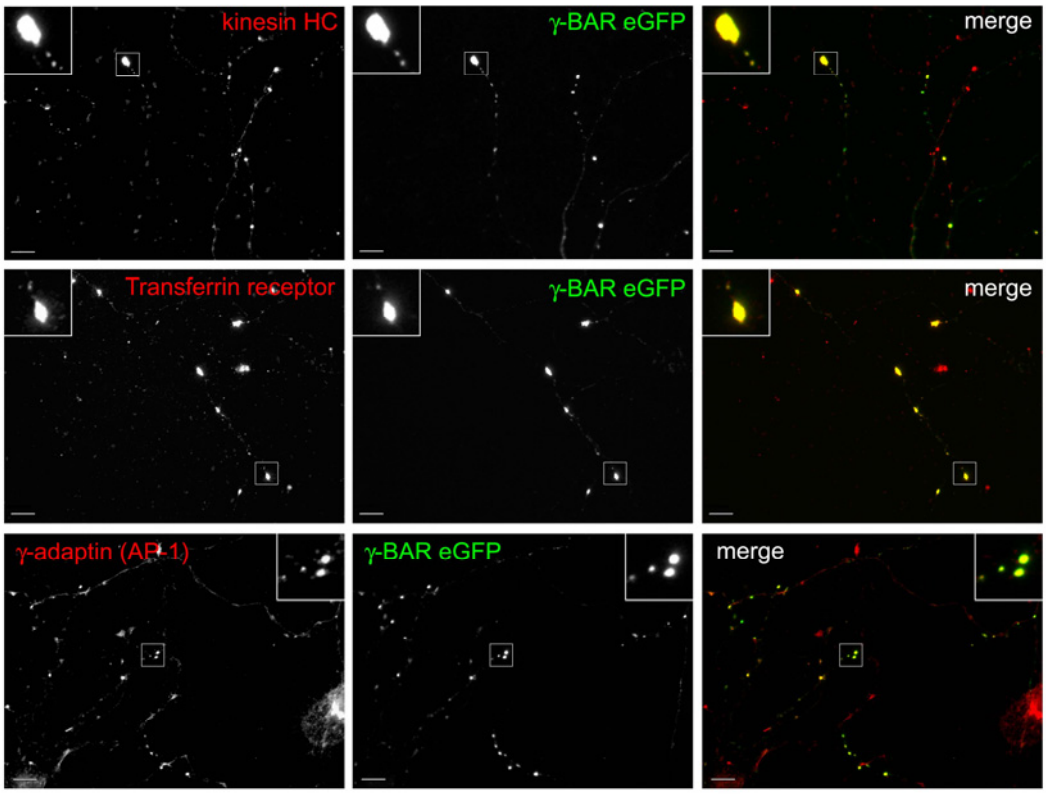

Figure 3-32: γ-BAR-eGFP co-localizes with AP-1, TfR and kinesin KIF5 in cultured neurons
Plasmids encoding eGFP-tagged γ-BAR (splice variant) were transfected into cultured hippocampal neurons at DIV 9 using Effectene and fixed 24 hours after transfection (DIV 10). Cells were processed for immunofluorescence staining using antibodies against conventional kinesin HC (upper panel), transferrin receptor (middle panel) and γ-adaptin (lower panel). Insets show 3-fold magnified view of boxed areas. The scale bar is 10 µm.

3.7.2 Influence of γ-BAR on neurite outgrowth in developing neurons

Recent studies revealed that the recycling endosomal compartment is involved in a variety of membrane trafficking events and might thereby control cellular processes ranging from cellular polarization over cytokinesis to cell fate specification (van Ijzendoorn, 2006). REs can also serve as an intermediate sorting station for proteins from the TGN *en route* to the plasma membrane as well as back to the TGN. They might also be a sorting station for proteins, such as the 46 kDa cation-independent mannose-6-phosphate receptor (MPR46), destined for the late endosomal/ lysosomal pathway and back (Lin et al., 2004). Furthermore, in neurons it has been shown that REs are crucial for postsynaptic AMPA receptor trafficking and the regulation of synaptic plasticity (Park et al., 2004) as well as the delivery of membrane material for the growth of dendritic spines (Park et al., 2006). We thus speculated that recycling endosomes might be involved in the delivery of membrane bounded organelles for neurite outgrowth, a process that is highly dependent on the redistribution of membranes and associated proteins towards the site of membrane addition, in this case the growth cones of neurites. A possible source of membrane material are REs. As γ-BAR is associated with and might regulate the transport of REs, it could well be involved in the process of neurite outgrowth and/ or axon formation in developing neurons. In fact, in a microscopy based screen to identify novel proteins involved in neurite formation and extension, γ-BAR was found to influence the length of neurites formed by PC12 cells upon stimulation with NGF (Laketa et al., 2007). Thus, we analyzed the effect of γ-BAR overexpression or knockdown on neurite outgrowth in primary hippocampal neurons. We transfected neurons prepared from E18 rat embryos directly after preparation using the Amaxa Nucleofector technology before plating them onto coverslips. Neurite length was analyzed 26 and 54 hours after transfection (stage 2 and 3 of neuronal development) by measuring the length of the longest neurite that would eventually become the axon.

Overexpression of eGFP-tagged γ-BAR full length reduced neurite length by about 30% after 54 hours compared to cells expressing eGFP. These data parallel the effects observed in NGF-stimulated PC12 cells (Laketa et al., 2007). A kinesin binding deficient γ-BAR truncation mutant (aa 1-140) had a less pronounced effect and reduced neurite length by about 15%.

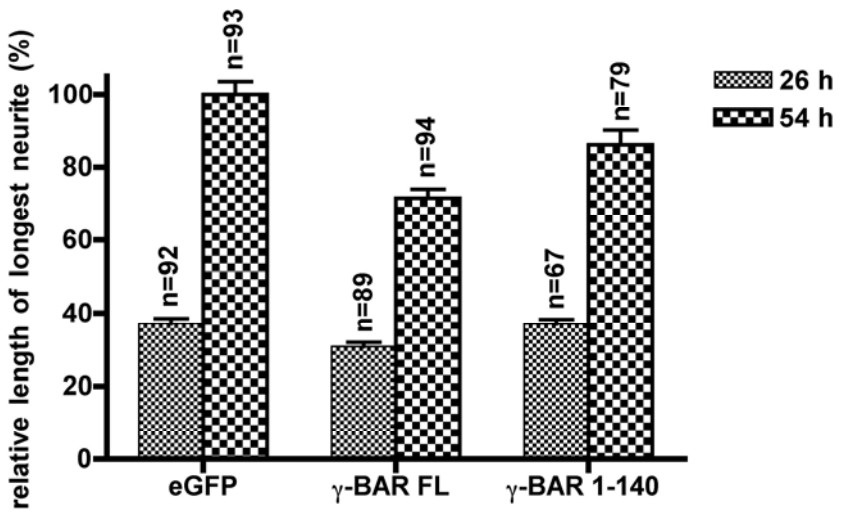

Figure 3-33: γ-BAR overexpression reduces the length of growing neurites

Primary hippocampal neurons prepared from E18 rat embryos were transfected with constructs encoding the indicated proteins (eGFP, eGFP-tagged γ-BAR full length and aa 1-140) directly after preparation using the Amaxa Nucleofector technology and plated onto coverslips. Cells were fixed 26 and 54 hours after transfection and immunostained with an antibody against eGFP to enhance signal intensities. The length of the longest neurite of each transfected cell was measured in bright field images (phase) by drawing a freehand line along the neurite and using the measure function of the software (Scion Image, Scion Corporation). The average neurite length of eGFP transfected control cells after 54 hours was set to 100%. n represents the number of cells analyzed from three independent experiments (for γ-BAR aa 1-140 only two experiments were performed). Error bars correspond to s.e.m.. The differences of the means between eGFP and γ-BAR FL were statistically significant in all three experiments (unpaired t-test, two-tailed P value: $P<0.0001$).

In order to complement these data, we used siRNA-mediated knockdown to inhibit γ-BAR expression in hippocampal neurons and analyzed neurite length as described above. 21-mer siRNAs against rat γ-BAR were synthesized. These siRNAs were highly efficient as assessed by their ability to knockdown expression of eGFP-tagged rat γ-BAR in transfected Cos7 cells (Figure 3-34, panel C). We chose a siRNA exhibiting nearly 100% knockdown efficiency towards the co-transfected rat protein and used a scrambled siRNA as control. Hippocampal neurons prepared from E18 rat embryos were transfected with synthetic siRNAs directly after preparation (Amaxa Nucleofector), plated and analyzed 54 hours after transfection as described above. Knockdown of γ-BAR resulted in about 50% longer neurites compared to control siRNA treated cells (Figure 3-34, panel B). It should be noted that the absolute length of the control siRNA treated neurons was significantly shorter than normally seen for

cultured hippocampal neurons at this stage of development, i.e. 54 hours after preparation (Frank Bradke, personal communication). This phenomenon can not be explained yet, but might be due to the siRNA transfection procedure or fixation artifacts. Further experiments analyzing the effects of other γ-BAR and control siRNAs are clearly necessary to clarify this point.

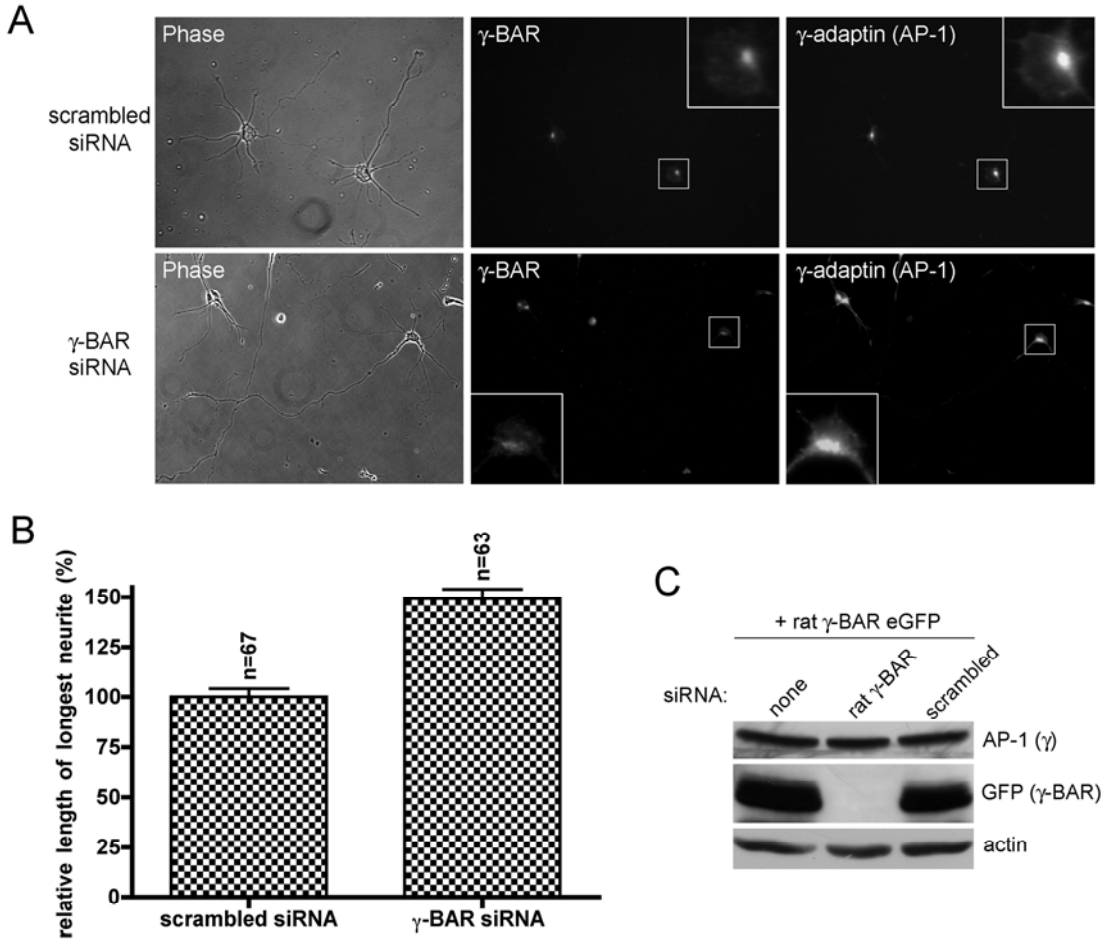

Figure 3-34: γ-BAR knockdown increases the length of growing neurites

(A) Synthetic siRNAs against rat γ-BAR or a control siRNA (scrambled) were transfected into primary hippocampal neurons directly after preparation from E18 rat embryos. The cells were plated onto coverslips and analyzed 54 hours after transfection by immunostaining using antibodies against γ-BAR and γ-adaptin. Cells that showed no or reduced staining of γ-BAR after treatment with the γ-BAR siRNA were chosen for analysis and the length of the longest neurite (see phase images) was measured as described. Insets represent 3-fold magnification of boxed areas.

(B) Quantification of the neurite length in scrambled (control) vs. γ-BAR siRNA treated neurons. The average neurite length of control treated cells was set to 100%. n indicates the number of cells analyzed from two independent experiments. Error bars represent s.e.m. The difference of the means is statistically significant (unpaired t-test, two-tailed P value: $P<0.0001$).

(C) Cos7 cells were co-transfected with plasmids encoding eGFP-tagged rat γ-BAR and siRNAs against rat γ-BAR or a control siRNA (scrambled) in order to test knockdown efficiency of the siRNAs used in (A). Triton X-100 extracts were prepared from the cells 24 hours after transfection and subjected to SDS-PAGE and immunoblotting using antibodies against GFP (detection of transfected rat γ-BAR) as well as γ-adaptin (AP-1) and actin as controls. The rat γ-BAR siRNA efficiently suppressed the expression of co-transfected rat γ-BAR.

4 Discussion

4.1 γ-BAR exclusively interacts with the γ-adaptin ear domain of AP-1

γ-BAR has recently been identified as a novel protein involved in intracellular, post-Golgi trafficking events. Before the start of this thesis work, it was known that γ-BAR directly interacts with the ear domain of the γ-adaptin subunit of the adaptor complex AP-1 and thus has been established as another member of the growing family of AP-1 associated accessory proteins. Although, a large number of accessory factors that bind the α-adaptin subunit of AP-2 have been identified and characterized (Slepnev and De Camilli, 2000), relatively few accessory proteins are known to interact with AP-1. These include, in addition to γ-BAR, γ-synergin, Rabaptin-5, EpsinR, NECAP, aftiphilin and p56. However, the specific function of most of them in AP-1-dependent sorting remains unclear. The identification of a GGA- and γ-adaptin ear-binding motif (GAE) with the consensus sequence ΨG(P/D/E)(Ψ/L/M) (Ψ represents an aromatic residue) in all of the known AP-1 accessory proteins (Collins et al., 2003; Mattera et al., 2004; Miller et al., 2003) might provide a basis to identify further AP-1 interactors. Indeed, γ-BAR harbors three similar motifs and all of them were shown to bind the γ-adaptin ear domain *in vitro* (Neubrand et al., 2005). However, further analysis of the mode of interaction revealed, that these motifs might not be the only γ-adaptin interacting sites within γ-BAR, since mutation of all three motifs did not completely abolish binding to AP-1. Other modes of interaction might contribute to the binding including a coiled-coil region of γ-BAR (Neubrand et al., 2005) and/ or additional motifs that do not fit the defined consensus sequence, i.e. the peptide sequence WENDF (aa 260-264 of human γ-BAR) (work in our lab by Kukhtina et al.).

We and others (Neubrand et al., 2005) were able to demonstrate a direct interaction of γ-BAR with γ-adaptin ear domains *in vitro* using purified proteins. However, it was not shown, whether there is an exclusive specificity of γ-BAR towards the γ-ear or whether it might be able to bind other ear domains as well. We therefore purified γ-ears of AP-1, α-ears of AP-2 and the β-ears of AP-1, -2 and -3 (β1, β2, β3A) for *in vitro* binding experiments. These studies have clearly demonstrated that out of the five different domains tested only γ-adaptin ear directly interacts with γ-BAR. However, we can not rule out that γ-BAR might directly interact with δ-ears of AP-3, ε-ears of AP-4 or any of the GGA ear domains. The latter might bind to γ-BAR, since it has been shown that the three γ-adaptin binding motifs are also able to bind GGA1 ears *in vitro*, but with much

lower affinity. However, this interaction could not be confirmed *in vivo* by immunoprecipitation experiments (Neubrand et al., 2005). Thus, taking all data into account, a specific and exclusive interaction of γ-BAR with the γ-adaptin ear domain of AP-1 seems most likely at this point. This specific interaction confirms the hypothesis, that different adaptor complexes and alternative adaptors interact with distinct sets of accessory proteins which may act at distinct steps of vesicle formation at the different sites of the intracellular trafficking. However, the general mechanisms involved in adaptor-mediated sorting seem to be similar, which is reflected by a pool of accessory proteins that are shared among different adaptor proteins (McNiven and Thompson, 2006; Traub, 2005).

4.2 γ-BAR is associated with membranes due to palmitoylation of amino-terminal cysteine residues

We analyzed the membrane binding activity of γ-BAR. Endogenous γ-BAR was almost completely associated with membranes at steady state and almost no γ-BAR was detectable in the cytosolic protein fraction of HeLa cells. Furthermore, the ability of γ-BAR to associate with membranes seems to be independent of its AP-1 binding activity, as a truncation mutant that had lost its ability to associate with membranes (γ-BAR Δ51) was still able to bind AP-1 *in vitro* and vice versa (γ-BAR 1-100). Hence, other mechanisms must exist that mediate γ-BAR membrane association.

The covalent attachment of lipid moieties is an essential modification found in many proteins that are associated with membranes (Bijlmakers and Marsh, 2003). There are four major types of modification in eukaryotes: co-translational amino-terminal myristoylation or carboxy-terminal isoprenylation of cytosolic proteins, attachment of glycophosphatidyl inositol (GPI) to plasma membrane proteins, and post-translational palmitoylation of many integral and peripheral membrane proteins. Palmitoylation is the most common and most versatile modification. Palmitic acid is added to the free thiol group of cysteines, although other saturated (e.g. myristic or stearic) or unsaturated (e.g. oleic and arachidonic) fatty acids can be used as well (Resh, 1999). Thus, palmitoylation is alternatively referred to as S-acylation.

We could show that three amino-terminal cysteine residues (Cys 4, 5 and 9) are critical for the association of γ-BAR with membranes. Mutation of all three cysteines to serines

results in a complete cytosolic distribution of the protein when overexpressed in cells. Furthermore, we could show that these cysteine residues are targets for post-translational palmitoylation, since treatment with the palmitoylation inhibitor 2-Bromopalmitate (2-BrP) results in a cytosolic distribution of overexpressed γ-BAR similar to that seen for the 3x cysteine to serine mutant.

Palmitoylation is a reversible modification of proteins and is catalyzed by specific membrane-bound enzymes called protein acyltransferases (PATs) or palmitoyl transferases. Recently, a family of such PATs has been discovered, first in *Saccharomyces cerevisiae* (Lobo et al., 2002; Roth et al., 2002) and subsequently in mammalian cells (Fukata et al., 2004; Huang et al., 2004; Keller et al., 2004; Swarthout et al., 2005). PATs exhibit specific expression patterns, subcellular localizations and substrate specificities. Thus, the localization of a certain transferase might define the subcellular localization of its substrates by attaching them to the membrane of a specific organelle. Depalmitoylation is mediated by acylprotein thioesterases (APTs), but so far these are less well characterized. Only one such enzyme, APT1, is known that removes palmitate from proteins on the cytosolic surface of membranes (Duncan and Gilman, 1998; Yeh et al., 1999). The fates of attached palmitates to proteins can be different. Proteins can be transiently modified by consecutive action of a PAT and an APT and may cycle between a membrane-attached and a cytosolic state. Such cycling between palmitoylated and depalmitoylated states can also regulate trafficking between different compartments, as it has been shown for Ras proteins and other monomeric GTPases. Ras is post-translationally modified by farnesylation in the cytoplasm and exhibits a weak affinity for Golgi membranes in that state. Subsequent palmitoylation by Golgi-localized PATs mediates membrane trapping and facilitates trafficking to the plasma membrane. There, Ras is depalmitoylated by APT, which releases it into the cytosol where it can rebind to Golgi membranes (Goodwin et al., 2005; Rocks et al., 2005). Thus, dynamic palmitoylation may regulate the intracellular distribution of certain proteins. Alternatively, proteins can be permanently modified with palmitate, which is transferred to a protein by a PAT and remains associated with it. In fact, many proteins appear to be stably palmitoylated and thus may keep their membrane association and subcellular distribution throughout lifetime, for example certain viral membrane glycoproteins (Schmidt and Schlesinger, 1980; Veit and Schmidt, 1993).

The latter is probably also the case for γ-BAR. This assumption is supported by the following lines of evidence: (i) We see an almost complete association of γ-BAR with

membranes. Thus, only a very small pool of cytosolic γ-BAR seems to be present in cells at steady-state. This is in contrast with its direct binding partner AP-1 which always maintains a cytosolic pool (data not shown). (ii) All three cysteine residues seem to be important for membrane association. Palmitoylation at several sites may keep the protein stably associated with membranes. Indeed, the SNARE protein SNAP-25 (synaptosome-associated protein of 25 kDa) also appears to be stably palmitoylated at two central cysteines (Kang et al., 2004).

We can not rule out the possibility that the glycine residue at position 2 of γ-BAR is a target for co-translational myristoylation after the cleavage of the initiator amino acid methionine. In fact, many palmitoylated proteins are dual-lipid modified and require a transient association with membranes mediated by myristate to allow for palmitoylation by membrane associated PATs (Resh, 1999). In these cases, both modifications are essential for correct membrane targeting of the modified protein (van't Hof and Resh, 1997). We showed that the amino-terminal glycine residue of γ-BAR is not crucial for its membrane association. Mutating this residue to alanine does not have any influence on its subcellular distribution. Thus, it appears that myristoylation is not required for the palmitoylation of γ-BAR and its correct membrane association.

Taken together, we postulate that γ-BAR functions in the recruitment of AP-1 to specific sites of membranes and thus regulates its membrane association and function within the TGN and endosomes (discussed later on). The specificity of γ-BAR to associate with particular membranes might be achieved by a specific subcellular localization of the enzyme (PAT) that modifies γ-BAR.

4.3 γ-BAR regulates transport and positioning of recycling endosomes

4.3.1 γ-BAR associates with recycling endosomes

We could show that γ-BAR partially co-localizes with the adaptor complex AP-1 in a peri-nuclear compartment and also with TfR and Rab11, two markers for REs which are usually found in close proximity to the TGN. AP-1 has been implicated in trafficking both from the TGN as well as endosomes (Futter et al., 1998; Honing et al., 1997; Pagano et al., 2004; Peden et al., 2004; Robinson, 1990). There is a close inter-relationship between REs and the TGN, which is reflected by the fact that the localization of both organelles is largely overlapping, and that specific markers for one compartment display at least some enrichment in the other. Furthermore, the exocyst complex, which serves to direct exocytic cargo to active sites of secretion within the plasma membrane, is an effector of RE-associated Rab11 (Zhang et al., 2004) and has been shown to regulate trafficking of cargo (i.e. *Drosophila* E-cadherin) from REs to the plasma membrane (Langevin et al., 2005). Thus, the TGN and REs could be seen as a twin-compartment with overlapping functions. This suggestion is further supported by the recent finding that Rab6-interacting protein 1 (R6IP1), originally identified as a Rab6-binding protein, also binds to Rab11a and may couple Rab6 and Rab11 function at the TGN and REs, respectively (Miserey-Lenkei et al., 2007). We therefore refer to this twin-compartment as the TGN-RE boundary (Schmidt and Haucke, 2007).

Overexpression of eGFP-tagged γ-BAR in HeLa cells results in a re-localization of TGN-RE derived membranes to the cell periphery, where they accumulate in patches underneath the plasma membrane. TGN-RE markers (AP-1, TfR, Rab11), that co-localize with endogenous γ-BAR, are co-enriched in the re-located compartment. Furthermore, the compartment is also positive for TGN46, a marker that has originally been associated with the TGN, but cycles between TGN and the plasma membrane, thereby traversing REs *en route* (Ghosh et al., 1998; Stanley and Howell, 1993). Additionally, MPRs are found in peripheral accumulations. After the delivery of newly synthesized lysosomal acid hydrolases to early and late endosomes, MPRs return to the TGN to mediate further rounds of sorting. The pathways of MPR recycling are diverse and not entirely clear, but involve sorting through various compartments including REs and the plasma membrane (Ghosh et al., 2003). Retrograde endosome-to-TGN transport of TGN46 (and its rat homolog TGN38) and MPRs depends on a conserved molecular machinery called retromer (Bonifacino and Rojas, 2006; Seaman, 2005). This

machinery, which mediates budding and cargo selection at endosomes, consists of several components including sorting nexin (Snx) proteins and depends on the function of several other trafficking proteins including Rab9, AP-1, EpsinR, dynamin and clathrin (Carroll et al., 2001; Diaz and Pfeffer, 1998; Lauvrak et al., 2004; Lombardi et al., 1993; Meyer et al., 2000; Saint-Pol et al., 2004). Consistent with the reported role of clathrin in budding from endosomes, we also found clathrin in the accumulated peripheral compartment.

However, markers for other compartments, including early endosomes (EEA1), late endosomes/ lysosomes (LAMP-1), cis-Golgi (GM130), mitochondria (Cyt. C) and the plasma membrane (AP-2) are absent from the peripheral TGN/ recycling endosomal compartment. The relocalization of the compartment is most probably an overexpression artifact mediated by the excess of γ-BAR. However, based on these results we postulate that γ-BAR regulates intracellular trafficking and positioning of TGN/ RE-derived organelles. We and others (Neubrand et al., 2005) do not see a complete co-localization of endogenous γ-BAR and AP-1, which might indicate that γ-BAR regulates only a subpool of AP-1 by recruiting it to the TGN/ recycling endosomal boundary. A distinct pool of AP-1 could function in trafficking from endosomes or the TGN independently of γ-BAR. Indeed, AP-1 is also found on smaller discrete structures throughout the cell which lack endogenous γ-BAR staining (not shown; see also Neubrand et al., 2005).

4.3.2 Recycling endosomal positioning depends on conventional kinesins

The re-localization of TGN/ recycling endosomal membranes by γ-BAR overexpression must clearly depend on intracellular transport processes. These transport processes are driven by motor proteins, such as kinesins, that move cargo vesicles and organelles along cytoskeletal filaments, e.g. microtubules. In our studies, we found that γ-BAR directly interacts with the light chains of conventional kinesins, both *in vitro* (affinity purifications) and *in vivo* (co-immunoprecipitations). Furthermore, we could show that this interaction is mediated by a conserved motif consisting of a critical tryptophan residue surrounded by several acidic residues. This motif has also been found in other kinesin light chain binding proteins, like calsyntenin-1 (Konecna et al., 2006) or the vaccinia virus envelope protein A36R (Ward and Moss, 2004). Furthermore, overexpressed γ-BAR directs co-overexpressed kinesin light chains as well as

endogenous conventional kinesin into the peripheral TGN/ RE compartment in HeLa cells.

Functional analysis of this interaction reveals that the γ-BAR induced re-localization of TGN/ RE-membranes in HeLa cells depends on the presence of intact microtubules. When treating γ-BAR overexpressing cells with nocodazole, which depolymerizes microtubules, the peripherally accumulated compartment gets dispersed throughout the cell. In line with that, knock down of ubiquitous conventional kinesin KIF5B results in a much stronger perinuclear accumulation of overexpressed γ-BAR. This indicates, that the γ-BAR induced re-localization of the perinuclear compartment indeed depends on the action of conventional kinesins.

Conventional kinesins have been implicated in the transport of a variety of different membrane cargo, including mitochondria, lysosomes, endoplasmic reticulum and certain neuronal transport carriers, as well as non-membranous cargo such as mRNA granules, tubulin oligomers and intermediate filaments (Hirokawa and Takemura, 2005). However, so far only actin-based motor proteins, members of the non-conventional myosin V protein family, have been implicated in the intracellular transport of recycling endosomal cargo. Myosin motors are recruited to certain organelles by the action of Rabs and Rab-interacting proteins. For example, Rab11a is known to interact with myosin Vb (Lapierre et al., 2001), and both proteins bind to Rab11 family interacting protein 2 (Rab11-FIP2) (Hales et al., 2002). All three proteins are involved in the recycling of a variety of receptors, including TfR (Hales et al., 2002; Lapierre et al., 2001; Lindsay and McCaffrey, 2002).

In order to test whether conventional kinesins might also be involved in the transport or the intracellular positioning of recycling endosomes, we analyzed the distribution of REs in HeLa cells after knockdown of KIF5B in comparison to control siRNA treated cells. We observed a more pronounced peri-nuclear accumulation of REs after loading the cells with fluorescenctly labeled Tf. In fact, it seems that the recycling endosomal compartment collapses into a condensed peri-nuclear spot in KIF5B-depleted cells. We propose that conventional kinesins are important for the intracellular positioning and transport of REs, and this function appears to be regulated by γ-BAR. γ-BAR could thus function as an adaptor to recruit the motor protein to the organelle membrane. Other proteins have been identified that serve as adaptors for motor-cargo interactions, including AP-1 for the transport of MPR containing organelles by KIF13A (Nakagawa et al., 2000), and the LIN10/ LIN2/ LIN7 complex for KIF17 mediated transport of

NMDA receptor-containing vesicles (Setou et al., 2000). Additionally, Rab5 was shown to regulate the recruitment of KIF16B to early endosomes (Hoepfner et al., 2005), in this case via an indirect mechanism. Thus, γ-BAR might be a specific adaptor for KIF5 linking it to RE. As conventional kinesins transport a variety of different cargos, specificity towards certain organelles and directions of transport might be achieved by specific adaptors that localize to a particular compartment. Calsyntenin-1, another adaptor for KIF5, has recently been implicated in the docking of vesicular and tubulovesicular organelles transported along axons (Konecna et al., 2006). Other specific adaptors for conventional kinesins are the JIP family of proteins, which have been implicated in docking different types of transport vesicles containing the integral membrane proteins APP or APOER2. Another example is GRIP1 which connects AMPA receptor subunits (GluR2)-containing vesicles to KIF5.

4.3.3 γ-BAR affects the rate of transferrin recycling

Since we found that γ-BAR is associated with REs and regulates their intracellular positioning and transport by direct interaction with kinesin KIF5 motor proteins, we analyzed whether it might be functionally involved in the recycling of cargo towards the plasma membrane. To test this, we analyzed the effects of γ-BAR overexpression and knockdown on Tf-recycling. Overexpression of γ-BAR caused a retention of internalized Tf in a peripheral compartment and recycling from that compartment to the plasma membrane was delayed. The intracellular localization of endosomes is determined by a delicate balance between plus and minus end-directed motor proteins. γ-BAR overexpression leads to a massive recruitment of plus end-directed motor proteins to RE thereby shifting their intracellular distribution. This shift might cause the compartment to be unavailable for other factors which are needed for correct targeting, for example myosin motor proteins that work together with kinesins in the transport of organelles to the plasma membrane (Huang et al., 1999). This is in line with similar effects observed for motor proteins that transport other types of endosomes. KIF16B regulates the positioning of EEA1-positive early endosomes and overexpression of the motor causes a transloction of EEs to the cell periphery (Hoepfner et al., 2005). This effect parallels our observation that γ-BAR overexpression dramatically alters the distribution of TfR-positive REs. Furthermore, EGF receptors trapped in EEs of KIF16B overexpressing cells are incapable of entering the degradative pathway. Thus, EGF receptor degradation appears to be nearly abolished in these cells. These results

parallel the effects of γ-BAR overexpression on the rate of Tf-recycling. The fact that Tf-recycling is only delayed but not abolished can be explained by the existence of several possible routes for recycling of TfR to the plasma membrane (Maxfield and McGraw, 2004).

We also analyzed the role of γ-BAR in Tf recycling in cells depleted of γ-BAR by quantitative assays using [^{125}I]-labeled Tf. Silencing of γ-BAR expression accelerated the recycling of transferrin compared to control siRNA treated cells. In contrast, no effects of γ-BAR depletion on the rate of Tf-internalization could be observed, further confirming that γ-BAR is specifically involved in recycling and not in endocytic uptake. These data suggest that γ-BAR regulates the balance between slow and fast tracks of Tf recycling by KIF5-mediated positioning of REs. In this scenario, γ-BAR silencing might interfere with the correct targeting of REs to a peri-nuclear location, thereby shifting the balance of Tf recycling towards a fast pathway mediated through Rab4-positive EEs (van der Sluijs et al., 1992; Van Der Sluijs et al., 1991). It has previously been shown that other AP-1 accessory proteins exhibit similar effects on Tf recycling (Hirst et al., 2005). Knockdown of aftiphilin and, to a lesser extent, p200 also increased the rate of Tf recycling, whereas knockdown of AP-1 decreased the rate of recycling. The function of aftiphilin and p200 in this context is still unknown. AP-1 has been shown to localize to early and recycling endosomes (Futter et al., 1998; Peden et al., 2004) and to be required for the formation of recycling vesicles from endosomes (Pagano et al., 2004). Thus, AP-1 might be involved in fast and slow pathways of recycling. By contrast, AP-1-binding accessory proteins might act on a specific subset of endosomes and thus could selectively interfere with trafficking via the slow or fast recycling pathway. In the case of aftiphilin-depleted cells, movement of internalized Tf from EEs to REs might be disturbed, causing Tf to be recycled via a faster, more direct pathway from Rab4-containing EEs. Similarly, γ-BAR knockdown may cause REs to be unavailable for Tf-recycling due to incorrect positioning and thus enable internalized Tf to recycle faster via an EE route. This hypothesis is supported by other studies on the role of different endosomal Rab proteins on the recycling of plasma membrane proteins. It was shown recently that Rab8a and Rab11a define spatially and functionally distinct routes of recycling, although both proteins interact with the same motor protein, myosin Vb (Roland et al., 2007). The authors speculate that, in the case of inhibition of one pathway, alternative pathways may be used for recycling. Thus, Tf molecules that are

blocked from entering Rab11a-mediated recycling may be able to shunt into a fast Rab8a/ Rab4-dependent route (Provance et al., 2004).

It should be noted that the hypothesis that recycling of Tf may be directed into a faster pathway upon γ-BAR depletion has still to be proven. One experiment would be to investigate the intracellular distribution of Tf-loaded endosomes in γ-BAR-depleted cells. Aftiphilin and p200 depletions were shown to cause an accumulation of transferrin mainly in peripheral endosomes, whereas in control siRNA treated cells Tf is present in both peripheral and perinuclear endosomes (Hirst et al., 2005). Thus, γ-BAR knockdown might have similar effects on the localization of internalized Tf.

4.4 Role of γ-BAR in neuronal transport processes and development

REs are involved in a variety of processes of neuronal membrane traffic, thereby regulating neuronal development and polarization (Schmidt and Haucke, 2007). We analyzed the localization of endogenous and overexpressed γ-BAR in hippocampal neurons in culture. Endogenous γ-BAR mostly localizes to a perinuclear compartment where it is found together with AP-1 and TfR. However, overexpressed γ-BAR localizes to axonal vesicle clusters and growth cones and re-distributes AP-1 and TfR into these clusters. This is remarkable, since TfRs are normally excluded from the axonal compartment. This effect may not reflect a specific sorting defect, but rather a more general re-localization of REs and associated proteins like AP-1 and TfR. In this respect these observations parallel the effect of γ-BAR overexpression in HeLa cells. Additionally, we found endogenous kinesin heavy chain to be enriched in γ-BAR-containing clusters along neurites. This might indicate that also in neurons the re-localization of RE material is dependent on conventional kinesins.

Given the fact that γ-BAR may regulate the positioning and transport of REs by the interaction with kinesin motors, we hypothesized that it could influence axonal growth during neuronal development. We therefore analyzed the effect of γ-BAR overexpression and depletion on neurite outgrowth in embryonic hippocampal neurons in culture. We found that γ-BAR overexpression reduces the length of the growing axon at stage 3 of development (54 hours after plating) by about 30% compared to control cells. This is in complete agreement with earlier studies analyzing the effect of γ-BAR overexpression on neurite outgrowth in PC12 cells (Laketa et al., 2007). We also

investigated the effect of a kinesin binding-deficient truncation mutant (γ-BAR 1-140), which displayed a less dramatic effect and reduced the length of growing neurites only by about 15%. Depletion of γ-BAR seems to increase the length of neurites in hippocampal neurons by about 50% at stage 3, 54 hours after plating. However, these are preliminary results, since the absolute neurite length of neurons treated with control siRNAs is significantly smaller than normally found at this stage of development. Thus, these experiments ought to be repeated including additional control and γ-BAR-targeting siRNAs.

If the results hold true, the observed effects on neurite length could be explained by the following model: γ-BAR may regulate the steady-state distribution of REs by the recruitment of plus end-directed microtubule motor proteins that are in balance with minus end-directed microtubule and actin based myosin motors. Overexpression of γ-BAR causes a massive recruitment of conventional kinesins to REs, which results in a re-localization and accumulation of these organelles along neurites and in growth cones. There, they might be unavailable for other components, like myosin motors or proteins involved in plasma membrane targeting and fusion, which are needed for the correct targeting to sites of plasma membrane growth. This effect might be similar to the effect of γ-BAR overexpression on Tf-recycling in HeLa cells, where the correct targeting of Tf-containing organelles to the plasma membrane seems to be impaired. Alternatively, γ-BAR depletion might direct recycling endosomal membrane traffic towards faster pathways, thereby facilitating faster neurite growth, similar to the accelerated Tf recycling phenotype observed in HeLa cells.

The increase in neurite length upon γ-BAR knockdown observed here strikingly re-assembles a recently characterized effect of Arp2/3 on axon elongation (Strasser et al., 2004). The authors found that inhibition of the Arp2/3 complex by the expression of dominant negative N-WASP domains significantly increased neurite length. In another study, silencing of Arp3 and Abp1, a presumed positive regulator of Arp2/3, causes similar effects, leading to an increase in axon length by about 50% (Pinyol et al., 2007). Given the fact that we identified Arp2/3 as a putative binding partner of γ-BAR in affinity purifications, our observed effect of γ-BAR knockdown on neurite length may in fact also reflect an Arp2/3-dependent phenotype. Therefore, it would be of great interest to further investigate, whether γ-BAR directly or indirectly associates with Arp2/3 and whether this is of any functional relevance for Arp2/3 mediated actin polymerization and branching.

5 Summary and Conclusions

We aimed at elucidating the function of the AP-1 interacting protein γ-BAR in non-neuronal as well as neuronal membrane traffic.

We showed that γ-BAR specifically interacts with γ-ear but not with the α-ear domain of AP-2 or the β-ear domains of AP-1, -2 and -3. At steady-state, γ-BAR is completely associated with membranes mediated by post-translational palmitoylation. We postulate that this represents a permanent modification which keeps γ-BAR stably associated with intracellular membranes.

Endogenous γ-BAR partially co-localized with AP-1, TfR and Rab11 in a perinuclear TGN/ RE compartment. Overexpression of γ-BAR caused a massive re-localization of this compartment to the cell periphery. Additionally, the compartment contained TGN46 and MPR46, further confirming that it is of TGN/ recycling endosomal origin. In contrast, organellar marker proteins for EEs, LEs/ lysosomes, cis-Golgi, mitochondria or the plasmalemma were absent from the peripheral compartment.

We identified conventional kinesin (KIF5) as a direct binding partner of γ-BAR. Binding was mediated by the light chains (Klc2) of kinesin heterotetramers and was critically dependent on a tryptophan-based acidic motif, which has already been identified in other Klc-binding proteins. Strikingly, overexpressed γ-BAR re-distributed co-expressed Klc2 as well as endogenous kinesin KIF5. Nocodazole-induced microtubule depolymerization caused a dispersal of the peripherally accumulated compartment in γ-BAR overexpressing cells. Similar to that, KIF5B knockdown inhibited relocalization of overexpressed γ-BAR to the cell periphery. Furthermore, KIF5B depletion caused an enhanced accumulation of internalized Tf in the perinuclear area. We conclude, that γ-BAR may regulate the intracellular positioning and trafficking of REs by serving as an adaptor for plus-end directed motor proteins of the kinesin KIF5 family. Such intracellular positioning of organelles has been shown to be regulated by a delicate balance between plus and minus end-directed microtubule as well as actin-based myosin motor proteins.

On a functional level, we analyzed the effect of γ-BAR on the recycling of Tf. Internalized Tf localized to the peripheral compartment in γ-BAR overexpressing cells and its recycling was retarded. Conversely, γ-BAR depletion accelerated the rate of Tf recycling. We conclude that the intracellular positioning of REs by a γ-BAR/ KIF5 complex may be critical for Tf trafficking. Ablation of γ-BAR may interfere with the

correct targeting of peri-nuclear REs and thus might shift recycling of Tf towards a fast, Rab4-dependent EE pathway.

Moreover, we have started to analyze the function of γ-BAR in neuronal membrane traffic. Upon overexpression, γ-BAR redistributed AP-1, TfR and conventional kinesin to axonal vesicle clusters and growth cones. Preliminary data suggest that γ-BAR may affect the length of growing neurites in developing hippocampal neurons; while γ-BAR overexpression may reduce the length of outgrowing axons, γ-BAR knockdown appears to increase their length. These results ought to be confirmed using additional siRNAs. Our observations could indicate a role of γ-BAR/ KIF5-mediated positioning and trafficking of REs in neuronal differentiation.

Taken all data together, we propose that a γ-BAR/ kinesin KIF5 complex serves as an important regulator of RE dynamics. REs are implicated in diverse cell physiological processes ranging from the regulation of cell signaling to polarization, cytokinesis, morphogenesis and long-term synaptic plasticity. Thus, it will be an exciting endeavor for the future to investigate whether γ-BAR has a role in at least some of the processes known to involve REs. Furthermore, it will be interesting to see whether γ-BAR may have additional interaction partners implicated in related or distinct cellular functions, for example Arp2/3 mediated actin polymerization and branching. The latter process has been implicated in cellular motility, growth and the regulation of neurite extension.

Bibliography

Ahle, S. and Ungewickell, E. (1986). Purification and properties of a new clathrin assembly protein. *Embo J* **5**, 3143-9.

Albertinazzi, C., Za, L., Paris, S. and de Curtis, I. (2003). ADP-ribosylation factor 6 and a functional PIX/p95-APP1 complex are required for Rac1B-mediated neurite outgrowth. *Mol Biol Cell* **14**, 1295-307.

Alberts, B., Johnson, A., Lewis, J., Raff, M., Roberts, K. and Walter, P. (2002). Molecular Biology of the Cell. New York: Garland Publishing.

Alberts, P., Rudge, R., Hinners, I., Muzerelle, A., Martinez-Arca, S., Irinopoulou, T., Marthiens, V., Tooze, S., Rathjen, F., Gaspar, P. et al. (2003). Cross talk between tetanus neurotoxin-insensitive vesicle-associated membrane protein-mediated transport and L1-mediated adhesion. *Mol Biol Cell* **14**, 4207-20.

Ang, A. L., Folsch, H., Koivisto, U. M., Pypaert, M. and Mellman, I. (2003). The Rab8 GTPase selectively regulates AP-1B-dependent basolateral transport in polarized Madin-Darby canine kidney cells. *J Cell Biol* **163**, 339-50.

Ang, A. L., Taguchi, T., Francis, S., Folsch, H., Murrells, L. J., Pypaert, M., Warren, G. and Mellman, I. (2004). Recycling endosomes can serve as intermediates during transport from the Golgi to the plasma membrane of MDCK cells. *J Cell Biol* **167**, 531-43.

Arimura, N. and Kaibuchi, K. (2007). Neuronal polarity: from extracellular signals to intracellular mechanisms. *Nat Rev Neurosci* **8**, 194-205.

Baas, P. W., Deitch, J. S., Black, M. M. and Banker, G. A. (1988). Polarity orientation of microtubules in hippocampal neurons: uniformity in the axon and nonuniformity in the dendrite. *Proc Natl Acad Sci U S A* **85**, 8335-9.

Bananis, E., Murray, J. W., Stockert, R. J., Satir, P. and Wolkoff, A. W. (2000). Microtubule and motor-dependent endocytic vesicle sorting in vitro. *J Cell Biol* **151**, 179-86.

Bielli, A., Thornqvist, P. O., Hendrick, A. G., Finn, R., Fitzgerald, K. and McCaffrey, M. W. (2001). The small GTPase Rab4A interacts with the central region of cytoplasmic dynein light intermediate chain-1. *Biochem Biophys Res Commun* **281**, 1141-53.

Bijlmakers, M. J. and Marsh, M. (2003). The on-off story of protein palmitoylation. *Trends Cell Biol* **13**, 32-42.

Boman, A. L., Zhang, C., Zhu, X. and Kahn, R. A. (2000). A family of ADP-ribosylation factor effectors that can alter membrane transport through the trans-Golgi. *Mol Biol Cell* **11**, 1241-55.

Bonifacino, J. S. (2004). The GGA proteins: adaptors on the move. *Nat Rev Mol Cell Biol* **5**, 23-32.

Bonifacino, J. S. and Rojas, R. (2006). Retrograde transport from endosomes to the trans-Golgi network. *Nat Rev Mol Cell Biol* **7**, 568-79.

Bonifacino, J. S. and Traub, L. M. (2003). Signals for sorting of transmembrane proteins to endosomes and lysosomes. *Annu Rev Biochem* **72**, 395-447.

Bradke, F. and Dotti, C. G. (1999). The role of local actin instability in axon formation. *Science* **283**, 1931-4.

Bradke, F. and Dotti, C. G. (2000). Establishment of neuronal polarity: lessons from cultured hippocampal neurons. *Curr Opin Neurobiol* **10**, 574-81.

Brambell, F. W. (1923). The activity of the Golgi apparatus in the neurones of Helix aspersa. *J Physiol* **57**, 415-21.

Brown, D. A., Crise, B. and Rose, J. K. (1989). Mechanism of membrane anchoring affects polarized expression of two proteins in MDCK cells. *Science* **245**, 1499-501.

Bucci, C., Parton, R. G., Mather, I. H., Stunnenberg, H., Simons, K., Hoflack, B. and Zerial, M. (1992). The small GTPase rab5 functions as a regulatory factor in the early endocytic pathway. *Cell* **70**, 715-28.

Burack, M. A., Silverman, M. A. and Banker, G. (2000). The role of selective transport in neuronal protein sorting. *Neuron* **26**, 465-72.

Carroll, K. S., Hanna, J., Simon, I., Krise, J., Barbero, P. and Pfeffer, S. R. (2001). Role of Rab9 GTPase in facilitating receptor recruitment by TIP47. *Science* **292**, 1373-6.

Casanova, J. E., Apodaca, G. and Mostov, K. E. (1991). An autonomous signal for basolateral sorting in the cytoplasmic domain of the polymeric immunoglobulin receptor. *Cell* **66**, 65-75.

Casanova, J. E., Wang, X., Kumar, R., Bhartur, S. G., Navarre, J., Woodrum, J. E., Altschuler, Y., Ray, G. S. and Goldenring, J. R. (1999). Association of Rab25 and Rab11a with the apical recycling system of polarized Madin-Darby canine kidney cells. *Mol Biol Cell* **10**, 47-61.

Caviston, J. P. and Holzbaur, E. L. (2006). Microtubule motors at the intersection of trafficking and transport. *Trends Cell Biol* **16**, 530-7.

Christoforidis, S., McBride, H. M., Burgoyne, R. D. and Zerial, M. (1999). The Rab5 effector EEA1 is a core component of endosome docking. *Nature* **397**, 621-5.

Collins, B. M., McCoy, A. J., Kent, H. M., Evans, P. R. and Owen, D. J. (2002). Molecular architecture and functional model of the endocytic AP2 complex. *Cell* **109**, 523-35.

Collins, B. M., Praefcke, G. J., Robinson, M. S. and Owen, D. J. (2003). Structural basis for binding of accessory proteins by the appendage domain of GGAs. *Nat Struct Biol* **10**, 607-13.

Craig, A. M. and Banker, G. (1994). Neuronal polarity. *Annu Rev Neurosci* **17**, 267-310.

Craig, H. M., Reddy, T. R., Riggs, N. L., Dao, P. P. and Guatelli, J. C. (2000). Interactions of HIV-1 nef with the mu subunits of adaptor protein complexes 1, 2, and 3: role of the dileucine-based sorting motif. *Virology* **271**, 9-17.

Crottet, P., Meyer, D. M., Rohrer, J. and Spiess, M. (2002). ARF1.GTP, tyrosine-based signals, and phosphatidylinositol 4,5-bisphosphate constitute a minimal machinery to recruit the AP-1 clathrin adaptor to membranes. *Mol Biol Cell* **13**, 3672-82.

Cyr, J. L., Pfister, K. K., Bloom, G. S., Slaughter, C. A. and Brady, S. T. (1991). Molecular genetics of kinesin light chains: generation of isoforms by alternative splicing. *Proc Natl Acad Sci U S A* **88**, 10114-8.

de Anda, F. C., Pollarolo, G., Da Silva, J. S., Camoletto, P. G., Feiguin, F. and Dotti, C. G. (2005). Centrosome localization determines neuronal polarity. *Nature* **436**, 704-8.

Dell'Angelica, E. C., Mullins, C. and Bonifacino, J. S. (1999). AP-4, a novel protein complex related to clathrin adaptors. *J Biol Chem* **274**, 7278-85.

Dell'Angelica, E. C., Ohno, H., Ooi, C. E., Rabinovich, E., Roche, K. W. and Bonifacino, J. S. (1997). AP-3: an adaptor-like protein complex with ubiquitous expression. *Embo J* **16**, 917-28.

Dell'Angelica, E. C., Puertollano, R., Mullins, C., Aguilar, R. C., Vargas, J. D., Hartnell, L. M. and Bonifacino, J. S. (2000). GGAs: a family of ADP ribosylation factor-binding proteins related to adaptors and associated with the Golgi complex. *J Cell Biol* **149**, 81-94.

Deneka, M., Neeft, M. and van der Sluijs, P. (2003). Regulation of membrane transport by rab GTPases. *Crit Rev Biochem Mol Biol* **38**, 121-42.

Deora, A. A., Gravotta, D., Kreitzer, G., Hu, J., Bok, D. and Rodriguez-Boulan, E. (2004). The basolateral targeting signal of CD147 (EMMPRIN) consists of a single leucine and is not recognized by retinal pigment epithelium. *Mol Biol Cell* **15**, 4148-65.

Diaz, E. and Pfeffer, S. R. (1998). TIP47: a cargo selection device for mannose 6-phosphate receptor trafficking. *Cell* **93**, 433-43.

Diefenbach, R. J., Mackay, J. P., Armati, P. J. and Cunningham, A. L. (1998). The C-terminal region of the stalk domain of ubiquitous human kinesin heavy chain contains the binding site for kinesin light chain. *Biochemistry* **37**, 16663-70.

Donaldson, J. G., Finazzi, D. and Klausner, R. D. (1992). Brefeldin A inhibits Golgi membrane-catalysed exchange of guanine nucleotide onto ARF protein. *Nature* **360**, 350-2.

Doray, B., Ghosh, P., Griffith, J., Geuze, H. J. and Kornfeld, S. (2002). Cooperation of GGAs and AP-1 in packaging MPRs at the trans-Golgi network. *Science* **297**, 1700-3.

Doray, B. and Kornfeld, S. (2001). Gamma subunit of the AP-1 adaptor complex binds clathrin: implications for cooperative binding in coated vesicle assembly. *Mol Biol Cell* **12**, 1925-35.

Doray, B., Lee, I., Knisely, J., Bu, G. and Kornfeld, S. (2007). The gamma/sigma1 and alpha/sigma2 hemicomplexes of clathrin adaptors AP-1 and AP-2 harbor the dileucine recognition site. *Mol Biol Cell* **18**, 1887-96.

Dotti, C. G. and Poo, M. M. (2003). Neuronal polarization: building fences for molecular segregation. *Nat Cell Biol* **5**, 591-4.

Dotti, C. G., Sullivan, C. A. and Banker, G. A. (1988). The establishment of polarity by hippocampal neurons in culture. *J Neurosci* **8**, 1454-68.

Duden, R. (2003). ER-to-Golgi transport: COP I and COP II function (Review). *Mol Membr Biol* **20**, 197-207.

Duncan, J. A. and Gilman, A. G. (1998). A cytoplasmic acyl-protein thioesterase that removes palmitate from G protein alpha subunits and p21(RAS). *J Biol Chem* **273**, 15830-7.

El-Husseini, A. E. and Vincent, S. R. (1999). Cloning and characterization of a novel RING finger protein that interacts with class V myosins. *J Biol Chem* **274**, 19771-7.

Ellis, M. A., Potter, B. A., Cresawn, K. O. and Weisz, O. A. (2006). Polarized biosynthetic traffic in renal epithelial cells: sorting, sorting, everywhere. *Am J Physiol Renal Physiol* **291**, F707-13.

Fang, C., Deng, L., Keller, C. A., Fukata, M., Fukata, Y., Chen, G. and Luscher, B. (2006). GODZ-mediated palmitoylation of GABA(A) receptors is required for normal assembly and function of GABAergic inhibitory synapses. *J Neurosci* **26**, 12758-68.

Feng, Y., Press, B. and Wandinger-Ness, A. (1995). Rab 7: an important regulator of late endocytic membrane traffic. *J Cell Biol* **131**, 1435-52.

Ferreira, A. and Rapoport, M. (2002). The synapsins: beyond the regulation of neurotransmitter release. *Cell Mol Life Sci* **59**, 589-95.

Fiedler, K. and Simons, K. (1995). The role of N-glycans in the secretory pathway. *Cell* **81**, 309-12.

Folsch, H., Ohno, H., Bonifacino, J. S. and Mellman, I. (1999). A novel clathrin adaptor complex mediates basolateral targeting in polarized epithelial cells. *Cell* **99**, 189-98.

Folsch, H., Pypaert, M., Maday, S., Pelletier, L. and Mellman, I. (2003). The AP-1A and AP-1B clathrin adaptor complexes define biochemically and functionally distinct membrane domains. *J Cell Biol* **163**, 351-62.

Fukata, M., Fukata, Y., Adesnik, H., Nicoll, R. A. and Bredt, D. S. (2004). Identification of PSD-95 palmitoylating enzymes. *Neuron* **44**, 987-96.

Futter, C. E., Connolly, C. N., Cutler, D. F. and Hopkins, C. R. (1995). Newly synthesized transferrin receptors can be detected in the endosome before they appear on the cell surface. *J Biol Chem* **270**, 10999-1003.

Futter, C. E., Gibson, A., Allchin, E. H., Maxwell, S., Ruddock, L. J., Odorizzi, G., Domingo, D., Trowbridge, I. S. and Hopkins, C. R. (1998). In polarized MDCK cells basolateral vesicles arise from clathrin-gamma-adaptin-coated domains on endosomal tubules. *J Cell Biol* **141**, 611-23.

Gallusser, A. and Kirchhausen, T. (1993). The beta 1 and beta 2 subunits of the AP complexes are the clathrin coat assembly components. *Embo J* **12**, 5237-44.

Gan, Y., McGraw, T. E. and Rodriguez-Boulan, E. (2002). The epithelial-specific adaptor AP1B mediates post-endocytic recycling to the basolateral membrane. *Nat Cell Biol* **4**, 605-9.

Garrido, J. J., Fernandes, F., Giraud, P., Mouret, I., Pasqualini, E., Fache, M. P., Jullien, F. and Dargent, B. (2001). Identification of an axonal determinant in the C-terminus of the sodium channel Na(v)1.2. *Embo J* **20**, 5950-61.

Ghosh, P., Dahms, N. M. and Kornfeld, S. (2003). Mannose 6-phosphate receptors: new twists in the tale. *Nat Rev Mol Cell Biol* **4**, 202-12.

Ghosh, P. and Kornfeld, S. (2004). The GGA proteins: key players in protein sorting at the trans-Golgi network. *Eur J Cell Biol* **83**, 257-62.

Ghosh, R. N., Mallet, W. G., Soe, T. T., McGraw, T. E. and Maxfield, F. R. (1998). An endocytosed TGN38 chimeric protein is delivered to the TGN after trafficking through the endocytic recycling compartment in CHO cells. *J Cell Biol* **142**, 923-36.

Glater, E. E., Megeath, L. J., Stowers, R. S. and Schwarz, T. L. (2006). Axonal transport of mitochondria requires milton to recruit kinesin heavy chain and is light chain independent. *J Cell Biol* **173**, 545-57.

Goley, E. D. and Welch, M. D. (2006). The ARP2/3 complex: an actin nucleator comes of age. *Nat Rev Mol Cell Biol* **7**, 713-26.

Goodwin, J. S., Drake, K. R., Rogers, C., Wright, L., Lippincott-Schwartz, J., Philips, M. R. and Kenworthy, A. K. (2005). Depalmitoylated Ras traffics to and from the Golgi complex via a nonvesicular pathway. *J Cell Biol* **170**, 261-72.

Gorvel, J. P., Chavrier, P., Zerial, M. and Gruenberg, J. (1991). rab5 controls early endosome fusion in vitro. *Cell* **64**, 915-25.

Gravotta, D., Deora, A., Perret, E., Oyanadel, C., Soza, A., Schreiner, R., Gonzalez, A. and Rodriguez-Boulan, E. (2007). AP1B sorts basolateral proteins in recycling and biosynthetic routes of MDCK cells. *Proc Natl Acad Sci U S A* **104**, 1564-9.

Griffiths, G. and Simons, K. (1986). The trans Golgi network: sorting at the exit site of the Golgi complex. *Science* **234**, 438-43.

Gross, S. P. (2004). Hither and yon: a review of bi-directional microtubule-based transport. *Phys Biol* **1**, R1-11.

Guo, X., Macleod, G. T., Wellington, A., Hu, F., Panchumarthi, S., Schoenfield, M., Marin, L., Charlton, M. P., Atwood, H. L. and Zinsmaier, K. E. (2005). The GTPase dMiro is required for axonal transport of mitochondria to Drosophila synapses. *Neuron* **47**, 379-93.

Hales, C. M., Vaerman, J. P. and Goldenring, J. R. (2002). Rab11 family interacting protein 2 associates with Myosin Vb and regulates plasma membrane recycling. *J Biol Chem* **277**, 50415-21.

Hao, M. and Maxfield, F. R. (2000). Characterization of rapid membrane internalization and recycling. *J Biol Chem* **275**, 15279-86.

Harris, B. Z. and Lim, W. A. (2001). Mechanism and role of PDZ domains in signaling complex assembly. *J Cell Sci* **114**, 3219-31.

Hernandez-Deviez, D. J., Roth, M. G., Casanova, J. E. and Wilson, J. M. (2004). ARNO and ARF6 regulate axonal elongation and branching through downstream activation of phosphatidylinositol 4-phosphate 5-kinase alpha. *Mol Biol Cell* **15**, 111-20.

Hinners, I. and Tooze, S. A. (2003). Changing directions: clathrin-mediated transport between the Golgi and endosomes. *J Cell Sci* **116**, 763-71.

Hirling, H., Steiner, P., Chaperon, C., Marsault, R., Regazzi, R. and Catsicas, S. (2000). Syntaxin 13 is a developmentally regulated SNARE involved in neurite outgrowth and endosomal trafficking. *Eur J Neurosci* **12**, 1913-23.

Hirokawa, N., Pfister, K. K., Yorifuji, H., Wagner, M. C., Brady, S. T. and Bloom, G. S. (1989). Submolecular domains of bovine brain kinesin identified by electron microscopy and monoclonal antibody decoration. *Cell* **56**, 867-78.

Hirokawa, N. and Takemura, R. (2005). Molecular motors and mechanisms of directional transport in neurons. *Nat Rev Neurosci* **6**, 201-14.

Hirst, J., Borner, G. H., Harbour, M. and Robinson, M. S. (2005). The aftiphilin/p200/gamma-synergin complex. *Mol Biol Cell* **16**, 2554-65.

Hirst, J., Bright, N. A., Rous, B. and Robinson, M. S. (1999). Characterization of a fourth adaptor-related protein complex. *Mol Biol Cell* **10**, 2787-802.

Hirst, J., Lui, W. W., Bright, N. A., Totty, N., Seaman, M. N. and Robinson, M. S. (2000). A family of proteins with gamma-adaptin and VHS domains that facilitate trafficking between the trans-Golgi network and the vacuole/lysosome. *J Cell Biol* **149**, 67-80.

Hirst, J., Motley, A., Harasaki, K., Peak Chew, S. Y. and Robinson, M. S. (2003). EpsinR: an ENTH domain-containing protein that interacts with AP-1. *Mol Biol Cell* **14**, 625-41.

Hirst, J. and Robinson, M. S. (1998). Clathrin and adaptors. *Biochim Biophys Acta* **1404**, 173-93.

Hoepfner, S., Severin, F., Cabezas, A., Habermann, B., Runge, A., Gillooly, D., Stenmark, H. and Zerial, M. (2005). Modulation of receptor recycling and degradation by the endosomal kinesin KIF16B. *Cell* **121**, 437-50.

Hofmann, M. W., Honing, S., Rodionov, D., Dobberstein, B., von Figura, K. and Bakke, O. (1999). The leucine-based sorting motifs in the cytoplasmic domain of the invariant chain are recognized by the clathrin adaptors AP1 and AP2 and their medium chains. *J Biol Chem* **274**, 36153-8.

Honing, S., Sosa, M., Hille-Rehfeld, A. and von Figura, K. (1997). The 46-kDa mannose 6-phosphate receptor contains multiple binding sites for clathrin adaptors. *J Biol Chem* **272**, 19884-90.

Hopkins, C. R. (1983). Intracellular routing of transferrin and transferrin receptors in epidermoid carcinoma A431 cells. *Cell* **35**, 321-30.

Hopkins, C. R., Gibson, A., Shipman, M., Strickland, D. K. and Trowbridge, I. S. (1994). In migrating fibroblasts, recycling receptors are concentrated in narrow tubules in the pericentriolar area, and then routed to the plasma membrane of the leading lamella. *J Cell Biol* **125**, 1265-74.

Horton, A. C. and Ehlers, M. D. (2003). Neuronal polarity and trafficking. *Neuron* **40**, 277-95.

Horton, A. C. and Ehlers, M. D. (2004). Secretory trafficking in neuronal dendrites. *Nat Cell Biol* **6**, 585-91.

Huang, J. D., Brady, S. T., Richards, B. W., Stenolen, D., Resau, J. H., Copeland, N. G. and Jenkins, N. A. (1999). Direct interaction of microtubule- and actin-based transport motors. *Nature* **397**, 267-70.

Huang, K., Yanai, A., Kang, R., Arstikaitis, P., Singaraja, R. R., Metzler, M., Mullard, A., Haigh, B., Gauthier-Campbell, C., Gutekunst, C. A. et al. (2004). Huntingtin-interacting protein HIP14 is a palmitoyl transferase involved in palmitoylation and trafficking of multiple neuronal proteins. *Neuron* **44**, 977-86.

Hunziker, W. and Fumey, C. (1994). A di-leucine motif mediates endocytosis and basolateral sorting of macrophage IgG Fc receptors in MDCK cells. *Embo J* **13**, 2963-9.

Janvier, K., Kato, Y., Boehm, M., Rose, J. R., Martina, J. A., Kim, B. Y., Venkatesan, S. and Bonifacino, J. S. (2003). Recognition of dileucine-based sorting signals from HIV-1 Nef and LIMP-II by the AP-1 gamma-sigma1 and AP-3 delta-sigma3 hemicomplexes. *J Cell Biol* **163**, 1281-90.

Jordens, I., Fernandez-Borja, M., Marsman, M., Dusseljee, S., Janssen, L., Calafat, J., Janssen, H., Wubbolts, R. and Neefjes, J. (2001). The Rab7 effector protein RILP controls lysosomal transport by inducing the recruitment of dynein-dynactin motors. *Curr Biol* **11**, 1680-5.

Jordens, I., Marsman, M., Kuijl, C. and Neefjes, J. (2005). Rab proteins, connecting transport and vesicle fusion. *Traffic* **6**, 1070-7.

Junco, A., Bhullar, B., Tarnasky, H. A. and van der Hoorn, F. A. (2001). Kinesin light-chain KLC3 expression in testis is restricted to spermatids. *Biol Reprod* **64**, 1320-30.

Kaether, C., Skehel, P. and Dotti, C. G. (2000). Axonal membrane proteins are transported in distinct carriers: a two-color video microscopy study in cultured hippocampal neurons. *Mol Biol Cell* **11**, 1213-24.

Kalthoff, C., Groos, S., Kohl, R., Mahrhold, S. and Ungewickell, E. J. (2002). Clint: a novel clathrin-binding ENTH-domain protein at the Golgi. *Mol Biol Cell* **13**, 4060-73.

Kamal, A., Stokin, G. B., Yang, Z., Xia, C. H. and Goldstein, L. S. (2000). Axonal transport of amyloid precursor protein is mediated by direct binding to the kinesin light chain subunit of kinesin-I. *Neuron* **28**, 449-59.

Kanai, Y., Dohmae, N. and Hirokawa, N. (2004). Kinesin transports RNA: isolation and characterization of an RNA-transporting granule. *Neuron* **43**, 513-25.

Kanai, Y., Okada, Y., Tanaka, Y., Harada, A., Terada, S. and Hirokawa, N. (2000). KIF5C, a novel neuronal kinesin enriched in motor neurons. *J Neurosci* **20**, 6374-84.

Kang, R., Swayze, R., Lise, M. F., Gerrow, K., Mullard, A., Honer, W. G. and El-Husseini, A. (2004). Presynaptic trafficking of synaptotagmin I is regulated by protein palmitoylation. *J Biol Chem* **279**, 50524-36.

Katzmann, D. J., Odorizzi, G. and Emr, S. D. (2002). Receptor downregulation and multivesicular-body sorting. *Nat Rev Mol Cell Biol* **3**, 893-905.

Keen, J. H., Willingham, M. C. and Pastan, I. H. (1979). Clathrin-coated vesicles: isolation, dissociation and factor-dependent reassociation of clathrin baskets. *Cell* **16**, 303-12.

Keller, C. A., Yuan, X., Panzanelli, P., Martin, M. L., Alldred, M., Sassoe-Pognetto, M. and Luscher, B. (2004). The gamma2 subunit of GABA(A) receptors is a substrate for palmitoylation by GODZ. *J Neurosci* **24**, 5881-91.

Keller, P., Toomre, D., Diaz, E., White, J. and Simons, K. (2001). Multicolour imaging of post-Golgi sorting and trafficking in live cells. *Nat Cell Biol* **3**, 140-9.

Kennedy, M. J. and Ehlers, M. D. (2006). Organelles and trafficking machinery for postsynaptic plasticity. *Annu Rev Neurosci* **29**, 325-62.

Kim, D. H., Behlke, M. A., Rose, S. D., Chang, M. S., Choi, S. and Rossi, J. J. (2005). Synthetic dsRNA Dicer substrates enhance RNAi potency and efficacy. *Nat Biotechnol* **23**, 222-6.

Kirchhausen, T. (2000a). Clathrin. *Annu Rev Biochem* **69**, 699-727.

Kirchhausen, T. (2000b). Three ways to make a vesicle. *Nat Rev Mol Cell Biol* **1**, 187-98.

Kirchhausen, T. (2002). Clathrin adaptors really adapt. *Cell* **109**, 413-6.

Klausner, R. D., Donaldson, J. G. and Lippincott-Schwartz, J. (1992). Brefeldin A: insights into the control of membrane traffic and organelle structure. *J Cell Biol* **116**, 1071-80.

Kobayashi, T., Storrie, B., Simons, K. and Dotti, C. G. (1992). A functional barrier to movement of lipids in polarized neurons. *Nature* **359**, 647-50.

Konecna, A., Frischknecht, R., Kinter, J., Ludwig, A., Steuble, M., Meskenaite, V., Indermuhle, M., Engel, M., Cen, C., Mateos, J. M. et al. (2006). Calsyntenin-1 docks vesicular cargo to kinesin-1. *Mol Biol Cell* **17**, 3651-63.

Kreitzer, G., Schmoranzer, J., Low, S. H., Li, X., Gan, Y., Weimbs, T., Simon, S. M. and Rodriguez-Boulan, E. (2003). Three-dimensional analysis of post-Golgi carrier exocytosis in epithelial cells. *Nat Cell Biol* **5**, 126-36.

Kundu, A., Avalos, R. T., Sanderson, C. M. and Nayak, D. P. (1996). Transmembrane domain of influenza virus neuraminidase, a type II protein, possesses an apical sorting signal in polarized MDCK cells. *J Virol* **70**, 6508-15.

Laketa, V., Simpson, J. C., Bechtel, S., Wiemann, S. and Pepperkok, R. (2007). High-content microscopy identifies new neurite outgrowth regulators. *Mol Biol Cell* **18**, 242-52.

Langevin, J., Morgan, M. J., Sibarita, J. B., Aresta, S., Murthy, M., Schwarz, T., Camonis, J. and Bellaiche, Y. (2005). Drosophila exocyst components Sec5, Sec6, and Sec15 regulate DE-Cadherin trafficking from recycling endosomes to the plasma membrane. *Dev Cell* **9**, 355-76.

Lapierre, L. A., Kumar, R., Hales, C. M., Navarre, J., Bhartur, S. G., Burnette, J. O., Provance, D. W., Jr., Mercer, J. A., Bahler, M. and Goldenring, J. R. (2001). Myosin vb is associated with plasma membrane recycling systems. *Mol Biol Cell* **12**, 1843-57.

Lauvrak, S. U., Torgersen, M. L. and Sandvig, K. (2004). Efficient endosome-to-Golgi transport of Shiga toxin is dependent on dynamin and clathrin. *J Cell Sci* **117**, 2321-31.

Lawrence, C. J., Dawe, R. K., Christie, K. R., Cleveland, D. W., Dawson, S. C., Endow, S. A., Goldstein, L. S., Goodson, H. V., Hirokawa, N., Howard, J. et al. (2004). A standardized kinesin nomenclature. *J Cell Biol* **167**, 19-22.

Le Borgne, R., Schmidt, A., Mauxion, F., Griffiths, G. and Hoflack, B. (1993). Binding of AP-1 Golgi adaptors to membranes requires phosphorylated cytoplasmic domains of the mannose 6-phosphate/insulin-like growth factor II receptor. *J Biol Chem* **268**, 22552-6.

Le Gall, A. H., Powell, S. K., Yeaman, C. A. and Rodriguez-Boulan, E. (1997). The neural cell adhesion molecule expresses a tyrosine-independent basolateral sorting signal. *J Biol Chem* **272**, 4559-67.

Liebel, U., Starkuviene, V., Erfle, H., Simpson, J. C., Poustka, A., Wiemann, S. and Pepperkok, R. (2003). A microscope-based screening platform for large-scale functional protein analysis in intact cells. *FEBS Lett* **554**, 394-8.

Lin, S. X., Grant, B., Hirsh, D. and Maxfield, F. R. (2001). Rme-1 regulates the distribution and function of the endocytic recycling compartment in mammalian cells. *Nat Cell Biol* **3**, 567-72.

Lin, S. X., Gundersen, G. G. and Maxfield, F. R. (2002). Export from pericentriolar endocytic recycling compartment to cell surface depends on stable, detyrosinated (glu) microtubules and kinesin. *Mol Biol Cell* **13**, 96-109.

Lin, S. X., Mallet, W. G., Huang, A. Y. and Maxfield, F. R. (2004). Endocytosed cation-independent mannose 6-phosphate receptor traffics via the endocytic recycling compartment en route to the trans-Golgi network and a subpopulation of late endosomes. *Mol Biol Cell* **15**, 721-33.

Lindsay, A. J. and McCaffrey, M. W. (2002). Rab11-FIP2 functions in transferrin recycling and associates with endosomal membranes via its COOH-terminal domain. *J Biol Chem* **277**, 27193-9.

Lipschutz, J. H. and Mostov, K. E. (2002). Exocytosis: the many masters of the exocyst. *Curr Biol* **12**, R212-4.

Lisanti, M. P., Caras, I. W., Davitz, M. A. and Rodriguez-Boulan, E. (1989). A glycophospholipid membrane anchor acts as an apical targeting signal in polarized epithelial cells. *J Cell Biol* **109**, 2145-56.

Lobo, S., Greentree, W. K., Linder, M. E. and Deschenes, R. J. (2002). Identification of a Ras palmitoyltransferase in Saccharomyces cerevisiae. *J Biol Chem* **277**, 41268-73.

Lock, J. G. and Stow, J. L. (2005). Rab11 in recycling endosomes regulates the sorting and basolateral transport of E-cadherin. *Mol Biol Cell* **16**, 1744-55.

Lodish, H., Berk, A., Zipursky, L. S., Matsudaira, P., Baltimore, D. and Darnell, J. (2000). Molecular Cell Biology. New York: W. H. Freeman.

Lombardi, D., Soldati, T., Riederer, M. A., Goda, Y., Zerial, M. and Pfeffer, S. R. (1993). Rab9 functions in transport between late endosomes and the trans Golgi network. *Embo J* **12**, 677-82.

Lui, W. W., Collins, B. M., Hirst, J., Motley, A., Millar, C., Schu, P., Owen, D. J. and Robinson, M. S. (2003). Binding partners for the COOH-terminal appendage domains of the GGAs and gamma-adaptin. *Mol Biol Cell* **14**, 2385-98.

Mallard, F., Antony, C., Tenza, D., Salamero, J., Goud, B. and Johannes, L. (1998). Direct pathway from early/recycling endosomes to the Golgi apparatus revealed through the study of shiga toxin B-fragment transport. *J Cell Biol* **143**, 973-90.

Mardones, G. A., Burgos, P. V., Brooks, D. A., Parkinson-Lawrence, E., Mattera, R. and Bonifacino, J. S. (2007). The Trans-Golgi Network Accessory Protein p56

Promotes Long-Range Movement of GGA/Clathrin-containing Transport Carriers and Lysosomal Enzyme Sorting. *Mol Biol Cell* **18**, 3486-501.

Matter, K., Hunziker, W. and Mellman, I. (1992). Basolateral sorting of LDL receptor in MDCK cells: the cytoplasmic domain contains two tyrosine-dependent targeting determinants. *Cell* **71**, 741-53.

Mattera, R., Ritter, B., Sidhu, S. S., McPherson, P. S. and Bonifacino, J. S. (2004). Definition of the consensus motif recognized by gamma-adaptin ear domains. *J Biol Chem* **279**, 8018-28.

Maxfield, F. R. and McGraw, T. E. (2004). Endocytic recycling. *Nat Rev Mol Cell Biol* **5**, 121-32.

Mayor, S., Presley, J. F. and Maxfield, F. R. (1993). Sorting of membrane components from endosomes and subsequent recycling to the cell surface occurs by a bulk flow process. *J Cell Biol* **121**, 1257-69.

McMahon, H. T. and Mills, I. G. (2004). COP and clathrin-coated vesicle budding: different pathways, common approaches. *Curr Opin Cell Biol* **16**, 379-91.

McNiven, M. A. and Thompson, H. M. (2006). Vesicle formation at the plasma membrane and trans-Golgi network: the same but different. *Science* **313**, 1591-4.

Meyer, C., Zizioli, D., Lausmann, S., Eskelinen, E. L., Hamann, J., Saftig, P., von Figura, K. and Schu, P. (2000). mu1A-adaptin-deficient mice: lethality, loss of AP-1 binding and rerouting of mannose 6-phosphate receptors. *Embo J* **19**, 2193-203.

Miaczynska, M. and Zerial, M. (2002). Mosaic organization of the endocytic pathway. *Exp Cell Res* **272**, 8-14.

Miki, H., Okada, Y. and Hirokawa, N. (2005). Analysis of the kinesin superfamily: insights into structure and function. *Trends Cell Biol* **15**, 467-76.

Miller, G. J., Mattera, R., Bonifacino, J. S. and Hurley, J. H. (2003). Recognition of accessory protein motifs by the gamma-adaptin ear domain of GGA3. *Nat Struct Biol* **10**, 599-606.

Mills, I. G., Praefcke, G. J., Vallis, Y., Peter, B. J., Olesen, L. E., Gallop, J. L., Butler, P. J., Evans, P. R. and McMahon, H. T. (2003). EpsinR: an AP1/clathrin interacting protein involved in vesicle trafficking. *J Cell Biol* **160**, 213-22.

Miserey-Lenkei, S., Waharte, F., Boulet, A., Cuif, M. H., Tenza, D., El Marjou, A., Raposo, G., Salamero, J., Heliot, L., Goud, B. et al. (2007). Rab6-interacting Protein 1 Links Rab6 and Rab11 Function. *Traffic* **8**, 1385-1403.

Mostov, K., Su, T. and ter Beest, M. (2003). Polarized epithelial membrane traffic: conservation and plasticity. *Nat Cell Biol* **5**, 287-93.

Munro, S. (2004). Organelle identity and the organization of membrane traffic. *Nat Cell Biol* **6**, 469-72.

Nakada, C., Ritchie, K., Oba, Y., Nakamura, M., Hotta, Y., Iino, R., Kasai, R. S., Yamaguchi, K., Fujiwara, T. and Kusumi, A. (2003). Accumulation of anchored proteins forms membrane diffusion barriers during neuronal polarization. *Nat Cell Biol* **5**, 626-32.

Nakagawa, T., Setou, M., Seog, D., Ogasawara, K., Dohmae, N., Takio, K. and Hirokawa, N. (2000). A novel motor, KIF13A, transports mannose-6-phosphate receptor to plasma membrane through direct interaction with AP-1 complex. *Cell* **103**, 569-81.

Nakata, T. and Hirokawa, N. (1995). Point mutation of adenosine triphosphate-binding motif generated rigor kinesin that selectively blocks anterograde lysosome membrane transport. *J Cell Biol* **131**, 1039-53.

Neubrand, V. E., Will, R. D., Mobius, W., Poustka, A., Wiemann, S., Schu, P., Dotti, C. G., Pepperkok, R. and Simpson, J. C. (2005). Gamma-BAR, a novel AP-1-interacting protein involved in post-Golgi trafficking. *Embo J* **24**, 1122-33.

Nielsen, E., Severin, F., Backer, J. M., Hyman, A. A. and Zerial, M. (1999). Rab5 regulates motility of early endosomes on microtubules. *Nat Cell Biol* **1**, 376-82.

Odorizzi, G. and Trowbridge, I. S. (1997). Structural requirements for basolateral sorting of the human transferrin receptor in the biosynthetic and endocytic pathways of Madin-Darby canine kidney cells. *J Cell Biol* **137**, 1255-64.

Ohno, H., Stewart, J., Fournier, M. C., Bosshart, H., Rhee, I., Miyatake, S., Saito, T., Gallusser, A., Kirchhausen, T. and Bonifacino, J. S. (1995). Interaction of tyrosine-based sorting signals with clathrin-associated proteins. *Science* **269**, 1872-5.

Ohno, H., Tomemori, T., Nakatsu, F., Okazaki, Y., Aguilar, R. C., Foelsch, H., Mellman, I., Saito, T., Shirasawa, T. and Bonifacino, J. S. (1999). Mu1B, a novel adaptor medium chain expressed in polarized epithelial cells. *FEBS Lett* **449**, 215-20.

Orzech, E., Cohen, S., Weiss, A. and Aroeti, B. (2000). Interactions between the exocytic and endocytic pathways in polarized Madin-Darby canine kidney cells. *J Biol Chem* **275**, 15207-19.

Pagano, A., Crottet, P., Prescianotto-Baschong, C. and Spiess, M. (2004). In vitro formation of recycling vesicles from endosomes requires adaptor protein-1/clathrin and is regulated by rab4 and the connector rabaptin-5. *Mol Biol Cell* **15**, 4990-5000.

Page, L. J., Sowerby, P. J., Lui, W. W. and Robinson, M. S. (1999). Gamma-synergin: an EH domain-containing protein that interacts with gamma-adaptin. *J Cell Biol* **146**, 993-1004.

Park, M., Penick, E. C., Edwards, J. G., Kauer, J. A. and Ehlers, M. D. (2004). Recycling endosomes supply AMPA receptors for LTP. *Science* **305**, 1972-5.

Park, M., Salgado, J. M., Ostroff, L., Helton, T. D., Robinson, C. G., Harris, K. M. and Ehlers, M. D. (2006). Plasticity-induced growth of dendritic spines by exocytic trafficking from recycling endosomes. *Neuron* **52**, 817-30.

Pearse, B. M. (1976). Clathrin: a unique protein associated with intracellular transfer of membrane by coated vesicles. *Proc Natl Acad Sci U S A* **73**, 1255-9.

Peden, A. A., Oorschot, V., Hesser, B. A., Austin, C. D., Scheller, R. H. and Klumperman, J. (2004). Localization of the AP-3 adaptor complex defines a novel endosomal exit site for lysosomal membrane proteins. *J Cell Biol* **164**, 1065-76.

Pelissier, A., Chauvin, J. P. and Lecuit, T. (2003). Trafficking through Rab11 endosomes is required for cellularization during Drosophila embryogenesis. *Curr Biol* **13**, 1848-57.

Perret, E., Lakkaraju, A., Deborde, S., Schreiner, R. and Rodriguez-Boulan, E. (2005). Evolving endosomes: how many varieties and why? *Curr Opin Cell Biol* **17**, 423-34.

Pfeffer, S. R. and Rothman, J. E. (1987). Biosynthetic protein transport and sorting by the endoplasmic reticulum and Golgi. *Annu Rev Biochem* **56**, 829-52.

Pfister, K. K., Shah, P. R., Hummerich, H., Russ, A., Cotton, J., Annuar, A. A., King, S. M. and Fisher, E. M. (2006). Genetic analysis of the cytoplasmic dynein subunit families. *PLoS Genet* **2**, e1.

Pinyol, R., Haeckel, A., Ritter, A., Qualmann, B. and Kessels, M. M. (2007). Regulation of N-WASP and the Arp2/3 complex by Abp1 controls neuronal morphology. *PLoS ONE* **2**, e400.

Polishchuk, R. S., Polishchuk, E. V., Marra, P., Alberti, S., Buccione, R., Luini, A. and Mironov, A. A. (2000). Correlative light-electron microscopy reveals the tubular-saccular ultrastructure of carriers operating between Golgi apparatus and plasma membrane. *J Cell Biol* **148**, 45-58.

Poussu, A., Lohi, O. and Lehto, V. P. (2000). Vear, a novel Golgi-associated protein with VHS and gamma-adaptin "ear" domains. *J Biol Chem* **275**, 7176-83.

Prahlad, V., Yoon, M., Moir, R. D., Vale, R. D. and Goldman, R. D. (1998). Rapid movements of vimentin on microtubule tracks: kinesin-dependent assembly of intermediate filament networks. *J Cell Biol* **143**, 159-70.

Provance, D. W., Jr., Gourley, C. R., Silan, C. M., Cameron, L. C., Shokat, K. M., Goldenring, J. R., Shah, K., Gillespie, P. G. and Mercer, J. A. (2004). Chemical-genetic inhibition of a sensitized mutant myosin Vb demonstrates a role in peripheral-pericentriolar membrane traffic. *Proc Natl Acad Sci U S A* **101**, 1868-73.

Rahman, A., Friedman, D. S. and Goldstein, L. S. (1998). Two kinesin light chain genes in mice. Identification and characterization of the encoded proteins. *J Biol Chem* **273**, 15395-403.

Raiborg, C., Rusten, T. E. and Stenmark, H. (2003). Protein sorting into multivesicular endosomes. *Curr Opin Cell Biol* **15**, 446-55.

Rapoport, I., Chen, Y. C., Cupers, P., Shoelson, S. E. and Kirchhausen, T. (1998). Dileucine-based sorting signals bind to the beta chain of AP-1 at a site distinct and regulated differently from the tyrosine-based motif-binding site. *Embo J* **17**, 2148-55.

Ren, M., Xu, G., Zeng, J., De Lemos-Chiarandini, C., Adesnik, M. and Sabatini, D. D. (1998). Hydrolysis of GTP on rab11 is required for the direct delivery of transferrin from the pericentriolar recycling compartment to the cell surface but not from sorting endosomes. *Proc Natl Acad Sci U S A* **95**, 6187-92.

Resh, M. D. (1999). Fatty acylation of proteins: new insights into membrane targeting of myristoylated and palmitoylated proteins. *Biochim Biophys Acta* **1451**, 1-16.

Riggs, B., Rothwell, W., Mische, S., Hickson, G. R., Matheson, J., Hays, T. S., Gould, G. W. and Sullivan, W. (2003). Actin cytoskeleton remodeling during early Drosophila furrow formation requires recycling endosomal components Nuclear-fallout and Rab11. *J Cell Biol* **163**, 143-54.

Rink, J., Ghigo, E., Kalaidzidis, Y. and Zerial, M. (2005). Rab conversion as a mechanism of progression from early to late endosomes. *Cell* **122**, 735-49.

Ritter, B., Philie, J., Girard, M., Tung, E. C., Blondeau, F. and McPherson, P. S. (2003). Identification of a family of endocytic proteins that define a new alpha-adaptin ear-binding motif. *EMBO Rep* **4**, 1089-95.

Robinson, M. S. (1990). Cloning and expression of gamma-adaptin, a component of clathrin-coated vesicles associated with the Golgi apparatus. *J Cell Biol* **111**, 2319-26.

Robinson, M. S. (2004). Adaptable adaptors for coated vesicles. *Trends Cell Biol* **14**, 167-74.

Robinson, M. S. and Bonifacino, J. S. (2001). Adaptor-related proteins. *Curr Opin Cell Biol* **13**, 444-53.

Robinson, M. S. and Kreis, T. E. (1992). Recruitment of coat proteins onto Golgi membranes in intact and permeabilized cells: effects of brefeldin A and G protein activators. *Cell* **69**, 129-38.

Rocks, O., Peyker, A., Kahms, M., Verveer, P. J., Koerner, C., Lumbierres, M., Kuhlmann, J., Waldmann, H., Wittinghofer, A. and Bastiaens, P. I. (2005). An acylation cycle regulates localization and activity of palmitoylated Ras isoforms. *Science* **307**, 1746-52.

Rodionov, D. G. and Bakke, O. (1998). Medium chains of adaptor complexes AP-1 and AP-2 recognize leucine-based sorting signals from the invariant chain. *J Biol Chem* **273**, 6005-8.

Rodriguez-Boulan, E., Kreitzer, G. and Musch, A. (2005). Organization of vesicular trafficking in epithelia. *Nat Rev Mol Cell Biol* **6**, 233-47.

Rodriguez-Boulan, E. and Musch, A. (2005). Protein sorting in the Golgi complex: shifting paradigms. *Biochim Biophys Acta* **1744**, 455-64.

Roland, J. T., Kenworthy, A. K., Peranen, J., Caplan, S. and Goldenring, J. R. (2007). Myosin Vb interacts with Rab8a on a tubular network containing EHD1 and EHD3. *Mol Biol Cell* **18**, 2828-37.

Roquemore, E. P. and Banting, G. (1998). Efficient trafficking of TGN38 from the endosome to the trans-Golgi network requires a free hydroxyl group at position 331 in the cytosolic domain. *Mol Biol Cell* **9**, 2125-44.

Roth, A. F., Feng, Y., Chen, L. and Davis, N. G. (2002). The yeast DHHC cysteine-rich domain protein Akr1p is a palmitoyl transferase. *J Cell Biol* **159**, 23-8.

Roush, D. L., Gottardi, C. J., Naim, H. Y., Roth, M. G. and Caplan, M. J. (1998). Tyrosine-based membrane protein sorting signals are differentially interpreted by polarized Madin-Darby canine kidney and LLC-PK1 epithelial cells. *J Biol Chem* **273**, 26862-9.

Saint-Pol, A., Yelamos, B., Amessou, M., Mills, I. G., Dugast, M., Tenza, D., Schu, P., Antony, C., McMahon, H. T., Lamaze, C. et al. (2004). Clathrin adaptor epsinR is required for retrograde sorting on early endosomal membranes. *Dev Cell* **6**, 525-38.

Sampo, B., Kaech, S., Kunz, S. and Banker, G. (2003). Two distinct mechanisms target membrane proteins to the axonal surface. *Neuron* **37**, 611-24.

Scheiffele, P., Roth, M. G. and Simons, K. (1997). Interaction of influenza virus haemagglutinin with sphingolipid-cholesterol membrane domains via its transmembrane domain. *Embo J* **16**, 5501-8.

Schmidt, M. F. and Schlesinger, M. J. (1980). Relation of fatty acid attachment to the translation and maturation of vesicular stomatitis and Sindbis virus membrane glycoproteins. *J Biol Chem* **255**, 3334-9.

Schmidt, M. R. and Haucke, V. (2007). Recycling endosomes in neuronal membrane traffic. *Biol Cell* **99**, 333-42.

Schroer, T. A. (2004). Dynactin. *Annu Rev Cell Dev Biol* **20**, 759-79.

Schweizer, A., Kornfeld, S. and Rohrer, J. (1997). Proper sorting of the cation-dependent mannose 6-phosphate receptor in endosomes depends on a pair of aromatic amino acids in its cytoplasmic tail. *Proc Natl Acad Sci U S A* **94**, 14471-6.

Seabra, M. C. and Coudrier, E. (2004). Rab GTPases and myosin motors in organelle motility. *Traffic* **5**, 393-9.

Seabra, M. C. and Wasmeier, C. (2004). Controlling the location and activation of Rab GTPases. *Curr Opin Cell Biol* **16**, 451-7.

Seaman, M. N. (2005). Recycle your receptors with retromer. *Trends Cell Biol* **15**, 68-75.

Setou, M., Nakagawa, T., Seog, D. H. and Hirokawa, N. (2000). Kinesin superfamily motor protein KIF17 and mLin-10 in NMDA receptor-containing vesicle transport. *Science* **288**, 1796-802.

Setou, M., Seog, D. H., Tanaka, Y., Kanai, Y., Takei, Y., Kawagishi, M. and Hirokawa, N. (2002). Glutamate-receptor-interacting protein GRIP1 directly steers kinesin to dendrites. *Nature* **417**, 83-7.

Sheff, D. R., Daro, E. A., Hull, M. and Mellman, I. (1999). The receptor recycling pathway contains two distinct populations of early endosomes with different sorting functions. *J Cell Biol* **145**, 123-39.

Shiba, Y., Takatsu, H., Shin, H. W. and Nakayama, K. (2002). Gamma-adaptin interacts directly with Rabaptin-5 through its ear domain. *J Biochem (Tokyo)* **131**, 327-36.

Shirane, M. and Nakayama, K. I. (2006). Protrudin induces neurite formation by directional membrane trafficking. *Science* **314**, 818-21.

Short, B., Preisinger, C., Schaletzky, J., Kopajtich, R. and Barr, F. A. (2002). The Rab6 GTPase regulates recruitment of the dynactin complex to Golgi membranes. *Curr Biol* **12**, 1792-5.

Simmen, T., Honing, S., Icking, A., Tikkanen, R. and Hunziker, W. (2002). AP-4 binds basolateral signals and participates in basolateral sorting in epithelial MDCK cells. *Nat Cell Biol* **4**, 154-9.

Simpson, F., Bright, N. A., West, M. A., Newman, L. S., Darnell, R. B. and Robinson, M. S. (1996). A novel adaptor-related protein complex. *J Cell Biol* **133**, 749-60.

Simpson, J. C., Wellenreuther, R., Poustka, A., Pepperkok, R. and Wiemann, S. (2000). Systematic subcellular localization of novel proteins identified by large-scale cDNA sequencing. *EMBO Rep* **1**, 287-92.

Skibbens, J. E., Roth, M. G. and Matlin, K. S. (1989). Differential extractability of influenza virus hemagglutinin during intracellular transport in polarized epithelial cells and nonpolar fibroblasts. *J Cell Biol* **108**, 821-32.

Skop, A. R., Bergmann, D., Mohler, W. A. and White, J. G. (2001). Completion of cytokinesis in C. elegans requires a brefeldin A-sensitive membrane accumulation at the cleavage furrow apex. *Curr Biol* **11**, 735-46.

Slepnev, V. I. and De Camilli, P. (2000). Accessory factors in clathrin-dependent synaptic vesicle endocytosis. *Nat Rev Neurosci* **1**, 161-72.

Smith, C. J. and Pearse, B. M. (1999). Clathrin: anatomy of a coat protein. *Trends Cell Biol* **9**, 335-8.

Stanley, K. K. and Howell, K. E. (1993). TGN38/41: a molecule on the move. *Trends Cell Biol* **3**, 252-5.

Strasser, G. A., Rahim, N. A., VanderWaal, K. E., Gertler, F. B. and Lanier, L. M. (2004). Arp2/3 is a negative regulator of growth cone translocation. *Neuron* **43**, 81-94.

Swarthout, J. T., Lobo, S., Farh, L., Croke, M. R., Greentree, W. K., Deschenes, R. J. and Linder, M. E. (2005). DHHC9 and GCP16 constitute a human protein fatty acyltransferase with specificity for H- and N-Ras. *J Biol Chem* **280**, 31141-8.

Tai, A. W., Chuang, J. Z., Bode, C., Wolfrum, U. and Sung, C. H. (1999). Rhodopsin's carboxy-terminal cytoplasmic tail acts as a membrane receptor for cytoplasmic dynein by binding to the dynein light chain Tctex-1. *Cell* **97**, 877-87.

Takatsu, H., Yoshino, K. and Nakayama, K. (2000). Adaptor gamma ear homology domain conserved in gamma-adaptin and GGA proteins that interact with gamma-synergin. *Biochem Biophys Res Commun* **271**, 719-25.

Takei, K. and Haucke, V. (2001). Clathrin-mediated endocytosis: membrane factors pull the trigger. *Trends Cell Biol* **11**, 385-91.

Tanaka, Y., Kanai, Y., Okada, Y., Nonaka, S., Takeda, S., Harada, A. and Hirokawa, N. (1998). Targeted disruption of mouse conventional kinesin heavy chain, kif5B, results in abnormal perinuclear clustering of mitochondria. *Cell* **93**, 1147-58.

Terada, S., Kinjo, M. and Hirokawa, N. (2000). Oligomeric tubulin in large transporting complex is transported via kinesin in squid giant axons. *Cell* **103**, 141-55.

Thomas, D. C. and Roth, M. G. (1994). The basolateral targeting signal in the cytoplasmic domain of glycoprotein G from vesicular stomatitis virus resembles a variety of intracellular targeting motifs related by primary sequence but having diverse targeting activities. *J Biol Chem* **269**, 15732-9.

Thompson, A., Nessler, R., Wisco, D., Anderson, E., Winckler, B. and Sheff, D. (2007). Recycling endosomes of polarized epithelial cells actively sort apical and basolateral cargos into separate subdomains. *Mol Biol Cell* **18**, 2687-97.

Tikkanen, R., Obermuller, S., Denzer, K., Pungitore, R., Geuze, H. J., von Figura, K. and Honing, S. (2000). The dileucine motif within the tail of MPR46 is required for sorting of the receptor in endosomes. *Traffic* **1**, 631-40.

Traub, L. M. (2003). Sorting it out: AP-2 and alternate clathrin adaptors in endocytic cargo selection. *J Cell Biol* **163**, 203-8.

Traub, L. M. (2005). Common principles in clathrin-mediated sorting at the Golgi and the plasma membrane. *Biochim Biophys Acta* **1744**, 415-37.

Ullrich, O., Reinsch, S., Urbe, S., Zerial, M. and Parton, R. G. (1996). Rab11 regulates recycling through the pericentriolar recycling endosome. *J Cell Biol* **135**, 913-24.

Urbe, S., Huber, L. A., Zerial, M., Tooze, S. A. and Parton, R. G. (1993). Rab11, a small GTPase associated with both constitutive and regulated secretory pathways in PC12 cells. *FEBS Lett* **334**, 175-82.

Vale, R. D. (2003). The molecular motor toolbox for intracellular transport. *Cell* **112**, 467-80.

Vale, R. D., Reese, T. S. and Sheetz, M. P. (1985). Identification of a novel force-generating protein, kinesin, involved in microtubule-based motility. *Cell* **42**, 39-50.

van't Hof, W. and Resh, M. D. (1997). Rapid plasma membrane anchoring of newly synthesized p59fyn: selective requirement for NH2-terminal myristoylation and palmitoylation at cysteine-3. *J Cell Biol* **136**, 1023-35.

van der Sluijs, P., Hull, M., Webster, P., Male, P., Goud, B. and Mellman, I. (1992). The small GTP-binding protein rab4 controls an early sorting event on the endocytic pathway. *Cell* **70**, 729-40.

Van Der Sluijs, P., Hull, M., Zahraoui, A., Tavitian, A., Goud, B. and Mellman, I. (1991). The small GTP-binding protein rab4 is associated with early endosomes. *Proc Natl Acad Sci U S A* **88**, 6313-7.

van Ijzendoorn, S. C. (2006). Recycling endosomes. *J Cell Sci* **119**, 1679-81.

Vega, I. E. and Hsu, S. C. (2001). The exocyst complex associates with microtubules to mediate vesicle targeting and neurite outgrowth. *J Neurosci* **21**, 3839-48.

Veit, M. and Schmidt, M. F. (1993). Timing of palmitoylation of influenza virus hemagglutinin. *FEBS Lett* **336**, 243-7.

Verhey, K. J., Meyer, D., Deehan, R., Blenis, J., Schnapp, B. J., Rapoport, T. A. and Margolis, B. (2001). Cargo of kinesin identified as JIP scaffolding proteins and associated signaling molecules. *J Cell Biol* **152**, 959-70.

Wang, Y. J., Wang, J., Sun, H. Q., Martinez, M., Sun, Y. X., Macia, E., Kirchhausen, T., Albanesi, J. P., Roth, M. G. and Yin, H. L. (2003). Phosphatidylinositol 4 phosphate regulates targeting of clathrin adaptor AP-1 complexes to the Golgi. *Cell* **114**, 299-310.

Ward, B. M. and Moss, B. (2004). Vaccinia virus A36R membrane protein provides a direct link between intracellular enveloped virions and the microtubule motor kinesin. *J Virol* **78**, 2486-93.

Wasiak, S., Legendre-Guillemin, V., Puertollano, R., Blondeau, F., Girard, M., de Heuvel, E., Boismenu, D., Bell, A. W., Bonifacino, J. S. and McPherson, P. S. (2002). Enthoprotin: a novel clathrin-associated protein identified through subcellular proteomics. *J Cell Biol* **158**, 855-62.

Webb, Y., Hermida-Matsumoto, L. and Resh, M. D. (2000). Inhibition of protein palmitoylation, raft localization, and T cell signaling by 2-bromopalmitate and polyunsaturated fatty acids. *J Biol Chem* **275**, 261-70.

Wehrle-Haller, B. and Imhof, B. A. (2001). Stem cell factor presentation to c-Kit. Identification of a basolateral targeting domain. *J Biol Chem* **276**, 12667-74.

Wiemann, S., Weil, B., Wellenreuther, R., Gassenhuber, J., Glassl, S., Ansorge, W., Bocher, M., Blocker, H., Bauersachs, S., Blum, H. et al. (2001). Toward a catalog of human genes and proteins: sequencing and analysis of 500 novel complete protein coding human cDNAs. *Genome Res* **11**, 422-35.

Wilcke, M., Johannes, L., Galli, T., Mayau, V., Goud, B. and Salamero, J. (2000). Rab11 regulates the compartmentalization of early endosomes required for efficient transport from early endosomes to the trans-golgi network. *J Cell Biol* **151**, 1207-20.

Wilson, G. M., Fielding, A. B., Simon, G. C., Yu, X., Andrews, P. D., Hames, R. S., Frey, A. M., Peden, A. A., Gould, G. W. and Prekeris, R. (2005). The FIP3-Rab11 protein complex regulates recycling endosome targeting to the cleavage furrow during late cytokinesis. *Mol Biol Cell* **16**, 849-60.

Winckler, B. (2004). Scientiae forum / models and speculations pathways for axonal targeting of membrane proteins. *Biol Cell* **96**, 669-74.

Winckler, B., Forscher, P. and Mellman, I. (1999). A diffusion barrier maintains distribution of membrane proteins in polarized neurons. *Nature* **397**, 698-701.

Winckler, B. and Mellman, I. (1999). Neuronal polarity: controlling the sorting and diffusion of membrane components. *Neuron* **23**, 637-40.

Wisco, D., Anderson, E. D., Chang, M. C., Norden, C., Boiko, T., Folsch, H. and Winckler, B. (2003). Uncovering multiple axonal targeting pathways in hippocampal neurons. *J Cell Biol* **162**, 1317-28.

Yamashiro, D. J., Tycko, B., Fluss, S. R. and Maxfield, F. R. (1984). Segregation of transferrin to a mildly acidic (pH 6.5) para-Golgi compartment in the recycling pathway. *Cell* **37**, 789-800.

Yeaman, C., Le Gall, A. H., Baldwin, A. N., Monlauzeur, L., Le Bivic, A. and Rodriguez-Boulan, E. (1997). The O-glycosylated stalk domain is required for apical sorting of neurotrophin receptors in polarized MDCK cells. *J Cell Biol* **139**, 929-40.

Yeh, D. C., Duncan, J. A., Yamashita, S. and Michel, T. (1999). Depalmitoylation of endothelial nitric-oxide synthase by acyl-protein thioesterase 1 is potentiated by Ca(2+)-calmodulin. *J Biol Chem* **274**, 33148-54.

Zacchi, P., Stenmark, H., Parton, R. G., Orioli, D., Lim, F., Giner, A., Mellman, I., Zerial, M. and Murphy, C. (1998). Rab17 regulates membrane trafficking through apical recycling endosomes in polarized epithelial cells. *J Cell Biol* **140**, 1039-53.

Zeghouf, M., Guibert, B., Zeeh, J. C. and Cherfils, J. (2005). Arf, Sec7 and Brefeldin A: a model towards the therapeutic inhibition of guanine nucleotide-exchange factors. *Biochem Soc Trans* **33**, 1265-8.

Zerial, M. and McBride, H. (2001). Rab proteins as membrane organizers. *Nat Rev Mol Cell Biol* **2**, 107-17.

Zhai, R. G., Vardinon-Friedman, H., Cases-Langhoff, C., Becker, B., Gundelfinger, E. D., Ziv, N. E. and Garner, C. C. (2001). Assembling the presynaptic active zone: a characterization of an active one precursor vesicle. *Neuron* **29**, 131-43.

Zhang, X. M., Ellis, S., Sriratana, A., Mitchell, C. A. and Rowe, T. (2004). Sec15 is an effector for the Rab11 GTPase in mammalian cells. *J Biol Chem* **279**, 43027-34.

Zhu, Y., Doray, B., Poussu, A., Lehto, V. P. and Kornfeld, S. (2001). Binding of GGA2 to the lysosomal enzyme sorting motif of the mannose 6-phosphate receptor. *Science* **292**, 1716-8.

Appendix

a) List of Figures

b) List of Primers

primer	short name / use	sequence 5'-3'	length (bp)
MS1	AP-1γ_hinge_for_BamHI	CGC GGA TCC ATG GAA AAA GTG ACC ACA AAT GGC	33
MS2	AP-1γ_ear_for_BamHI	CGC GGA TCC ATG GGG CTT TCC TCA CAG CCT CTC	33
MS3	AP-1γ_hinge_rev_EcoRI	CCG GAA TTC TCA GCC TGG AGC GAT GTC ATT GAA	33
MS4	AP-1γ_ear_rev_EcoRI	CCG GAA TTC TCA TTG CCA GGA CTG AGG GGG	30
MS5	2c18_for_EcoRI	CCG GAA TTC ATG GGG AAC TGC TGC TG	26
MS6	2c18_rev_NotI	ATA AGA ATG CGG CCG CCT ATC GAG TCT GTT GAT CTG TGT	39
MS7	2c18_N-term_rev_NotI	ATA AGA ATG CGG CCG CCT ACT CTT CTT GTA AGG CTA ACT CTT TTT	45
MS8	2c18_C-term_for_EcoRI	CCG GAA TTC ATG GAC GAC AGC ACA TCC TTA G	31
MS9	2c18_middle_for_EcoRI	CCG GAA TTC ATG AAG TTA AGA CTA GAA GAA GAA GCT TTA TAC	42
MS10	2c18_middle_rev_NotI	ATA AGA ATG CGG CCG CCT AAT TTC CAC TAG TTG ATT TAG TTT TGG TC	47
MS11	2c18_aa140_for_EcoRI	CCG GAA TTC ATG TCC AAC AAT GGA GAA TAT CAA AGT TCA	39
MS12	2c18_aa140_rev_NotI	ATA AGA ATG CGG CCG CCT AGG AAG GAT GAT ATT GCT GCA C	40
MS13	syp_tail_for_BamHI	CGC GGA TCC ATG GAG ACA GGC TGG GCA GCC	30
MS14	syp_tail_rev_EcoRI	CCG GAA TTC TTA CAT CTG ATT GGA GAA GGA GGT GGG	36
MS15	syp_aa282_rev_EcoRI	CCG GAA TTC TTA GCC ACC GCC ACC GCT G	28
MS16	2c18_bp164_back-mutation	AGT GAT GAA GGG GAG AGC CCA GGA AGC	27
MS17	2c18_bp164_back-mutation_rev	GCT TCC TGG GCT CTC CCC TTC ATC ACT	27
MS18	2c18_aa52_for_EcoRI	CCG GAA TTC ATG GAT GAA GGG GAG AGC CC	29
MS19	2Z-tag_for_BamHI	CGC GGA TCC CCG ATG AAC AAA TTC AAC AAA GAA CAA CAA AAC G	43
MS20	2Z-tag_rev_EcoRI	CCG GAA TTC CGG GCC TAC TTT CGG CGC C	28
MS21	oligo_2c18_aa42-51_for	AAT TCA CAA TAG AGT TTG AGA ATC TAG TAG AAA GTT AGG C	40
MS22	oligo_2c18_aa42-51_rev	GGC CGC CTA ACT TTC TAC TAG ATT CTC AAA CTC TAT TGT G	40
MS23	2c18_aa61_for_EcoRI	CCG GAA TTC ATG CAT AGG CCT CTT ACT GAG G	31
MS24	2c18_aa76_for_EcoRI	CCG GAA TTC ATG CAT TAT GAT TCC ATT GCC GAA AAA C	37
MS25	synapsin_for_SalI	CGA TAC GCG TCG ACT CAT GAA CTA CCT GCG GCG	33
MS26	synapsin_rev_NotI	ATA AGA ATG CGG CCG CTC AGT CGG AGA AGA GGC T	34
MS27	synapsin_seq_bp537-558_for	GCC AGA CTT TGT GCT GAT CCG C	22
MS28	synapsin_seq_bp1616-1634_rev	CGG GCT GCT GGA GGT GCT C	19
MS29	2c18_rev_SalI	ATA CGC GTC GAC TTC GAG TCT GTT GAT CTG TGT CA	35
MS30	2c18_aa140_rev_SalI	ATA CGC GTC GAC TGG AAG GAT GAT ATT GCT GCA C	34
MS31	rat-2c18_rev_NotI	ATA AGA ATG CGG CCG CCT ACC GGA TCT GCT GAT CT	35
MS32	2c18_aa29_for_EcoRI	CCG GAA TTC ATG TCC AAG TAT TTT AGA ACA TGC TCA AGA	39
MS33	2c18_aa38_for_EcoRI	CCG GAA TTC ATG GGT GAG CAC TTG ACA ATA GAG TTT	36
MS34	mouse-2c18_rev_NotI	ATA AGA ATG CGG CCG CCT ATC GGA TCT GCT GGT CT	35
MS35	rat-BERP_for_BamHI	CGC GGA TCC ATG GCA AAG AGG GAG GAC A	28
MS36	rat-BERP_rev_XhoI	GGC CGC TCG AGC TAC TGG AGG TAT CGA TAG G	31

MS37	rat-BERP_aa421_for_BamHI	CGC GGA TCC ATG CCC GGA GAC TTG CCA C	28
MS38	rat-BERP_aa287_for_BamHI	CGC GGA TCC ATG CCA GAA AGG CCC CAT GAG	30
MS39	rat-BERP_aa420_rev_XhoI	GGC CGC TCG AGC TAT CTC AGG GCA CGC ACA C	31
MS40	mouse-KIF5C-tail_for_EcoRI	CCG GAA TTC ATG TTC CAA GAT AAG GAA AAG GAG CA	35
MS41	mouse-KIF5C-tail_rev_NotI	ATA AGA ATG CGG CCG CTT ATT TCT GGT AGT GAG TAG AGT TTG	42
MS42	mouse-KLC2_for_EcoRI	CCG GAA TTC ATG GCC ACG ATG GTG CTT C	28
MS43	mouse-KLC2_rev_NotI	ATA AGA ATG CGG CCG CTT AGC CCA CCA GGG AGC TT	35
MS44	mouse-p21_for_BamHI	CGC GGA TCC ATG CCG GCA TAC CAC TCT T	28
MS45	mouse-p21_rev_XhoI	GGC CGC TCG AGT CAC TGC CCA GGC CC	26
MS46	mouse-p21_aa33_myc_for	CAA AAA CTC ATC TCA GAA GAG GAT CTG CCT CGC GAG ACC AAA GA	44
Ms47	mouse-p21_aa32_myc_rev	ATC CTC TTC TGA GAT GAG TTT TTG TTC GGC GGG TCC TTT GAA CT	44
MS48	mouse-p41_for_BamHI	CGC GGA TCC ATG GCC TAC CAC AGC TTC	27
MS49	mouse-p41_rev_XhoI	GGC CGC TCG AGT CAT TTG ATT TTC AGG TCC TTC AAG	36
MS50	mouse-p41_aa182_myc_for	CAA AAA CTC ATC TCA GAA GAG GAT CTG CCT ACA CCG TGG GGC	42
MS51	mouse-p41_aa181_myc_rev	ATC CTC TTC TGA GAT GAG TTT TTG TTC GGC TGG CCG TTC TTC C	43
MS52	rat-BERP_aa289_rev_XhoI	GGC CGC TCG AGC TAC CTT TCT GGG AAG GCC TG	32
MS53	rat-BERP_aa149_rev_XhoI	GGC CGC TCG AGC TAC ACT GTG CCG TGT TCA CG	32
MS54	human-coronin1B_for_EcoRI	CCG GAA TTC ATG TCC TTC CGC AAA GTG GTC	30
MS55	human-coronin1B_rev_XbaI	TGC TCT AGA CTA CGC ATC CCC GTT CTC	27
MS56	rat-2c18_rev_SalI	ATA CGC GTC GAC TCC GGA TCT GCT GAT CTG TAT	33
MS57	2c18_AxxA_for_EcoRI	GGA ATT CAT GGG GAA CTG CTG CTG GAC GCA GTG CGC CGG ACT GGC TCG C	49
MS58	2c18_aa100_rev_SalI	ATA CGC GTC GAC TCT CTT CTT GTA AGG CTA ACT CTT TTT GAA TTT TCT C	49
MS59	2c18_AxxA-2nd_for	GAG CAC TTG ACA ATA GAG GCT GAG AAT GCA GTA GAA AGT GAT GAA GG	47
MS60	2c18_AxxA-2nd_rev	CCT TCA TCA CTT TCT ACT GCA TTC TCA GCC TCT ATT GTC AAG TGC TC	47
MS61	2c18_G2A_for_EcoRI	CCG GAA TTC ATG GCG AAC TGC TGC TGG ACG	30
MS62	2c18_C4,5,9S_for_EcoRI	CCG GAA TTC ATG GGG AAC AGC TCC TGG ACG CAG AGC TTC	39
MS63	2c18_aa10_for_EcoRI	CCG GAA TTC ATG TTC GGA CTG CTT CGC AAG	30
MS64	2c18_C4S_for_EcoRI	CCG GAA TTC ATG GGG AAC AGC TGC TGG ACG CAG TGC TTC G	40
MS65	2c18_C5S_for_EcoRI	CCG GAA TTC ATG GGG AAC TGC TCC TGG ACG CAG TGC TTC G	40
MS66	2c18_C9S_for_EcoRI	CCG GAA TTC ATG GGG AAC TGC TGC TGG ACG CAG AGC TTC G	40
MS67	2c18_C4,5S_for_EcoRI	CCG GAA TTC ATG GGG AAC AGC TCC TGG ACG CAG TGC TTC G	40
MS68	2c18_C4,9S_for_EcoRI	CCG GAA TTC ATG GGG AAC AGC TGC TGG ACG CAG AGC TTC G	40
MS69	2c18_C5,9S_for_EcoRI	CCG GAA TTC ATG GGG AAC TGC TCC TGG ACG CAG AGC TTC G	40
MS70	oligo_2c18 aa1-14_for_EcoRI	AAT TCA TGG GGA ACT GCT GCT GGA CGC AGT GCT TCG GAC TGC TTC GCA G	49
MS71	oligo_2c18 aa1-14_rev_SalI	TCG ACT GCG AAG CAG TCC GAA GCA CTG CGT CCA GCA GCA GTT CCC CAT G	49
MS72	2c18_rev_XbaI	TGC TCT AGA CTA TCG AGT CTG TTG ATC TGT GT	32
MS73	2c18_aa140_rev_XbaI	TGC TCT AGA CTA GGA AGG ATG ATA TTG CTG CAC	33
MS74	rab11A_for_BamHI	CGC GGA TCC ATG GGC ACC CGC GAC	24
MS75	rab11A_rev_XhoI	GGC CGC TCG AGT TAT ATG TTC TGA CAG CAC TGC AC	35
MS76	myc-tag_oligo1	CAT GGA GCA GAA ACT CAT CTC TGA AGA GGA TCT GG	35

MS77	myc-tag_oligo2	GAT CCC AGA TCC TCT TCA GAG ATG AGT TTC TGC TCC ATG GTA C	43
MS78	2c18_rev_SalI_pmRFP-N1	ATA CGC GTC GAC TGT CGA GTC TGT TGA TCT GTG TCA	36
MS79	2c18_FENL->AENA_for	GAG CAC TTG ACA ATA GAG GCT GAG AAT GCA GTA GAA AGT GAT GAA GG	47
MS80	2c18_FENL->AENA_rev	CCT TCA TCA CTT TCT ACT GCA TTC TCA GCC TCT ATT GTC AAG TGC TC	47
MS81	AP-1β1_ear_for_EcoRI	CCG GAA TTC GGC ACC CTT TCA GGA TCC	27
MS82	AP-1β1_ear_rev_SalI	ATA CGC GTC GAC TCA GTT CTT GAG GAT AGT CTC GTA G	37
MS83	EHD1_for_EcoRI	CCG GAA TTC ATG TTC AGC TGG GTG AGC AAG	30
MS84	EHD1_rev_NotI	ATA AGA ATG CGG CCG CTC ACT CGT GCC TCC GTT TG	35
MS85	EHD1_G429R_for	CGG CGA GCG GGC TGG	15
MS86	EHD1_G429R_rev	CCA GCC CGC TCG CCG	15
MS87	Sec6-sequencing primer_middle	CTT TGT TCC TCC TGG GAG	18
MS88	EHD1_wt(T72N-backmutation)_for	CAG CAC CGG CAA GAC CAC CTT CAT CCG CC	29
MS89	EHD1_wt(T72N-backmutation)_rev	GGC GGA TGA AGG TGG TCT TGC CGG TGC TG	29
MS90	2c18_W210A_for	CAT CCT TAG ACC TAG AGG CGG AAG ATG AAG AAG GAA TG	38
MS91	2c18_W210A_rev	CAT TCC TTC TTC ATC TTC CGC CTC TAG GTC TAA GGA TG	38
MS92	2c18_W260A_for	GAT TCC AAT GGG CTG GAG GCG GAA AAT GAT TTT GTT AGT G	40
MS93	2c18_W260A_rev	CAC TAA CAA AAT CAT TTT CCG CCT CCA GCC CAT TGG AAT C	40

c) Abbreviations

2-Br	2-bromopalmitate
2xYT	2x yeast trypton
aa	**amino acid**
ADP	adenosine diphosphate
AMPA	α-amino-3-hydroxy-5-methylisoxazole-4-propionic acid
AP	alkaline phosphatase
AP (-1,-2,-3,-4)	adaptor protein (or: 'assembly polypeptide') (-1, -2, -3, -4)
APOER2	apolipoprotein E receptor 2
APP	amyloid precursor protein
APT	acylprotein thioesterase
ARF	ADP-ribosylation factor
ATP	adenosine triphosphate
BCIP	**5-bromo-4-chloro-3-indolyl phosphate**
BFA	brefeldin A
bp	base pairs
BSA	bovine serum albumine
CAM	**cell adhesion molecule**
CCV	clathrin-coated vesicle
cDNA	complementary (copy) DNA
Ci	Curie
COP	coat protein
CPM	counts per minute
Cst1	Calsyntenin-1
Da	**Dalton**
DAPI	diamidophenylindole
ddH2O	double-distilled water
dH2O	distilled water
DIV	day in vitro
D-MEM	Dulbecco's minimal essential medium
DMF	dimethyl formamide
DMSO	dimethyl sulfoxide
DNA	deoxyribonucleic acid
dNTP	deoxynucleosidtriphosphate
DSS	Disuccinimidyl Suberate
DTT	dithiotreitol
E. coli	***Escherichia coli***
E18	embryonic day 18
ECL	enhanced chemiluminescence
EDTA	ethylenediaminetetraacetic acid
EE	early endosome
EEA1	early endosomal antigen 1
EGF(R)	epidermal growth factor (receptor)
eGFP	enhanced (engineered) green fluorescent protein
EHD	Eps15-homology domain
ENTH	epsin amino-terminal homology
ER	endoplasmic reticulum
ERC	endocytic recycling compartment
ERGIC	ER-Golgi intermediate compartment

et al.	et alii (and others)
EtBr	ethidiumbromide
EtOH	ethanol
FCS	**fetal calf serum**
Fig	figure
FIP	family of Rab11-interacting proteins
FL	full length
g	**acceleration of gravity**
g	gram
GAE	γ-adaptin ear
GAP	GTPase-activating protein
GAPDH	glutaraldehyd-3-phosphate dehydrogenase
γ-BAR	γ1-adaptin brefeldin A resistance
GDF	GDP-displacement factor
GDI	GDP-dissociation inhibitor
GDP	guanosine diphosphate
GEF	guanine nucleotide exchange factor
GGA	Golgi-localized, γ-ear containing, ARF-binding
GPI	glycophosphatidyl inositol
GRIP	glutamate receptor interacting protein
GST	glutathione S-transferase
GTP	guanosine triphosphate
h	**hour**
HA	hemagglutinin
HBSS	Hank's balanced salt solution
HC	heavy chain
HEK	human embryonic kidney
Hepes	4-(2-hydoxyethyl)piperazine-1-ethanesulfonic acid
His_6	6x Histidine
HRP	horseradish peroxidase
IB	**immunoblotting**
IF	immunofluorescence
Ig	immunoglobulin
IP	immunoprecipitation
IPTG	isopropylthio-β-D-galactoside
JIP	**JNK-binding scaffolding protein**
JNK	Jun N-terminal kinase
k	**kilo**
kb	kilo bases
KBS	kinesin binding segment
KHC	kinesin heavy chain
KIF	kinesin superfamily
KLC	kinesin light chain
l	**liter**
LAMP-1	lysosomal membrane glycoprotein-1
LB	Luria-Bertani
LC	light chain
LDL	low-density lipoprotein
LE	late endosome
LTD	long-term depression
LTP	long-term potentiation

µ	**micro**
m	milli
M	molar
MALDI-TOF	matrix-assisted laser desorption/ ionization – time of flight
MAP	mitogen activated protein
MDCK	Madin-Darby canine kidney
min	minute
MPR	mannose-6-phosphate receptor
mRNA	messenger RNA
MTOC	microtubule-organizing center
n	**nano**
NBT	nitro blue tetrazolium
NgCAM	neuron-glia cell adhesion molecule
NGF	nerve growth factor
NHS	N-hydroxysuccinimide
NMDA	N-methyl-D-aspartic acid
NMR	nuclear magnetic resonance
NSF	N-ethylmaleimide-sensitive fusion protein
Nuf	Nuclear-fallout
OD	**optical density**
PAGE	**polyacrylamide gel electrophoresis**
PAT	protein acyltransferase
PBS	phosphate buffered saline
PCR	polymerase chain reaction
PFA	para-formaldehyde
pH	preponderance of hydrogen ions
pI	isoelectric point
PI(3)P	phosphatidylinositol-3-phosphate
PMSF	phenylmethanesulfonyl fluoride
PNK	polynucleotide kinase
Ponceau S	3-hydoxy-4-[2-sulfo-4-(4-sulfophenylazo)phenylazo]-2,7-naphthalenedisulfonic acid
PX	PhoX homology
RBE	**rat brain extract**
RE	recycling endosome
RILP	Rab7-interacting lysosomal protein
RNA	ribonucleic acid
RNAi	RNA interference
rpm	rounds per minute
RT	room temperature
s.e.m.	**standard error of the mean**
SDS	sodium dodecylsulfate
SE	sorting endosome
sec	second
siRNA	small interfering RNA
SN	supernatant
SNAP	soluble NSF-attachment protein
SNARE	soluble NSF-attachment protein receptor
Std.	standard
Taq	***Thermus aquaticus***
TBE	Tris-borate-EDTA

TBS	Tris buffered saline
TCA	trichloroacetic acid
TE	Tris-EDTA
Tf	transferring
TfR	transferrin receptor
TGN	trans-Golgi network
TI-VAMP	tetanus neurotoxin-insensitive VAMP
T_M	melting temperature
TPR	tetratricopeptide repeat
Tris	Tris(hydroxymethyl)aminomethane
Triton X-100	octylphenol ethylene oxide condensate
TSM	Tris saline magnesium
U	**unit**
UV	ultraviolet
v/v	**volume per volume**
VAMP	vesicle-associated membrane protein
VSV(G)	vesicular stomatitis virus (glycoprotein)
w/o	**without**
w/v	weight per volume
w/w	weight per weight

d) Publications

Jia, J. Y., Lamer, S., Schumann, M., Schmidt, M. R., Krause, E. and Haucke, V. (2006). Quantitative proteomics analysis of detergent-resistant membranes from chemical synapses: evidence for cholesterol as spatial organizer of synaptic vesicle cycling. *Mol Cell Proteomics* **5**, 2060-71.

Schmidt, M. R. and Haucke, V. (2007). Recycling endosomes in neuronal membrane traffic. *Biol Cell* **99**, 333-42.

Schmidt, M. R., Doglio, L., Barak, N. L., Maritzen, T., Gensler, S., Gil, B., Dotti, C. G. and Haucke, V. Regulation of recycling endosomal membrane traffic by a γBAR-kinesin KIF5 complex. (submitted)

e) Curriculum vitae

Name:	Michael Roland Schmidt
Date of Birth:	April 11th, 1979
Place of Birth:	Eisenach, Germany
Marital status:	married
Nationality:	German

Education

since 04/2004	**Freie Universität Berlin** **PhD student with Prof. Dr. Volker Haucke** Institute of Chemistry and Biochemistry
since 10/2002	**Georg August University Göttingen** **MSc / PhD Program "Molecular Biology"** International Max Planck Research School Degree: Master of Science (MSc)
09/2001 - 05/2002	**McGill University Montréal, Canada** **Studies at the Faculty of Science** Transatlantic Science Student Exchange Program (TASSEP)
10/1998 - 08/2001	**Friedrich Schiller University Jena** **Studies in Biochemistry and Molecular Biology** Degree: "Vordiplom"
1997 - 1998	**Civil Service** Workshop for handicapped people
until 1997	**Ernst Abbe Gymnasium Eisenach** Degree: "Abitur"

Stipends

2002 - 2003	Stipend **International Max Planck Research School**
2002 - 2003	Stipend **Bayer AG**
2003 - 2006	PhD Stipend **Georg Christoph Lichtenberg**
2005	**EMBO** Short Term Fellowship

Contact Details

Address	Freie Universität Berlin, Institute of Chemistry and Biochemistry, Membrane Biochemistry, Takustr. 6, 14195 Berlin, Germany
Telephone	+49-30-838 56850
Permanent email	mschmidt@email.de